



# MID-BARATARIA SEDIMENT DIVERSION REPORT (DRAFT)

Ehab Meselhe, Ph.D., PE  
João Pereira, Ph.D., Hoon-Shin Jung,  
Ashok Khadka, Sadid Kazi

July 28, 2014

Produced for and funded by:  
HDR and CPRA



**THE WATER INSTITUTE  
OF THE GULF**

This page was intentionally left blank.

## TABLE OF CONTENTS

Figures .....	ii
Tables .....	v
Acknowledgments .....	vi
Overview and Objectives .....	1
1. Delft3D Modeling.....	2
1.1. Calibration and Validation of the Main Stem Hydrodynamics and Sediment Transport .....	2
1.2. Calibration and Validation of the Receiving Basin Hydrodynamics .....	13
1.3. Production Run with the Complete Model – Alternative 1 – 75,000 cfs ...	17
1.4. Production Run with the Complete Model – Alternative 2 – 50,000 cfs ...	41
2. River Response to the Diversion .....	56
3. FLOW-3D Modeling.....	60
3.1. Model Set up for Alternative Runs .....	60
3.2. Sediment / Water Ratios (SWRs) .....	63
Conclusions and Closing Remarks .....	64
References.....	66



## FIGURES

Figure 1. Main stem model domain, grid, and boundaries.....	2
Figure 2. Main stem stage calibration. ....	4
Figure 3. Main stem stage validation. ....	4
Figure 4. Main stem flow calibration.....	5
Figure 5. Main stem flow validation. ....	6
Figure 6. Depth averaged velocity transect calibration. ....	7
Figure 7. Depth-averaged velocity transect validation. ....	7
Figure 8. Main stem suspended fine load calibration.....	9
Figure 9. Main stem suspended fine load validation. ....	9
Figure 10. Main stem suspended sand load calibration. ....	10
Figure 11. Main stem suspended sand load validation.....	10
Figure 12. Main stem total suspended load calibration.....	11
Figure 13. Main stem total suspended load validation.....	11
Figure 14. Main stem bedload calibration.....	12
Figure 15. Main stem bedload validation. ....	12
Figure 16. Receiving basin model domain, grid, boundaries and CRMS stations used for stage calibration and validation. ....	14
Figure 17. Receiving basin stage calibration (calibration stations shown in bottom right quadrant). ....	15
Figure 18. Receiving basin stage validation (calibration stations shown in bottom right quadrant). ....	16
Figure 19. Production runs model domain, grid, and boundaries.....	18
Figure 20. Production runs: Alternative 1 - model initial bathymetry.....	18
Figure 21. Locations of soil boring information provided by HDR.....	20
Figure 22. Vertical profile of bed thickness for receiving basin showing the two different layers of soil used.....	20
Figure 23. Flow at Tarbert Landing: 1954-2003.....	22
Figure 24. Histogram for 1974-1983 river discharge. ....	23
Figure 25. Flow duration curves from simplified hydrograph and measured flows at Tarbert Landing (U.S. Army Corps of Engineers, Station ID: 01100). ....	23
Figure 26. Sand duration curve – probability of exceeding. Comparison between simplified and estimated hydrographs based on sediment transport rating curves. .....	24
Figure 27. Fine sediment duration curve – probability of exceeding. Comparison between simplified and estimated hydrographs based on sediment transport rating curves. ....	24



Figure 28. Five-year representative simplified flow hydrograph. ....	25
Figure 29. Simulation #1.1: Cumulative erosion and deposition after 5 years. ....	26
Figure 30. Simulation #1.1: Initial bed level (left panel) and Year-5 bed level (right panel). ....	27
Figure 31. Simulation #1.1: Annual erosion and deposition volumes. ....	28
Figure 32. Simulation #1.1: Cumulative erosion and deposition volumes for the 5-year simulation. ....	29
Figure 33. Simulation #1.2: Cumulative erosion and deposition after 5 years. A positive value indicates deposition and a negative value indicates erosion. ....	30
Figure 34. Simulation #1.2: Initial bed level (left panel) and Year 5 bed level (right panel). ....	31
Figure 35. Simulation #1.2: Annual erosion and deposition volumes. ....	32
Figure 36. Simulation #1.2: Cumulative erosion and deposition volumes. ....	33
Figure 37. Simulations #1.1 and #1.2: Longitudinal profile of bed elevation and stage for peak flow (year 3; $q = 1,180,000$ cfs) - outfall channel and part of the outfall area. ....	34
Figure 38. Simulations #1.1 and #1.2: Longitudinal profile of velocity for peak flow ( $q = 1,180,000$ cfs) - outfall channel and part of the outfall area. ....	35
Figure 39. Simulations #1.1 and #1.2: Cumulative erosion and deposition after 5 years. A positive value indicates deposition and a negative value indicates erosion. ....	36
Figure 40. Simulations #1.1 and #1.2: Comparison of final bed level. ....	36
Figure 41. Simulations #1.1 and #1.2: Comparison of cumulative erosion and deposition by polygon. ....	37
Figure 42. Annual evolution of the net volume change in the outfall area. ....	37
Figure 43. Hypsometric curves showing the land evolution in time. ....	38
Figure 44. Simulations #1.1 and #1.2: Comparison of stage at selected polygons. The points were selected near the center of the polygons. The points were mostly in open water areas. ....	39
Figure 45. Simulations #1.1 and #1.2: Comparison of instantaneous SWRs. ....	40
Figure 46. Simulation #2.1: Cumulative erosion and deposition after 5 years. A positive value indicates deposition and a negative value indicates erosion. ....	41
Figure 47. Simulation #2.1: Initial bed level (left panel) and Year-5 bed level (right panel). ....	42
Figure 48. Simulation #2.1: Annual erosion and deposition volumes. ....	43
Figure 49. Simulation #2.1: cumulative erosion and deposition volumes for the 5-year simulation. ....	44



Figure 50. Simulation #2.2: Cumulative erosion and deposition after 5 years. A positive value indicates deposition and a negative value indicates erosion. ....	45
Figure 51. Simulation #2.2: Initial bed level (left panel) and Year 5 bed level (right panel).....	46
Figure 52. Simulation #2.2: Annual erosion and deposition volumes. ....	47
Figure 53. Simulation #2.2: Cumulative erosion and deposition volumes. ....	48
Figure 54. Simulations #2.1 and #2.2: Longitudinal profile of bed elevation and stage for peak flow (year 3; $q = 1,180,000$ cfs) - outfall channel and part of the outfall area. ....	49
Figure 55. Simulations #2.1 and #2.2: Longitudinal profile of velocity for peak flow ( $q = 1,180,000$ cfs) - outfall channel and part of the outfall area. ....	50
Figure 56. Simulations #2.1 and #2.2: Cumulative erosion and deposition after 5 years. A positive value indicates deposition and a negative value indicates erosion. ....	50
Figure 57. Simulations #2.1 and #2.2: Comparison of final bed level. ....	51
Figure 58. Simulations #2.1 and #2.2: Comparison of cumulative erosion and deposition by polygon.....	52
Figure 59. Annual evolution of the net volume change in the outfall area.....	52
Figure 60. Hypsometric curves showing land evolution in time. ....	53
Figure 61. Simulations #2.1 and #2.2: Comparison of stage at selected polygons. ....	54
Figure 62. Simulations #2.1 and #2.2: Comparison of instantaneous SWRs. ....	55
Figure 63. Extended model domain for the Mississippi River channel opposite the diversion site.....	56
Figure 64. Simulated Mississippi River water discharge (Q) between 2008 – 2010. ....	57
Figure 65. Erosion and deposition volume in response to the diversion during 2008 – 2010. ....	58



## TABLES

Table 1. Main stem stage calibration and validation statistical analysis.....	5
Table 2. Main stem flow calibration and validation statistical analysis.....	6
Table 3. Main stem depth-averaged calibration and validation statistical analysis. .....	8
Table 4. Main stem suspended fine load calibration and validation statistical analysis. ....	10
Table 5. Main stem suspended sand load calibration and validation statistical analysis. ....	11
Table 6. Main stem total suspended load calibration and validation statistical analysis. ....	12
Table 7. Receiving basin stage calibration and validation statistical analysis.....	16
Table 8. Simulation #1.1: Retention rates by sediment size-class for the modeling period. ....	29
Table 9. Simulation #1.2: Retention rates by sediment size-class for the modeling period. ....	33
Table 10. Simulation #2.1: Retention rates by sediment size-class for the modeling period.....	44
Table 11. Simulation #2.2: Retention rates by sediment size-class for the modeling period.....	48
Table 12. Sediment budget for sand load for 2008 – 2010.....	58
Table 13. Sediment budget for fine sediment load for 2008 – 2010.....	59
Table 14. Sediment budget for total load for 2008 – 2010.....	59
Table 15. Specifications of four alternative runs used in the FLOW-3D simulations (bathymetry colored by elevation (ft)).....	61
Table 16. Wall roughness of model components. ....	62
Table 17. Boundary conditions used in the FLOW-3D simulations. ....	62
Table 18. Sediment/Water Ratio (SWR) for different flow conditions.....	63



## ACKNOWLEDGMENTS

The authors wish to thank the HDR team led by Bob Beduhn, Mark Forest, Neil McLellan, and Brinton Swift and well as the CPRA team led by Micaela Coner, Vida Carver, and Kodi Collins.

We would also like to acknowledge the help provided by Alex McCorquodale and Sina Amini (University of New Orleans) in developing the 5-year hydrograph used in the final production runs.

Lastly, this work was reviewed by Dr. Denise Reed, Dr. Mead Allison, Alaina Owens and Katelyn Costanza from the Water Institute of the Gulf (the Institute).

### **Suggested Citation**

The Water Institute of the Gulf (July 2014). Mid-Barataria Sediment Diversion Report. Prepared for HDR and CPRA. Prepared by Meselhe, E.A.; Pereira, J.F.; Jung, H., Khadka, A. and Sadid, K.



## OVERVIEW AND OBJECTIVES

This report summarizes the numerical modeling effort performed by the Water Institute as part of the overall engineering design of the Mid-Barataria Sediment Diversion. This report will be included as part of the full design report currently being prepared by HDR and will be ultimately submitted to CPRA.

The specific tasks described in this report include:

Task 1: Delft3D – Geomorphic model for the Mississippi River, through the 30% outfall channel design, and extending into the Barataria Basin outfall area for a minimum of eight miles. This task includes model development, calibration, validation and application and is intended to address the following:

- Investigation of the general geomorphic response of the area of Barataria Basin close to the diversion outfall within the first 5 years of diversion operation.
- Investigation of the sediment/water ratios calculated by the numerical model during periods in which the diversion is in operation.

Task 2: FLOW-3D – Hydraulic sediment particle tracking modeling for the Mississippi River, through the 30% outfall channel design, and extending one mile into the Barataria Basin outfall area. This task is intended to study the following:

- Sediment water ratios for the 30% channel design based on 700,000 cfs Mississippi River discharge.
- Sediment water ratios for the 30% channel design based on 970,000 cfs Mississippi River discharge.

This modeling effort focuses on the near-field outfall (receiving basin) area of the Mid-Barataria Sediment Diversion. The main objectives of this effort are to:

- Estimate the mass quantities and spatial trends of erosion and deposition in the outfall area
- Estimate the net-land gain over the first 5 years of the life of the diversion
- Determine the magnitude of deposition that occurs near the outlet mouth (basin side) of the outfall channel
- Estimate the increase of water surface elevation near the mouth of the outfall channel
- Discuss the potential impact of the diversion on the upstream sand bar

As this modeling effort focuses entirely on the near-field and the model domain is limited to a receiving basin area of 8 mi-by-8 mi near the mouth of the outfall channel, the results should not be used to:

- Infer the overall alteration of the water surface elevation over the entire Barataria basin
- Infer the total footprint of receiving basin land building resulting from the diversion over the first 5 years of operation.

Linking this model with a basinwide model and performing longer-term simulations (~ 50 years) would be necessary to address these issues.



## 1. DELFT3D MODELING

This chapter provides an overview of the Delft3D modeling effort. The Delft3D model has already been developed at the Water Institute for other studies. It has been refined based on newly available field observation and was re-calibrated as part of the effort presented herein. Below is a list summarizing the specific tasks performed in this effort:

- Calibration and validation of the main stem hydrodynamics and sediment transport
- Calibration and validation of the receiving basin hydrodynamics
- Production runs with the complete model (main stem + outfall channel + immediate outfall area of the receiving basin):
  - Alternative 1 – Version 1 - Diverted design flow of 75,000 cfs
  - Alternative 2 – Version 1 – Diverted design flow of 50,000 cfs

### 1.1. CALIBRATION AND VALIDATION OF THE MAIN STEM HYDRODYNAMICS AND SEDIMENT TRANSPORT

The calibration and validation of the Mississippi River channel adjacent to the diversion (Figure 1) were the first steps of the Delft3D modeling. This was a previously developed model, updated as part of this effort to include the following:

- 2013 multibeam bathymetry provided by HDR for the intake area
- 2012 multibeam bathymetry provided by the U.S. Army Corps of Engineers (USACE) for the remaining area of the river modeled beyond the intake area
- Updated parameter settings used by the Water Institute in other diversion projects, e.g., the Chézy formulation was used instead of the Manning's n formulation and the Van Rijn (1993) formula was used instead of the Van Rijn (1984) formula
- Set up of the Delft model in a two-dimensional (2-D) depth-averaged format

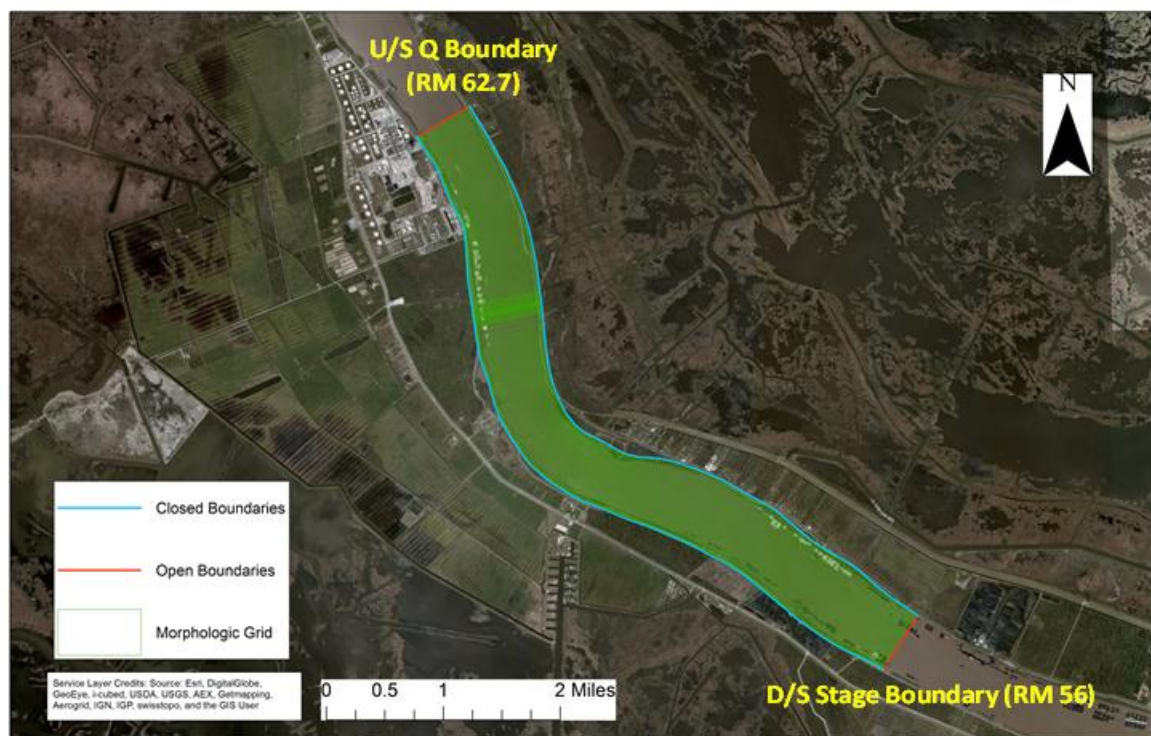


Figure 1. Main stem model domain, grid, and boundaries.



Based on the available hydrodynamic and sediment data, the following periods were selected for calibration and validation:

- Calibration: October 2008 to April 2010
- Validation: May 2010 to December 2012

Preliminary calibration simulations were performed in both 2-D and three-dimensional (3-D) mode (10 vertical sigma layers). From these, it was concluded that the 2-D model results were consistent with the 3-D model results. Thus, in order to save computational time, it was decided to select the 2-D model for the final calibration and validation.

The main stem model has a grid resolution ranging from 20 m-by-40 m to 40 m-by-80 m. A time-step of 0.10 minutes (6 sec) was used in all calibration and validation simulations.

The model was first calibrated and validated for hydrodynamics only. The following boundary conditions were used:

- U/S Boundary: Flow at Belle Chasse (U.S. Geological Survey [USGS] station ID: 07374525); gap for October 2008 filled based on Baton Rouge, Davis Pond and Caernarvon USGS data].
- D/S Boundary: Stage at RM 56 from a Mississippi River Regional Model (RM 138 to the Gulf) developed by the Institute.

Calibration and validation were performed for stage, flow, and depth-averaged transect velocities. For the model calibration and validation, the stage data were available at the USACE stations, while the flow and depth averaged transect velocity data were collected by Dr. Mead Allison and his team as part of the CPRA-funded, LCA Myrtle Grove study. These data are presented in Ramirez and Allison (2013).

Figure 2 and

Figure 3 display the stage calibration and validation performed at Alliance (RM 62). The performance of the model is summarized through the statistical analysis shown in Table 1. Based on guidance provided in Meselhe and Rodrigue (2013), the statistical analysis indicates that the model's performance is satisfactory.



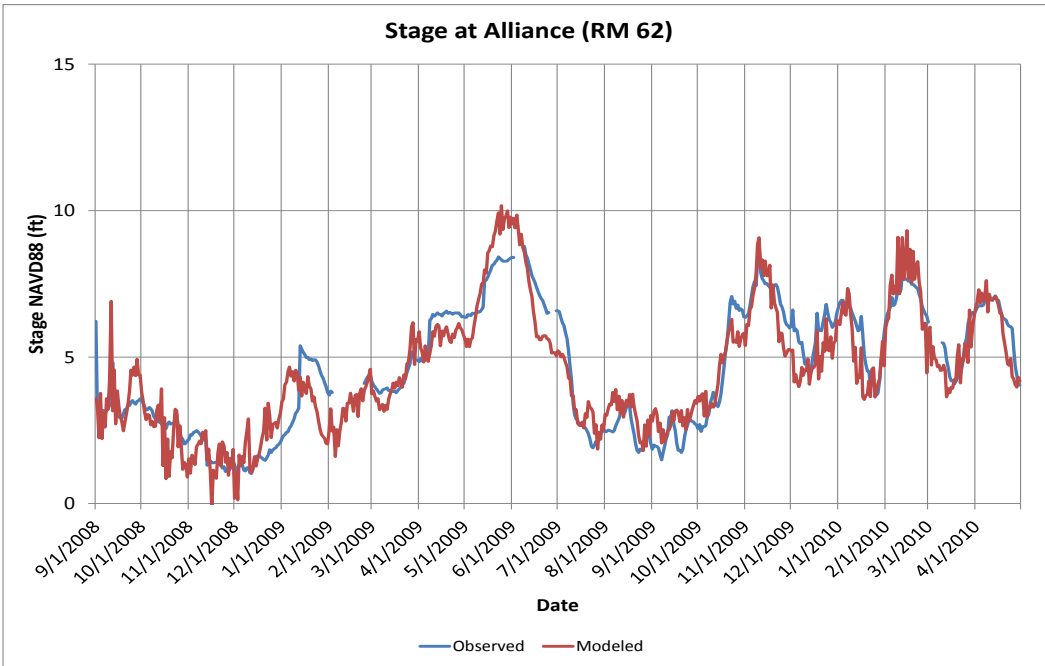


Figure 2. Main stem stage calibration.

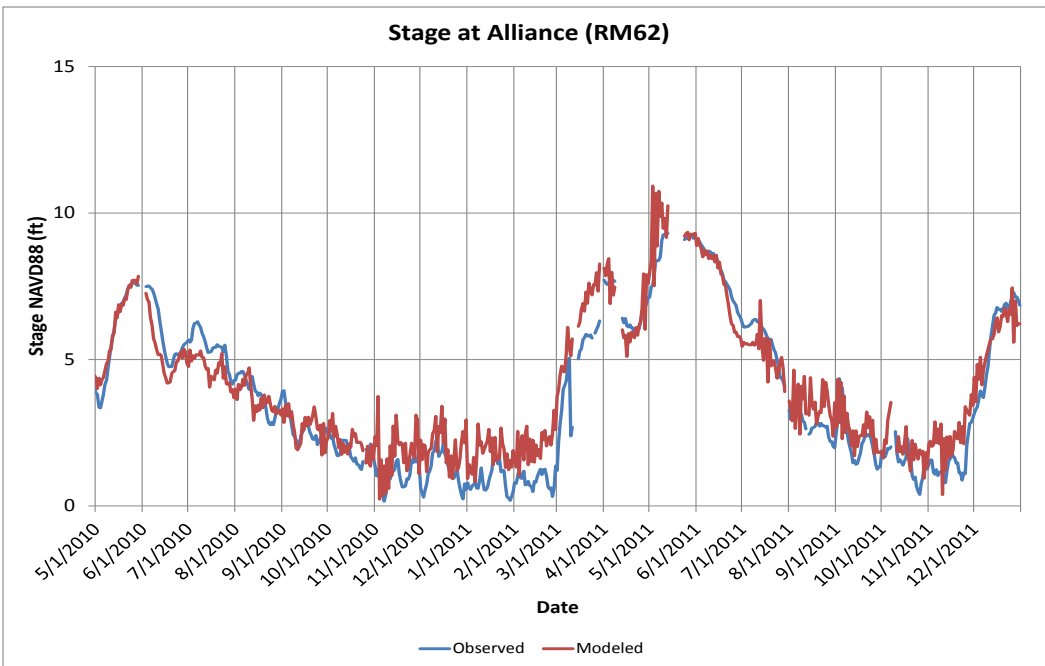


Figure 3. Main stem stage validation.



Modeled Period	Average Bias (ft)	Bias % of Range	RMSE%	Corr. Coef.
Calibration October 2008 to April 2010	-0.08	-1%	18%	0.91
Validation May 2010 to December 2012	0.33	5%	25%	0.95

Table 1. Main stem stage calibration and validation statistical analysis.

Flow calibration and validation were performed for RM 61.6. The corresponding statistical analysis of the results is provided in Table 2. The results presented in Figure 4 and Figure 5 and in Table 2 indicate that the model meets the standards presented in Meselhe and Rodrigue (2013). As such, the model performance is considered satisfactory.

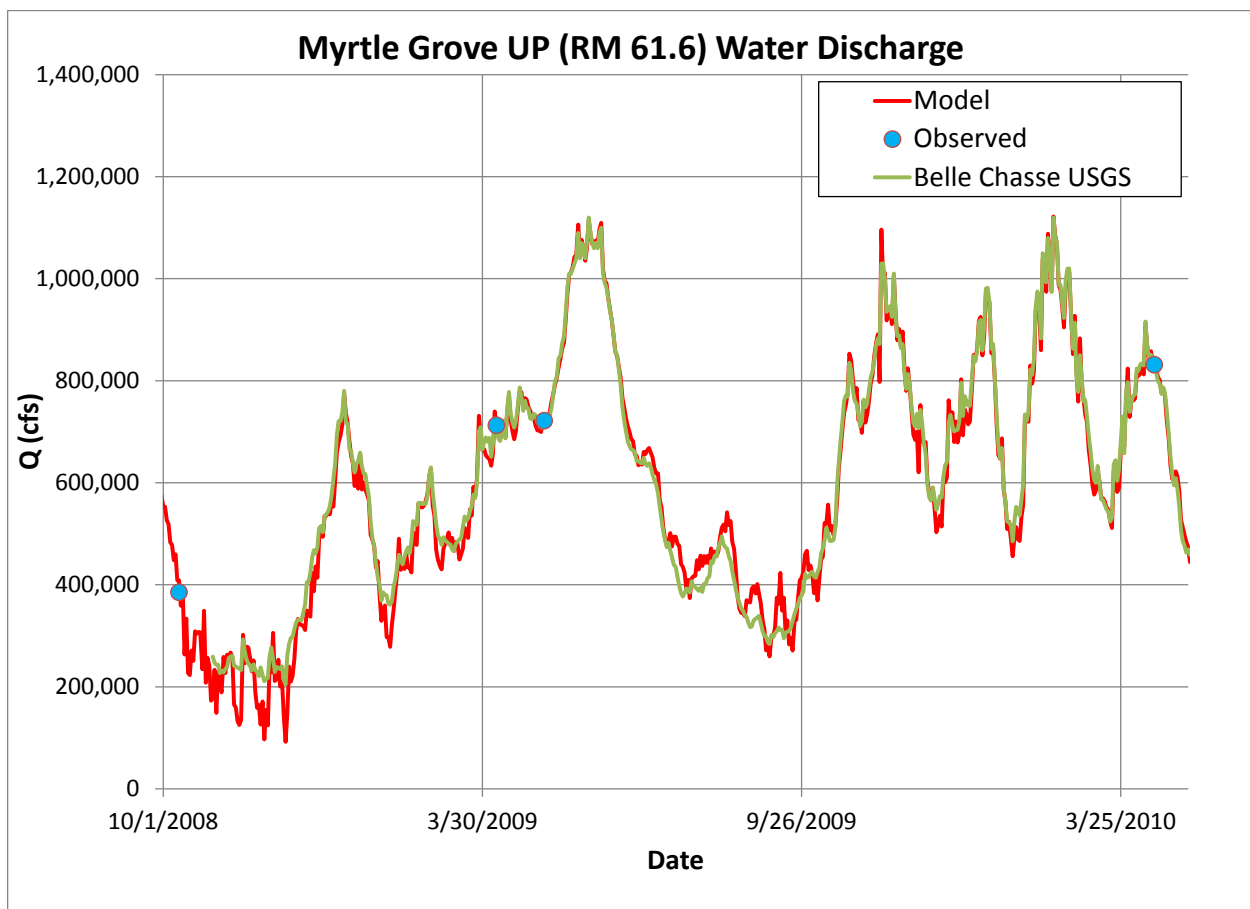


Figure 4. Main stem flow calibration.\*

\* Observed data are from boat-based ADCP measurements collected during the LCA Myrtle Grove study.



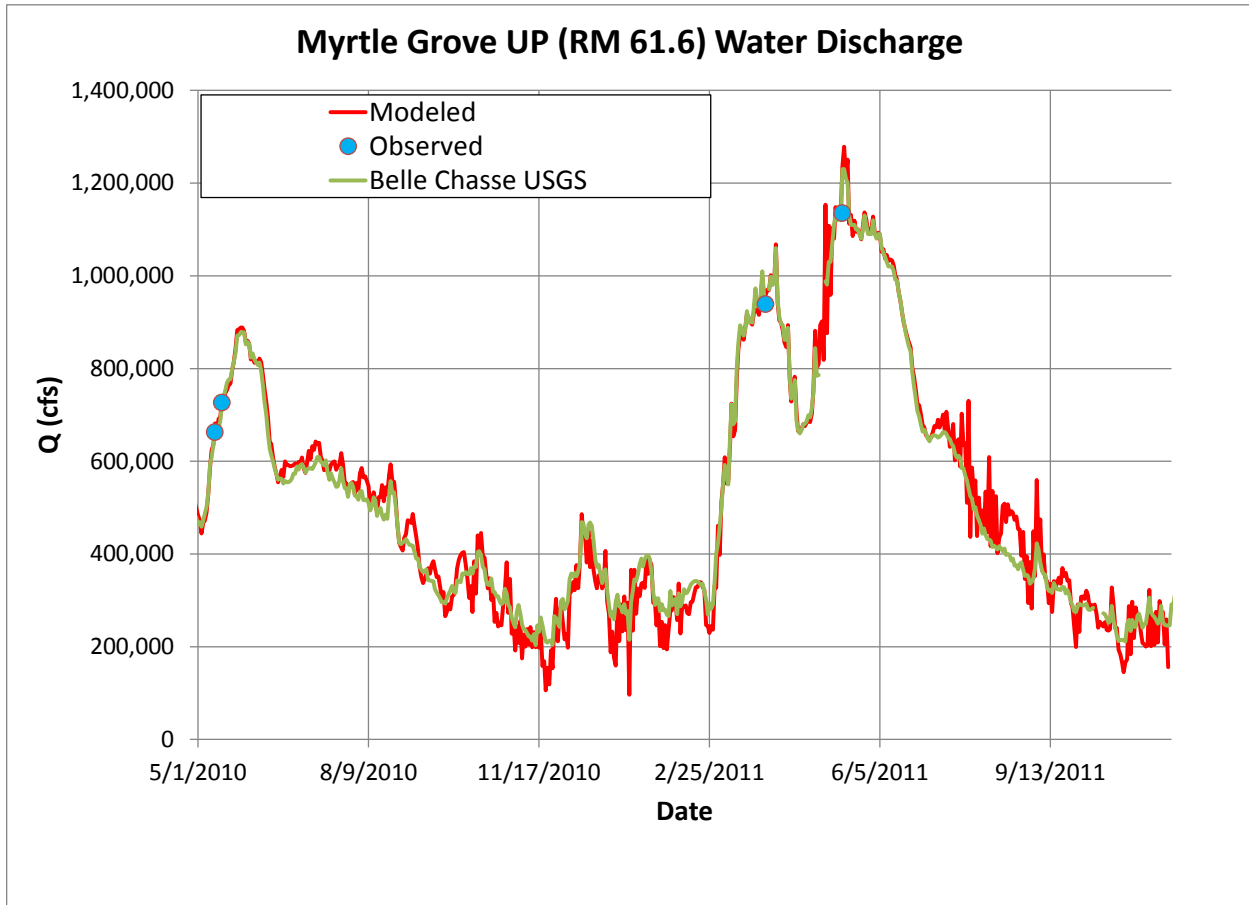


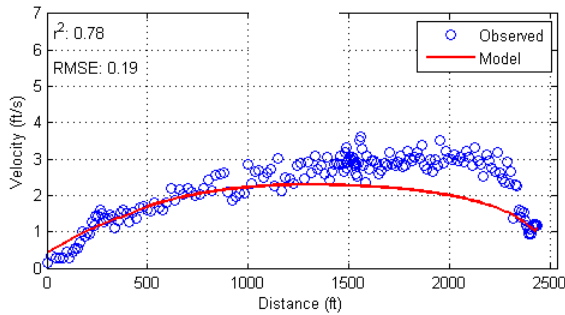
Figure 5. Main stem flow validation.\*

Modeled Period	Average Bias (cfs)	Bias (%)	RMSE%	Corr. Coef.
Calibration October 2008 to April 2010	-7,034	-1%	4%	0.99
Validation May 2010 to December 2012	35,789	4%	6%	1.00

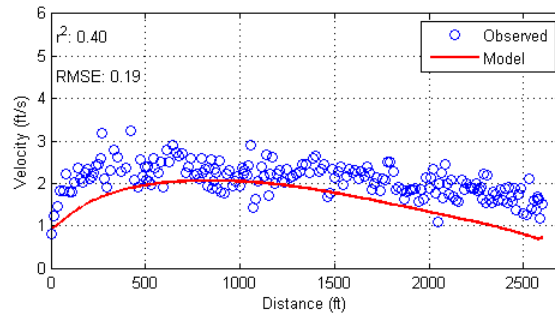
Table 2. Main stem flow calibration and validation statistical analysis.

The calibration and validation of depth-averaged velocity is presented in Figure 6 and Figure 7. There is good agreement between the model results and the measurements. The statistical analysis for the depth-averaged velocity is presented in Table 3.

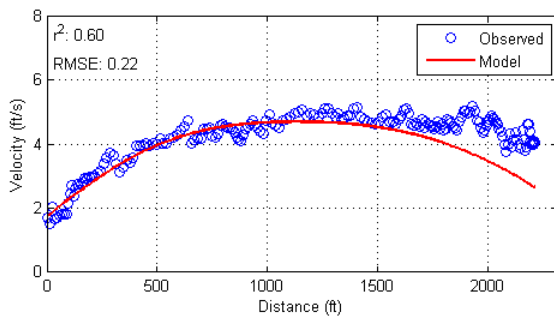




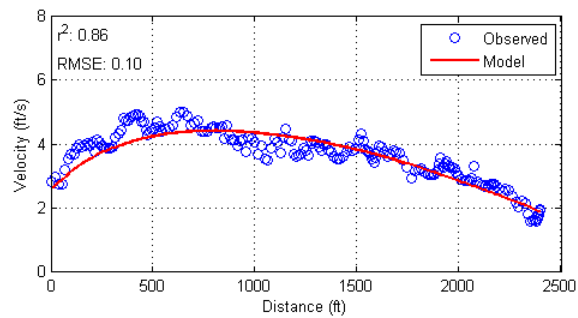
**RM 61.0, September 2009, Q = 350,000 cfs**



**RM58.3, September 2009, Q = 350,000 cfs**

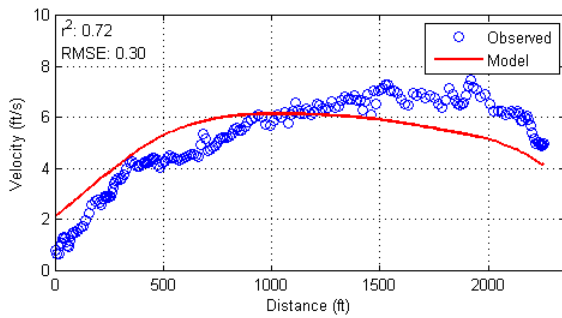


**RM 61.0, September 2009, Q = 350,000 cfs**

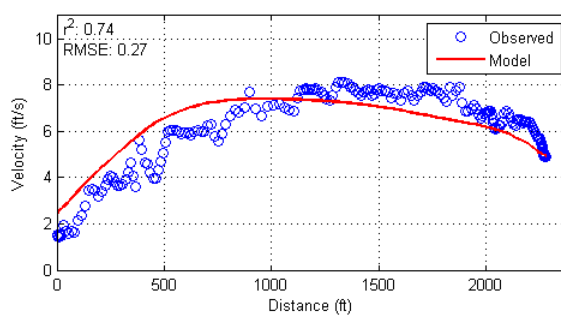


**RM 58.3, September 2009, Q = 700,000 cfs**

Figure 6. Depth averaged velocity transect calibration.\*



**RM 61.6, April 2011, Q = 970,000 cfs**



**RM 61.6, May 2011, Q = 1,150,000 cfs**

Figure 7. Depth-averaged velocity transect validation.\*

\* Observed data are from boat-based ADCP measurements collected during the LCA Myrtle Grove study.



Modeled Period	RMSE%	Corr. Coef.
Calibration October 2008 to April 2010	22%	0.80
Validation May 2010 to December 2012	28%	0.85

Table 3. Main stem depth-averaged calibration and validation statistical analysis.

The calibration and validation of sediment transport followed the hydrodynamics validation. The boundary conditions prescribed were:

- U/S boundary: Suspended sediment concentrations for the following size classes:
  - Sand: very fine sand ( $D_{50} = 83 \mu\text{m}$ ), fine sand ( $D_{50} = 167 \mu\text{m}$ ) and medium sand ( $D_{50} = 333 \mu\text{m}$ )
  - Mud (fine material): clay ( $D < 2 \mu\text{m}$ ) and silt ( $2 \mu\text{m} < D < 63 \mu\text{m}$ )

It should be noted that only the  $D_{50}$  is provided and the numerical model generates a distribution curve internally. The suspended sediment concentrations were estimated daily to be prescribed as inputs to the Delft3D model based on rating curves developed by the Water Institute using USGS measurements at Belle Chasse (RM 74) for the period 2008 to 2012. Separate rating curves were used for Sand and for Mud transport. The equations of the rating curves are:

- Suspended Sand Load (metric tons/day) =  $a*[1-\exp(-b*Q_w)]+c*[1-\exp(-d*Q_w)]$   
 $a = 7.716\text{E}+7$ ;  $b = 2.485\text{E}-7$ ;  $c = -5.748\text{E}+5$ ;  $d = 4.122\text{E}-5$
- Suspended Fine Load (metric tons/day) =  $A*Q_w^B$   
 $A = 0.0020$ ;  $B = 1.8589$

Calibration and validation of sediment transport was performed for suspended load and bedload. The sediment data were collected as part of the LCA Myrtle Grove study.

Figure 8 and

Figure 9 show the suspended fine load calibration and validation. The calibration was performed for two different transects where data were available: Myrtle Grove Up (RM 61.6) and Myrtle Grove Down (RM 58.0). For the validation period data were only available for Myrtle Grove Up (RM 61.6). For visual comparison, the USGS measurements at Belle Chasse (slightly outside the upstream end of the model domain) are also presented. The purpose of including such data in the plots is to examine the consistency of the boat-based measurements conducted by Dr. Allison and the USGS data. The outcome of this analysis indicates that the model is capable of capturing the order of magnitude and the temporal pattern of fluctuation of the suspended fine sediment transport. The statistical analysis results are presented in Table 4. The model performance is acceptable based on the metrics provided in Meselhe and Rodrigue (2013).

The calibration and validation of suspended sand load is shown in Figure 10 and Figure 11, and Table 5 illustrates the corresponding statistical analysis. Outcomes indicate that model performance is acceptable. Although the bias and RMSE values are not as good as those for suspended fine sediment, the correlation coefficient is considerably better. Overall, the model performance is acceptable for velocities and sediment transport based on the metrics provided in Meselhe and Rodrigue (2013).



Figure 12 and Figure 13 display the calibration and validation of total suspended load (suspended sand + suspended fines). The statistical analysis is presented in Table 6. The model performance is acceptable.

The bedload transport results are shown in Figure 14 and Figure 15. There are a smaller number of bedload measurements than there are for suspended load measurements. Thus, no statistical analysis was performed for bedload. The model approximates the magnitude of the bedload transport well compared to the field observations.

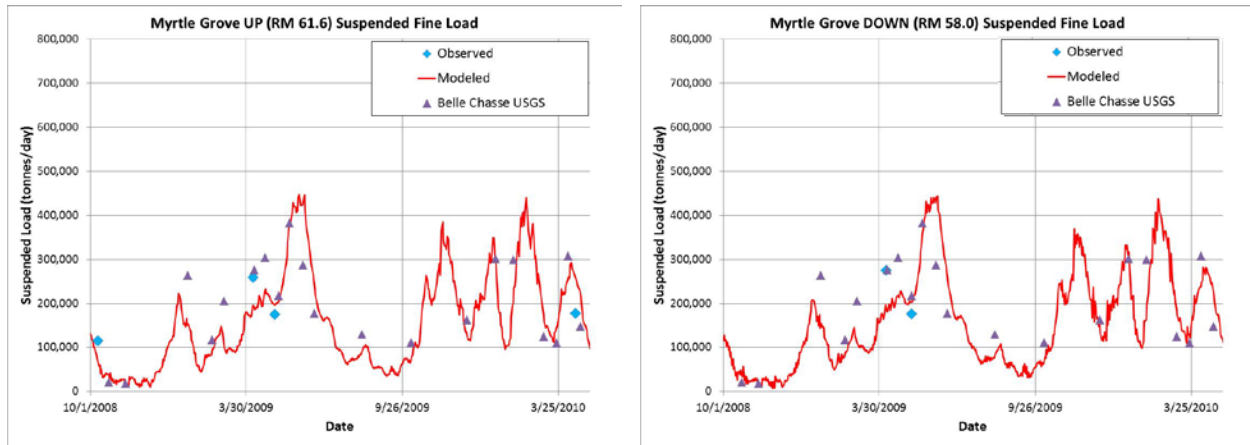


Figure 8. Main stem suspended fine load calibration.\*

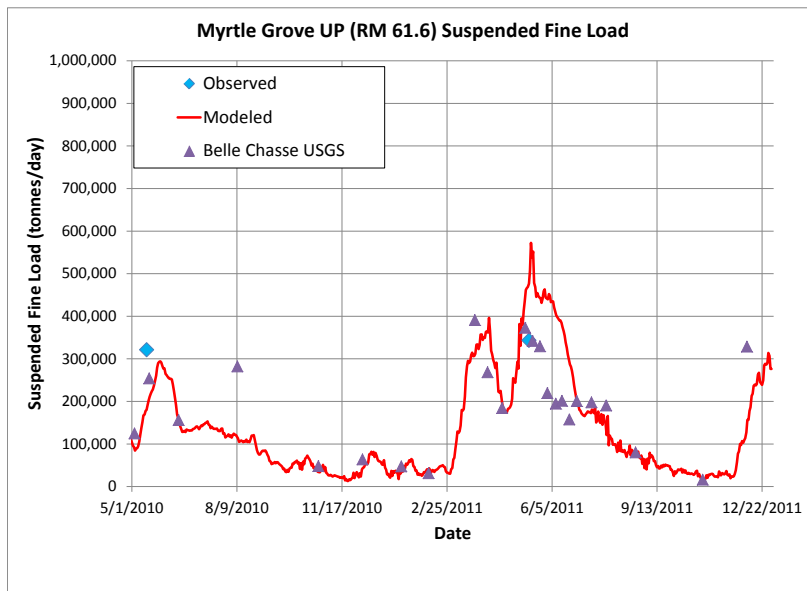


Figure 9. Main stem suspended fine load validation.\*

\* Observed data are from boat-based ADCP measurements collected during the LCA Myrtle Grove study.



Modeled Period	Average Measured (tonnes/d)	Average Modeled (tonnes/d)	Average Bias (tonnes/day)	Bias (%)	RMSE%	Corr. Coef.
Calibration October 08 to April 10	196,510	185,724	-10,786	-5%	30%	0.46
Validation May 10 to December 12	332,113	351,579	19,466	6%	N/A	N/A

Table 4. Main stem suspended fine load calibration and validation statistical analysis.

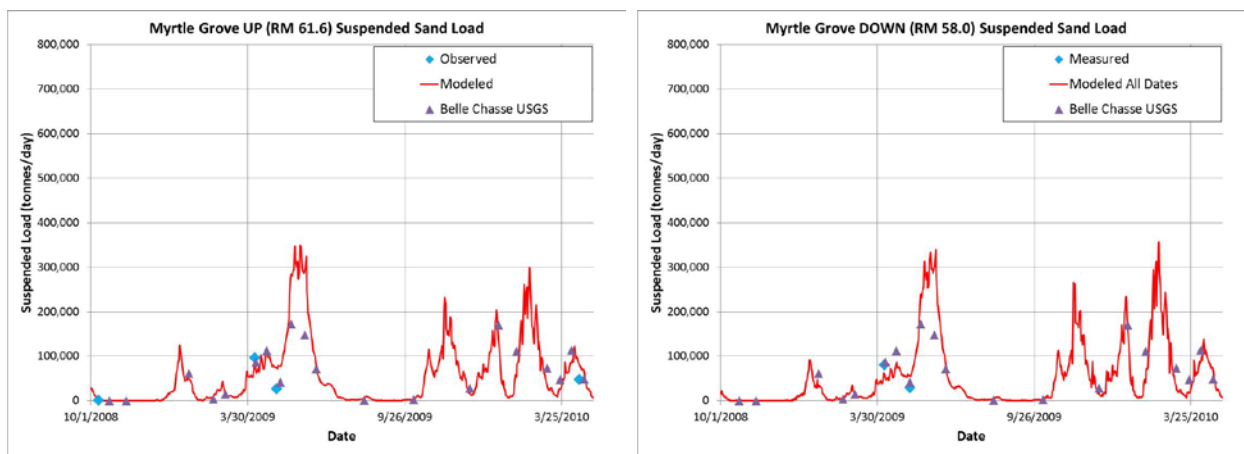


Figure 10. Main stem suspended sand load calibration.

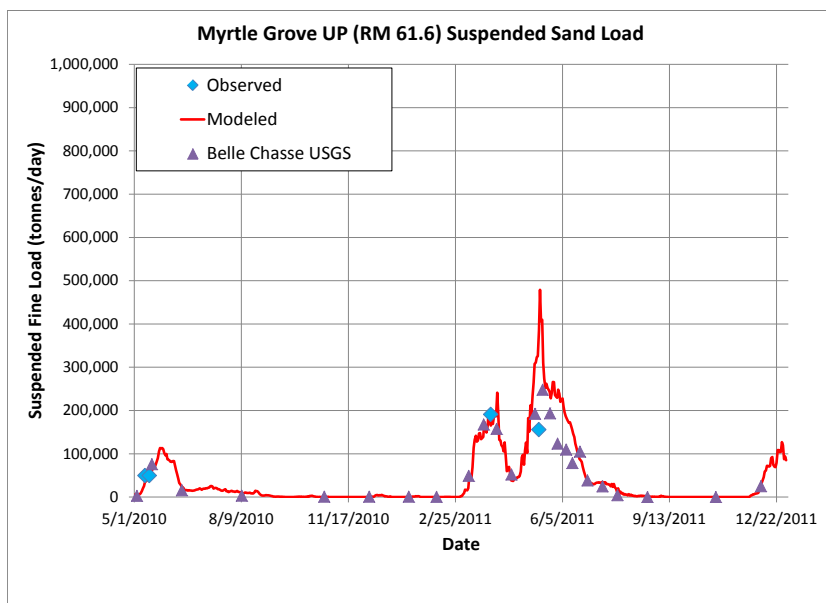


Figure 11. Main stem suspended sand load validation.



Modeled Period	Average Measured (tonnes/d)	Average Modeled (tonnes/d)	Average Bias (tonnes/day)	Bias (%)	RMSE%	Corr. Coef.
Calibration Oct 08 to Apr 10	47,238	59,667	12,429	26%	61%	0.64
Validation May 10 to Dec 12	111,362	158,360	46,998	42%	104%	0.71

Table 5. Main stem suspended sand load calibration and validation statistical analysis.

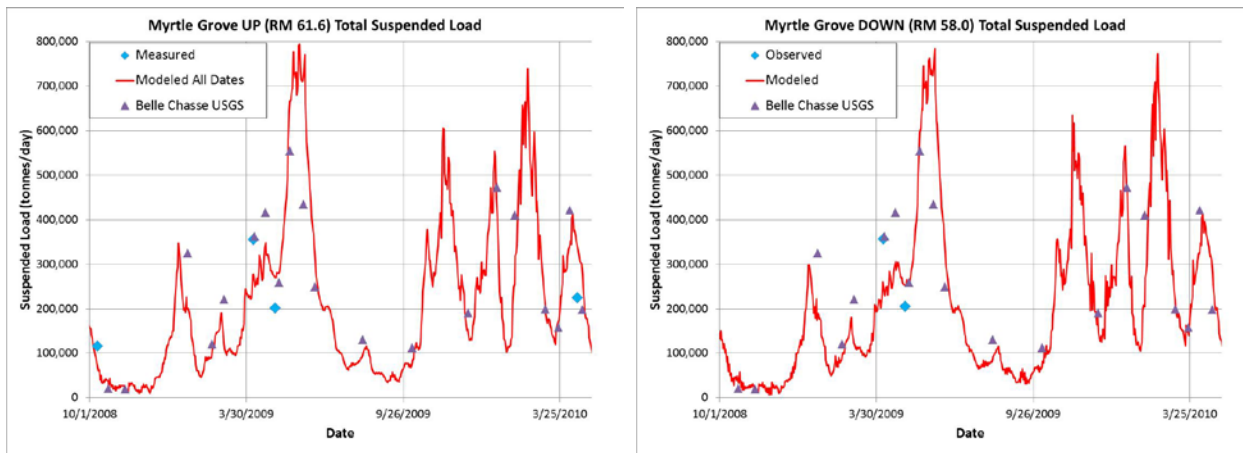


Figure 12. Main stem total suspended load calibration.

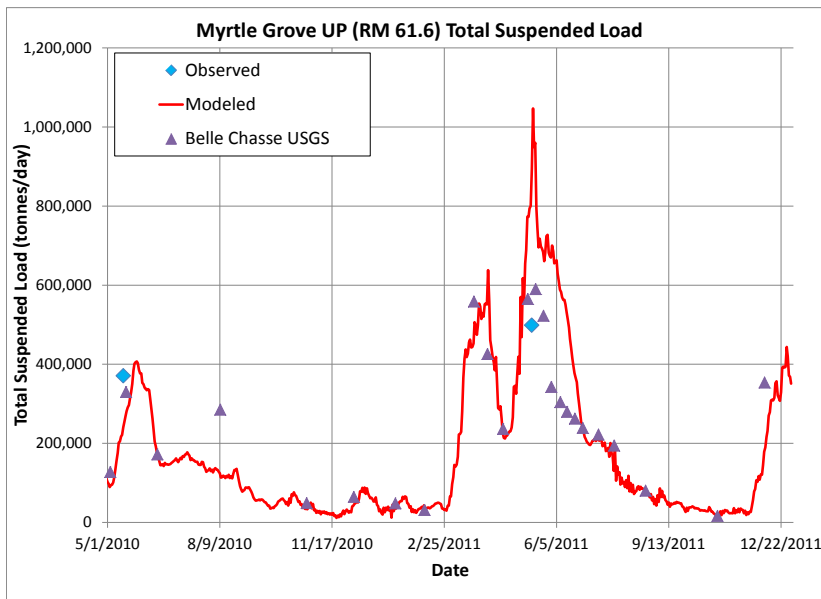


Figure 13. Main stem total suspended load validation.



Modeled Period	Average Measured (tonnes/d)	Average Modeled (tonnes/d)	Average Bias (tonnes/day)	Bias (%)	RMSE %	Corr. Coef.
Calibration October 08 to April 10	243,748	245,391	1,643	1%	34%	0.53
Validation May 10 to December 12	434,649	474,084	39,435	9%	N/A	N/A

Table 6. Main stem total suspended load calibration and validation statistical analysis.

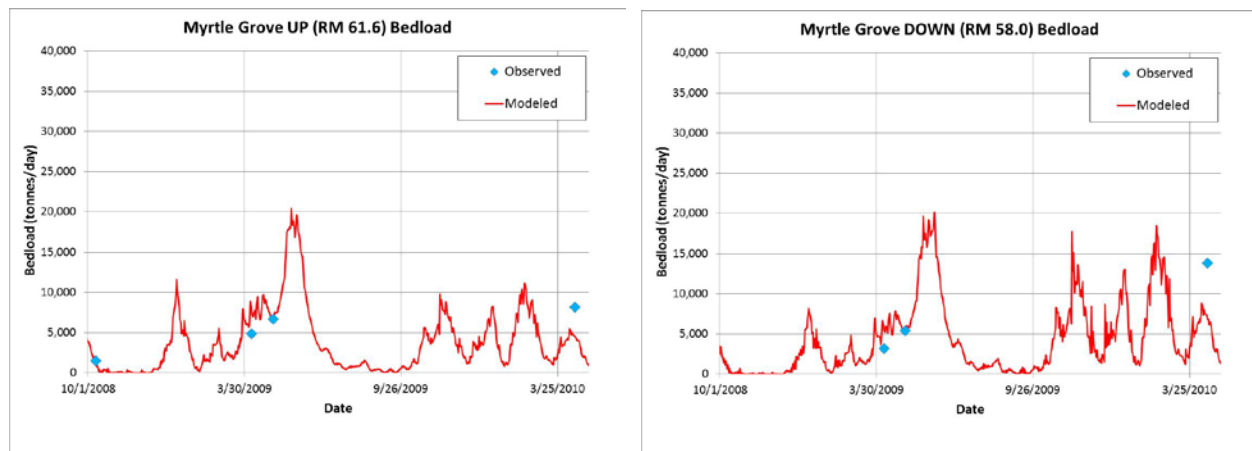


Figure 14. Main stem bedload calibration.

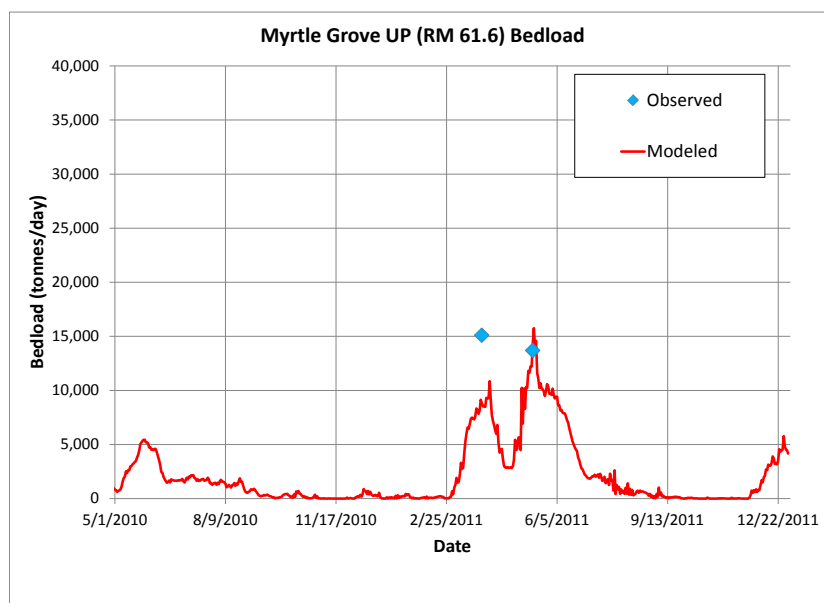


Figure 15. Main stem bedload validation.



## 1.2. CALIBRATION AND VALIDATION OF THE RECEIVING BASIN HYDRODYNAMICS

The following overall approach was used to set up the receiving basin model:

- Bathymetry data (provided by HDR) were used for the receiving basin.
- The model domain encompasses an area of 8 X 8 miles in the outfall area in the immediate vicinity of the mouth of the outfall channel.
- The grid (Figure 16) was generated with resolution ranging from 80 m-by-80 m to 100 m-by-200 m. The fine resolution areas focused around channels or high-gradient regions near the outfall channel mouth.
- After testing the model for stability, a time-step of 0.5 minutes (30 sec) was used. Typically the time step is governed by several factors, e.g. the grid resolution, the temporal gradient of the state variables, and the numerical scheme employed in the numerical model.
- The model was calibrated for roughness and a Chézy coefficient equal to 50 was used for all the domain. A spatial varying roughness would be considered for future phases of the project.

Calibration and validation of hydrodynamics were performed for the same periods that were used for the main stem modeling:

- Calibration: October 2008 to April 2010
- Validation: May 2010 to December 2012

The model was calibrated and validated for hydrodynamics. The following boundary conditions were used:

- Open boundary: Stage calculated based on the Coastwide Reference Monitoring System (CRMS) data for the six stations with available data closer to the open boundary (source: <http://coastal.la.gov/monitoring-data/>). The average daily value of the different stations was calculated and prescribed as a time-series to the model.
- Wind data from the National Oceanic and Atmospheric Administration (NOAA) station 8762482 at West Bank 1, Bayou Gauche were used to derive wind boundary conditions at hourly frequency.



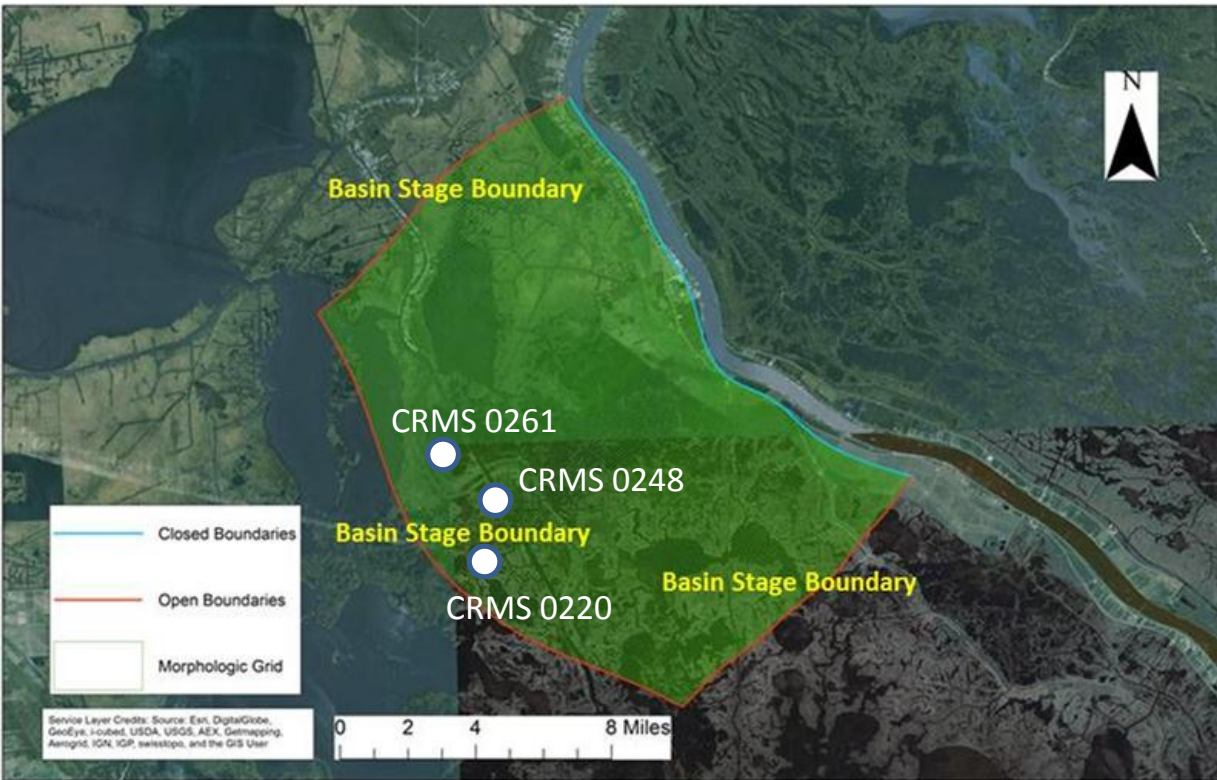


Figure 16. Receiving basin model domain, grid, boundaries and CRMS stations used for stage calibration and validation.

Calibration and validation were performed for stage, as mentioned previously. Observation data from CRMS stations 220, 248, and 261 (source: <http://coastal.la.gov/monitoring-data/>) were used for stage calibration. These stations were selected based on availability of data during the period of record of interest. Additional stations could be used in later phases of the project and as the model domain is expanded spatially. The bed roughness was the calibration parameter. Tests were performed with Chézy coefficient values between 40 and 70. The best results were obtained with a value of 50.

Figure 17 and Figure 18 display receiving basin stage calibration and validation performed using the three CRMS stations. The outcomes indicate the model is able to reproduce the measured stages. The performance of the model is assessed through a statistical analysis shown in Table 7.



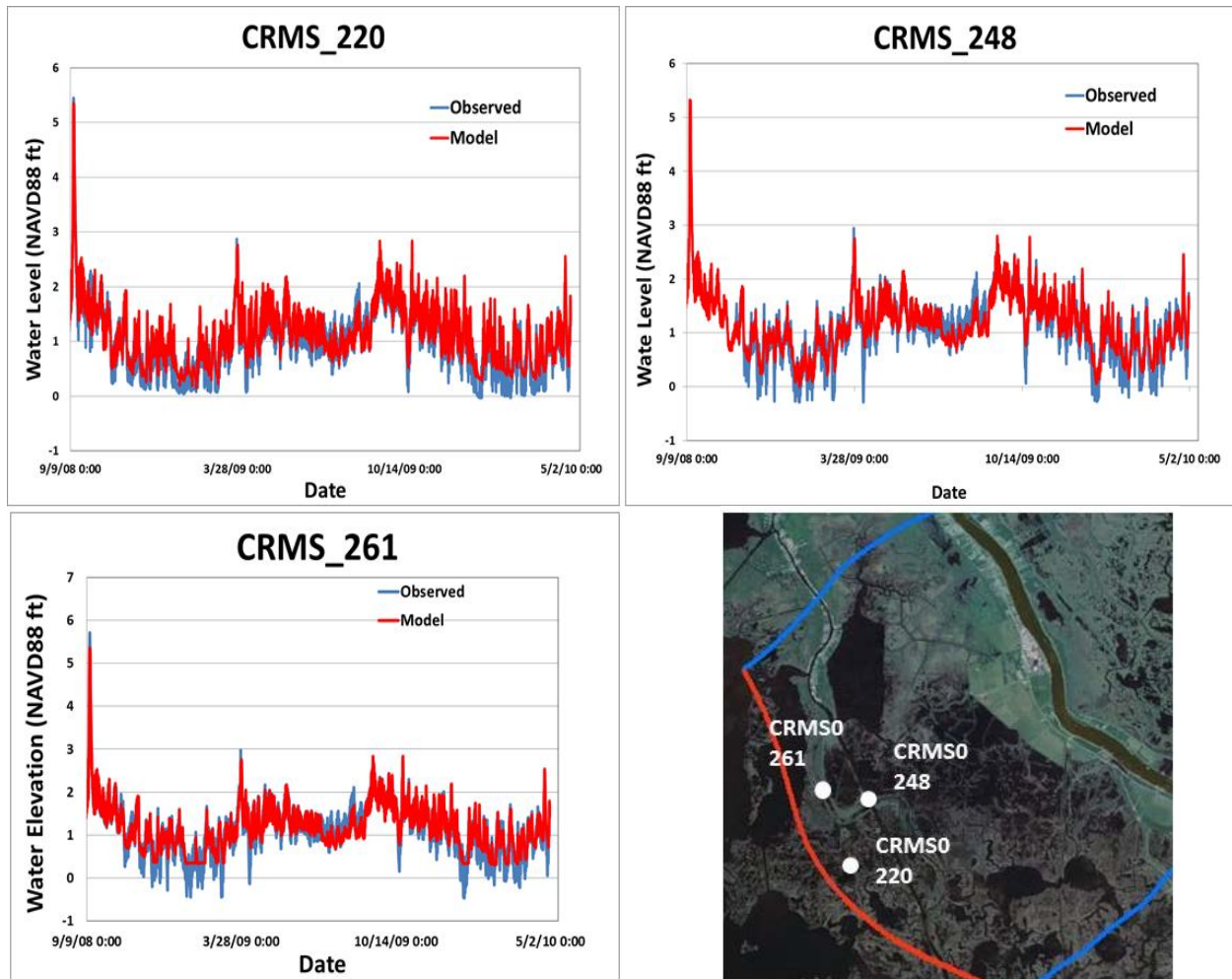


Figure 17. Receiving basin stage calibration (calibration stations shown in bottom right quadrant).



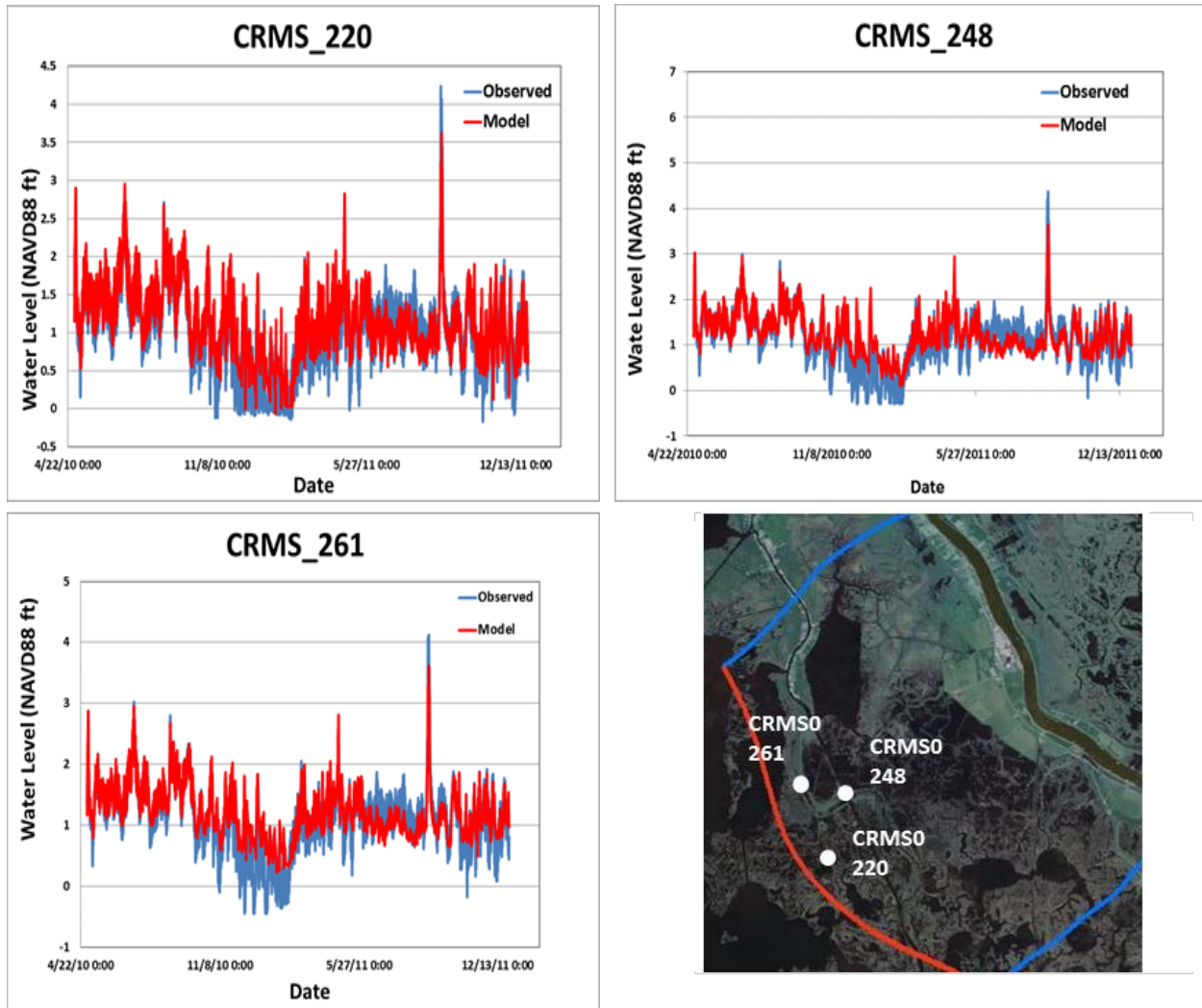


Figure 18. Receiving basin stage validation (calibration stations shown in bottom right quadrant).

Modeled Period	Average Bias (ft)	Bias % of Range	RMSE%	Corr. Coef.
Calibration Oct 2008 to Apr 2010	0.10	2%	6%	0.94
Validation May 2010 to Dec 2012	0.23	2%	8%	0.86

Table 7. Receiving basin stage calibration and validation statistical analysis.



### 1.3. PRODUCTION RUN WITH THE COMPLETE MODEL – ALTERNATIVE 1 – 75,000 CFS

The Delft3D analysis was based on the previous analysis performed for the West Bay Sediment Diversion by the Water Institute and its collaborators. Since detailed substrate information (e.g. soil erodibility) is not available for the outfall area, some of the model parameters and setup were defined in a similar manner to the West Bay modeling effort. The West Bay model was calibrated and validated against measurements of the diversion evolution (flow diverted, morphological changes) over the 10 years that the diversion has been open; as such, it was used as an analogue to obtain reliable settings for the Mid-Barataria diversion model. The model grid resolution ranged from 10 m-by-10 m in the outfall channel and intake area, to 100 m-by-200 m closer to the outer boundaries of the modeled outfall area. Figure 19 indicates the model domain, grid, and boundaries.

The surface (i.e., bathymetry and design structure, Figure 20) used in the simulations includes the following information:

- An approximate 5,000 ft (1,500 m) reach of the Mississippi River, the 30% design diversion channel, and 1 mi<sup>2</sup> (2.6 km<sup>2</sup>) of outfall into Barataria Basin provided by HDR. Two different designs were provided:
  - Alternative 1 – Version 1: 75,000 cfs diversion
  - Alternative 2 – Version 1: 50,000 cfs diversion
- An approximate 8 X 8 mile (13 X 13 km) area (centered on the outfall of the diversion channel) detailed surface of Barataria Basin including bathymetric information for channels provided by HDR
- A full Barataria Basin surface that has less bathymetric detail and is based on the most recent NOAA Digital Elevation Model (DEM) data
- USACE multibeam data collected in 2012 for the Mississippi River bathymetry beyond the 5,000-foot (1,500 m) reach provided by HDR



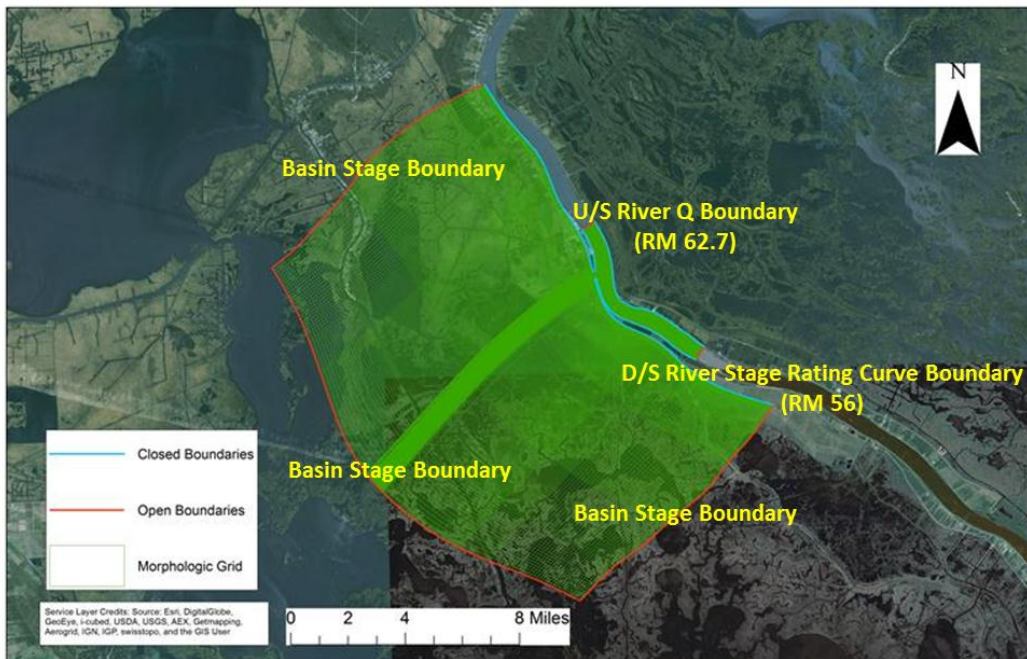


Figure 19. Production runs model domain, grid, and boundaries.

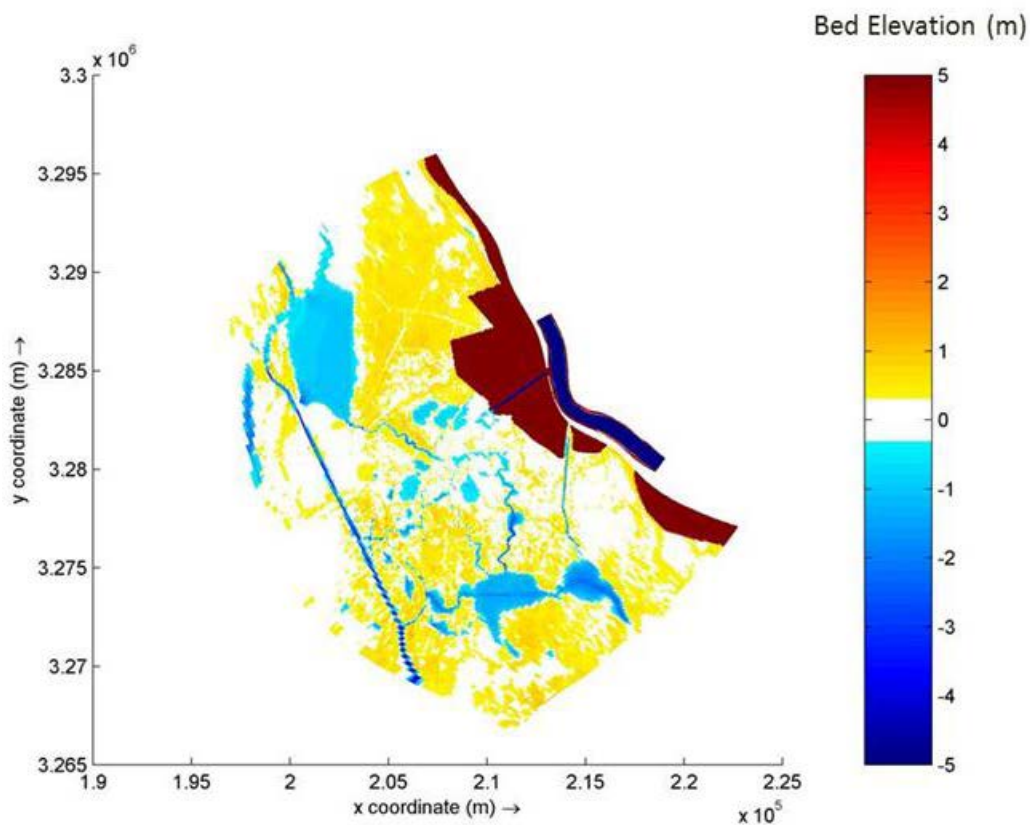


Figure 20. Production runs: Alternative 1 - model initial bathymetry.

*Note the scale used (5 m-to-5 m) was selected to highlight the water bodies and channels present.*



The Barataria Bay soil properties were based on soil boring information provided by HDR (Figure 21). The dataset included data collected by HDR and for other restoration projects in the vicinity of the outfall area of interest.

In Delft3D, it is necessary to provide critical shear stress erosion values for the fine (clay) material. The orders of magnitude of such values were obtained based on the data provided by HDR by using the studies of Pant (2013) and Léonard and Richard (2004).

The following six size classes were used in the production run modeling:

- Sand: very fine sand ( $D_{50} = 83 \mu\text{m}$ ), fine sand ( $D_{50} = 167 \mu\text{m}$ ) and medium sand ( $D_{50} = 333 \mu\text{m}$ )
- Mud (fine material): consolidated clay ( $D < 2 \mu\text{m}$ ; high shear stress), clay ( $D < 2 \mu\text{m}$ ; low shear stress) and silt ( $2 \mu\text{m} < D < 63 \mu\text{m}$ )

Two layers of spatially uniform thickness (Figure 22) were used for the receiving basin, based on the soil borings data provided by HDR:

- A top layer of 3.3 ft (1.0 m), composed of peaty soil (clay and silt) that is easier to erode. For the clay material a critical shear stress value between 0.1 - 1.0 Pa was used.
- A bottom layer of 56.0 ft (17.0 m), composed of consolidated mud and sand that is harder to erode. For the consolidated clay material a higher critical shear stress of 5.0 Pa was assigned.

Based on the available boring data, it was concluded that the mineral portion of the peat material initially present on the surface layer of the receiving basin (Figure 22) would have an average value for the critical shear stress against erosion in the range of 0.1 - 1.0 Pa (Pant, 2013; Sanford, 2008; Léonard & Richard, 2004). That range would represent material that had a chance to consolidate as well as newly deposited material. In Delft3D it is necessary to prescribe a critical shear stress for each size-class transport in suspension or present in the bed. Because clay dominates the surface layer, its critical shear stress will be the main parameter influencing the shear strength of the receiving basin surface layer.

The exact value of critical shear stress to represent the erodibility of the substrate material continues to be a subject of research efforts within the scientific community. Using this range, however, would allow one to present the land building projections within a reasonable range of uncertainty of this critical parameter. As such, two simulations were performed:

- Simulation 1.1: Critical shear stress for erosion of clay equal to 1.0 Pa
- Simulation 1.2: Critical shear stress for erosion of clay equal to 0.1 Pa

As discussed above, the results obtained with the two simulations were used to create an envelope of values for the land building obtained over a period of 5 years. It should be noted that information regarding the substrate soil strength is quite scarce, and as such we had to rely on anecdotal information to specify the critical shear stress value. As such, we used a range of critical shear stress for the clay layer to understand the sensitivity of the results to such parameter. It is recommended that more information be gathered in the field for future phases of this project.



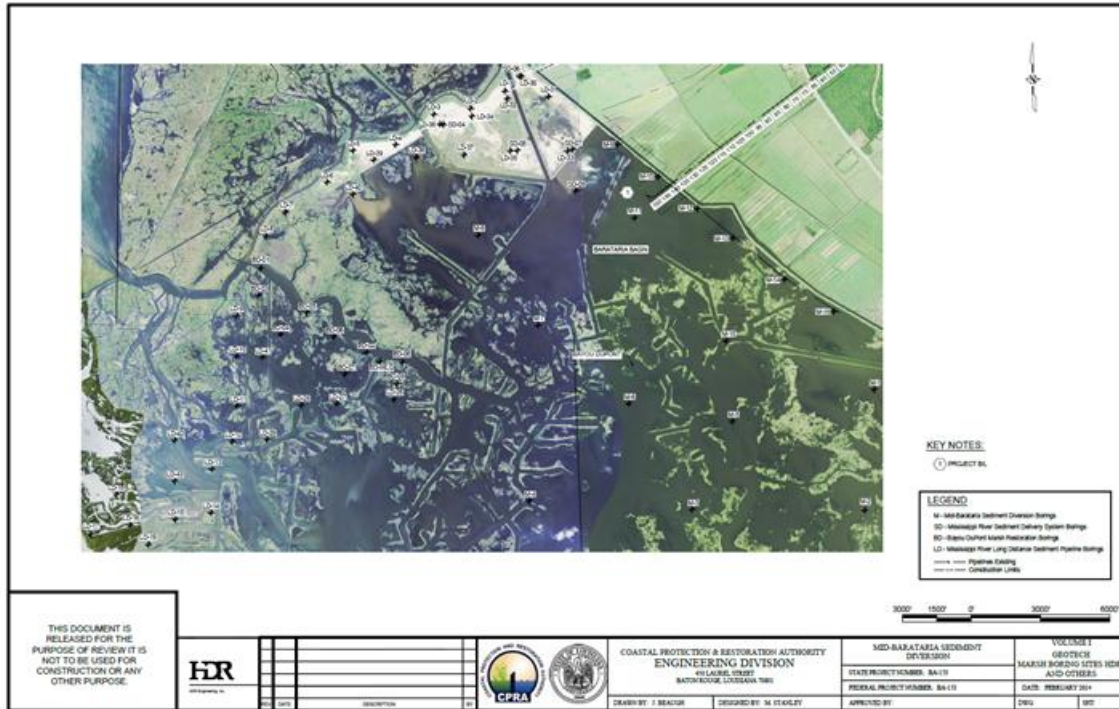


Figure 21. Locations of soil boring information provided by HDR.

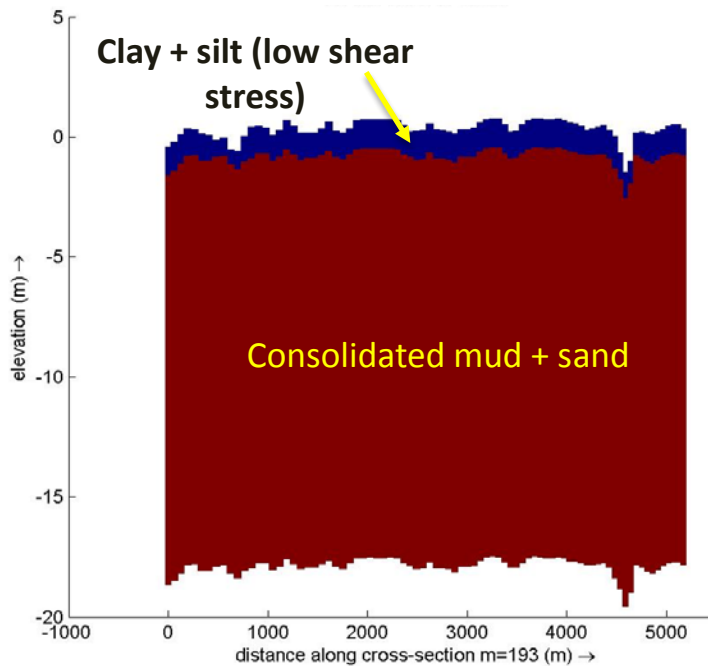


Figure 22. Vertical profile of bed thickness for receiving basin showing the two different layers of soil used.



As referred to earlier, the models were set up using the Chézy coefficient. Based on the Manning's  $n$  values provided by HDR, the following values were used:

- Main Stem: Chézy coefficient = 69
- Receiving Basin: Chézy coefficient = 50
- Outfall Channel: Chézy coefficient = 92

A 5-year hydrograph was used for this outfall area analysis. The hydrograph includes one wet year (large flood event), one dry year (small flood event), and three intermediate years. The data used to generate the hydrograph were derived from a 50-year historical data records at Tarbert Landing (USACE), and five years of suspended sediment concentration records at Baton Rouge, and Belle Chasse, Louisiana (USGS). The hydrograph was originally developed for the Mississippi River Hydrodynamic and Delta Management (MRHDM) Study. The approach to develop the hydrograph is summarized below:

- The 1954 to 2003 flow record at Tarbert Landing (Figure 23) was split into 10-year segments and flow duration curves were developed for each segment. It should be noted that the flows during the period of 1954 to 1963 were adjusted to reflect the flow split at the Old River Control Structure and to maintain consistency with the remainder of the hydrograph duration.
- These curves were used to obtain 10 mean flood discharge events for each 10% bin of the duration curve. An example is presented in Figure 24.
- For the discharge downstream of the Bonnet Carré Spillway, the maximum flow was limited to 1,250,000 cfs.
- The duration curves of the simplified discharge hydrographs were developed to be consistent with the duration curves of measured hydrographs (Figure 25)
- Sediment load duration curves developed for the 5-year simplified hydrograph were developed to be similar to the estimated sediment load for the measured hydrograph (based on Belle Chasse and Baton Rouge rating curves, described earlier in this document). An example is presented in Figure 26 and Figure 27.
- The average fine and sand loads used for the simplified 5-year data are also similar to the estimate loads obtained by applying the rating curves to the 50 years of flow measured at Tarbert Landing.
- The hydrograph has:
  - Two peaks per year. One of the peaks occurs in March and the other in May
  - Average annual number of days with  $Q > 600,000$  cfs between 100 and 120 days



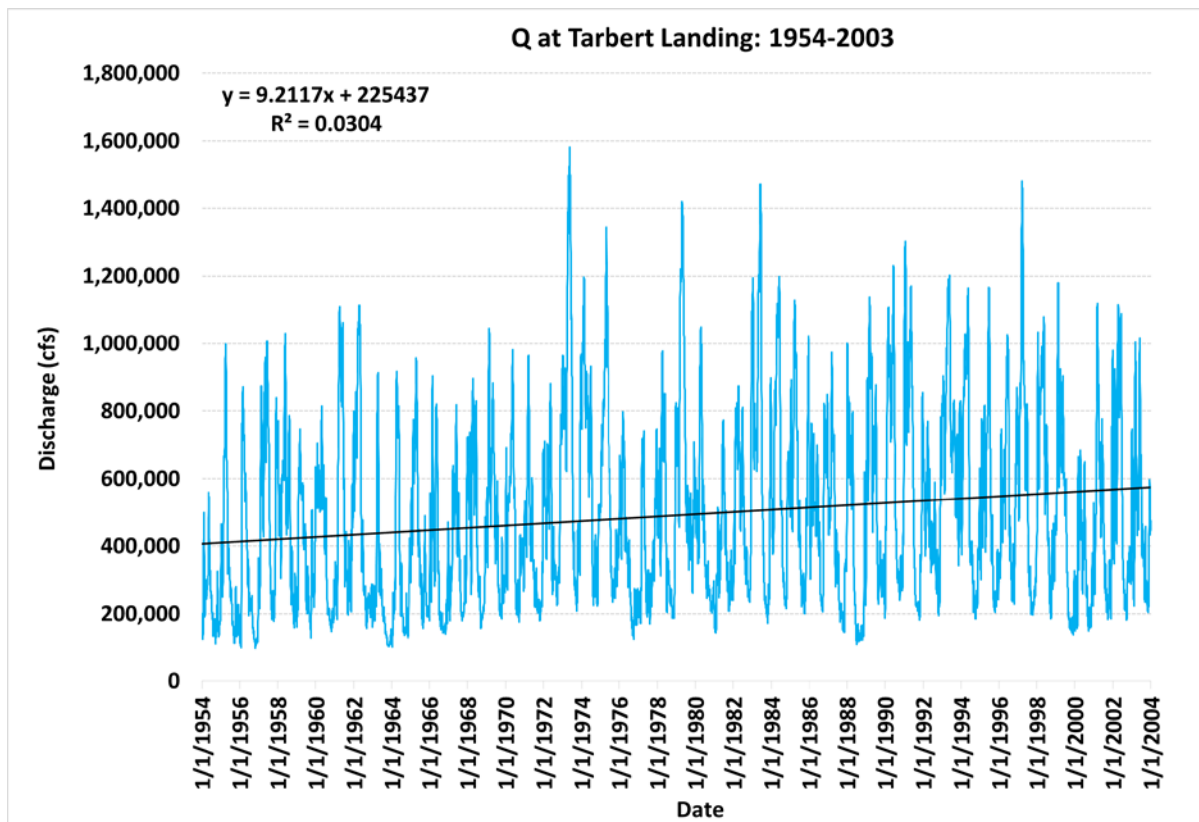


Figure 23. Flow at Tarbert Landing: 1954-2003.

The boundary conditions prescribed for stage and wind in the river and receiving basin are as follows:

- River D/S stage: Rating curve of stage versus flow based on flow measurements at Belle Chasse (USGS) and stage results at RM 56 obtained with a Mississippi River 2-D regional model that covers from RM 138 to the Passes for the period 2008 to 2012. It should be noted that sea level rise and subsidence were not considered in these simulations due to the short duration considered here (5 years). For future phases of the project where long term simulations (~ 50 years) will be performed seal level rise and subsidence should be included.
- Receiving basin stage: Time-series of the average value for each day of the year calculated based on CRMS data for the period 2008 to 2012.
- Wind data from NOAA station 8762482 at West Bank 1, Bayou Gauche were used to derive spatially uniform wind boundary conditions.

Preliminary runs used a simplified hydrograph that included only one peak event ( $Q > 600,000$  cfs) per year. Each peak lasted between 30 and 60 days. The results of the preliminary simulations were presented to HDR and CPRA during conference calls held on May 29 and June 16, 2014. These tests were used to assess the robustness of the model and for general troubleshooting, e.g., gate operations, numerical stability, and substrate setup in the outfall area.



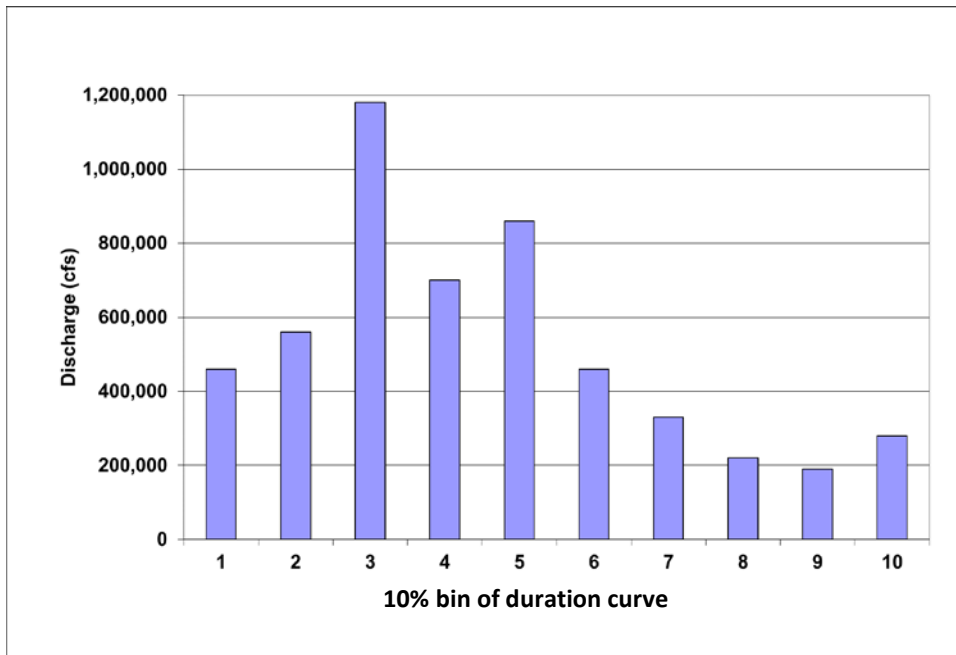


Figure 24. Histogram for 1974-1983 river discharge.

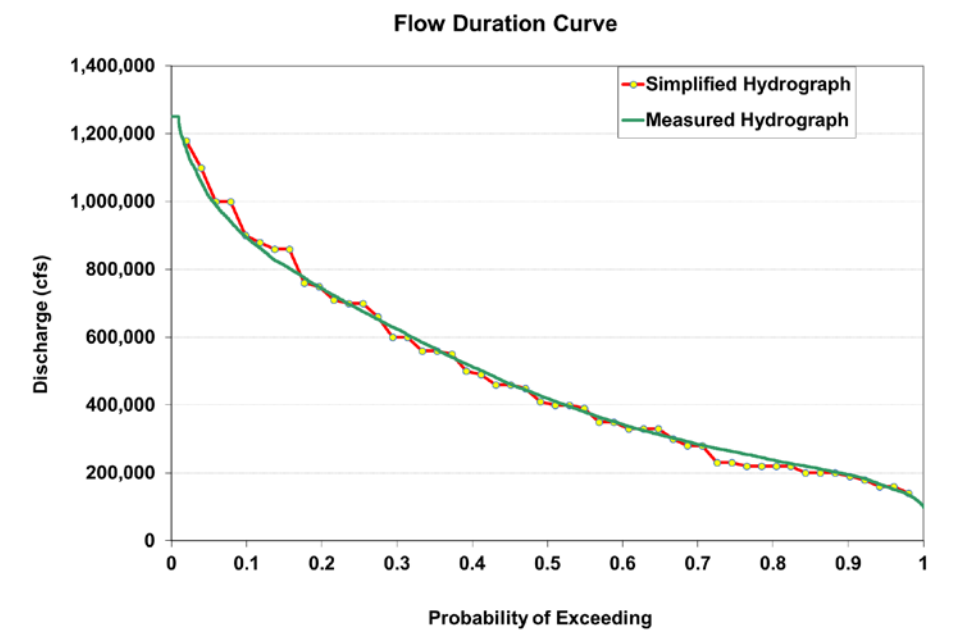


Figure 25. Flow duration curves from simplified hydrograph and measured flows at Tarbert Landing (U.S. Army Corps of Engineers, Station ID: 01100).



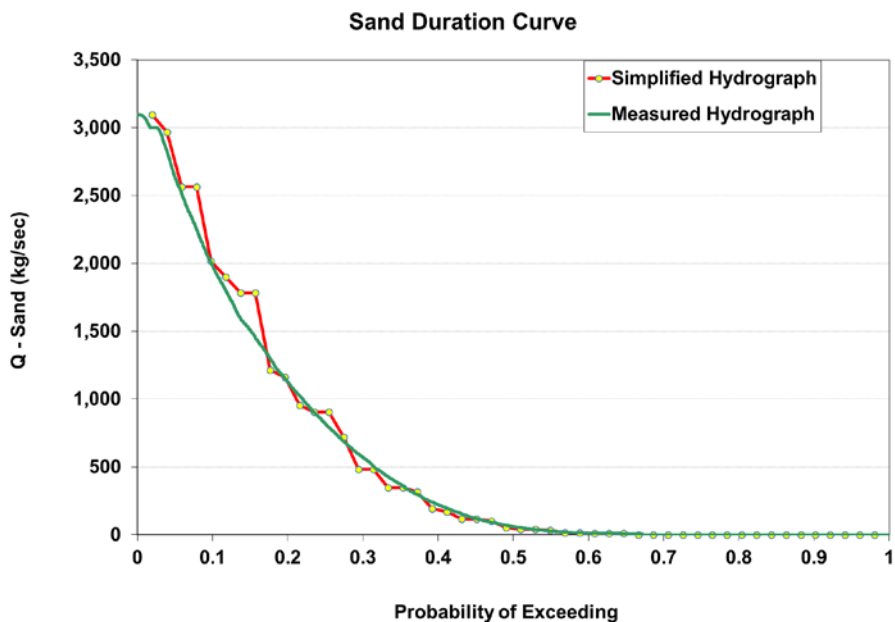


Figure 26. Sand duration curve – probability of exceeding. Comparison between simplified and estimated hydrographs based on sediment transport rating curves.

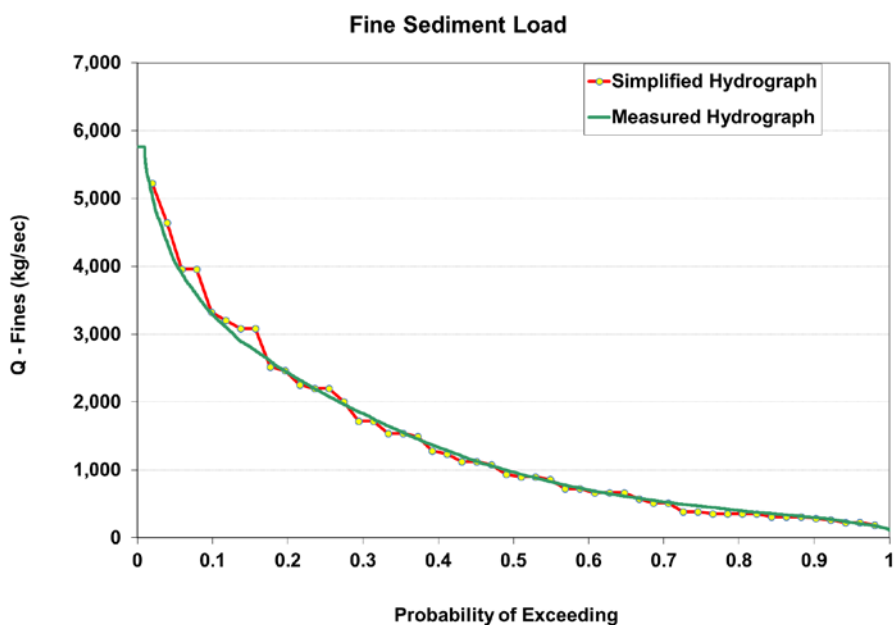


Figure 27. Fine sediment duration curve – probability of exceeding. Comparison between simplified and estimated hydrographs based on sediment transport rating curves.



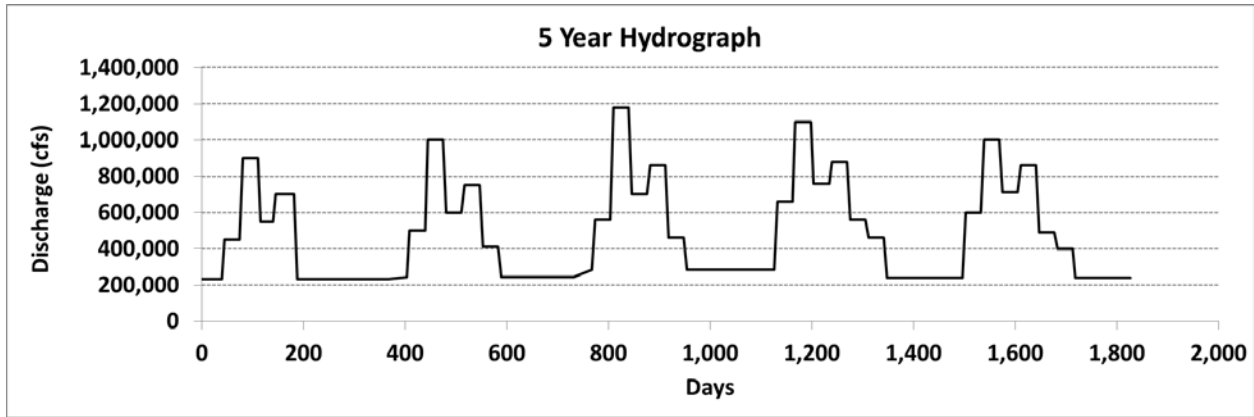


Figure 28. Five-year representative simplified flow hydrograph.



### Simulation #1.1: Critical shear stress for erosion of clay equal to 1.0 Pa

The cumulative erosional and depositional elevation change over the 5 years in the modeled receiving basin for Simulation #1.1 are presented in Figure 29. The largest erosion (deepening) values observed in the receiving basin are in the immediate vicinity of the mouth of the outfall channel, where high velocities are observed. Deposition (shoaling) is observed in the remainder of the model domain. Further, the carving of a bifurcating channel network characteristic of splay deposits in nature is visible (Figure 30).

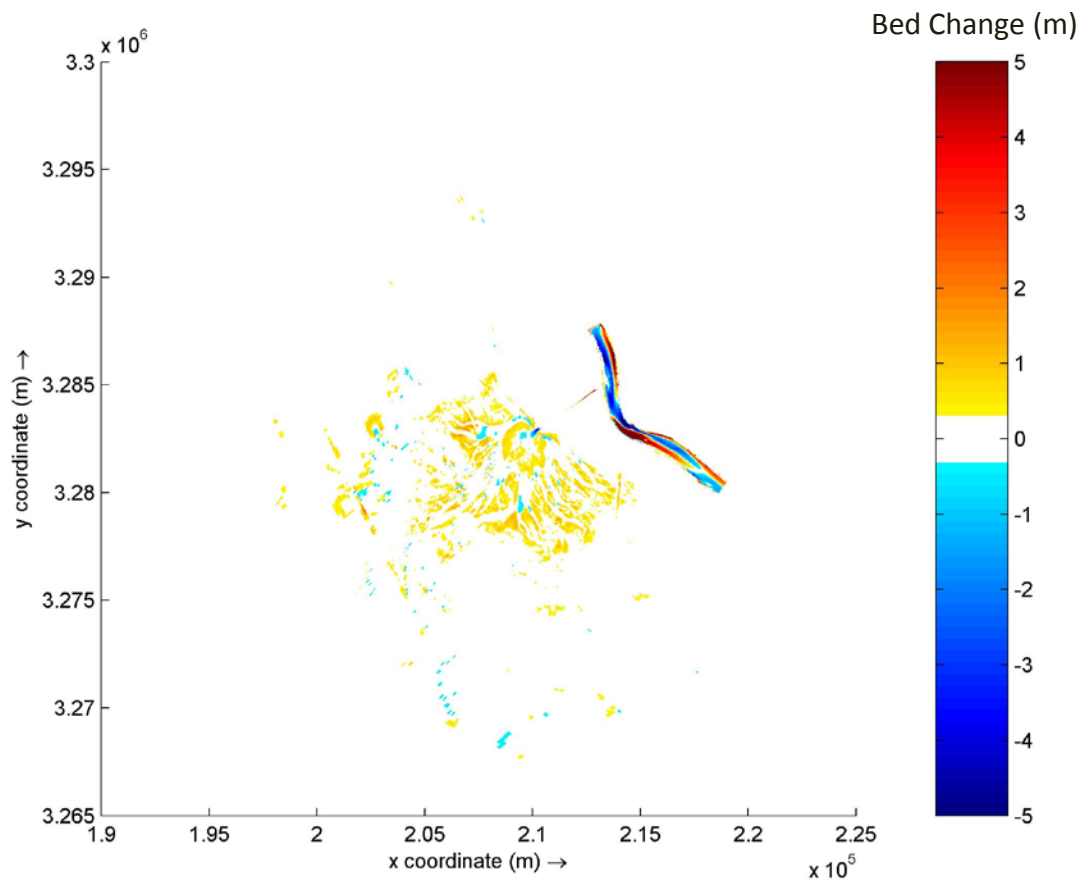


Figure 29. Simulation #1.1: Cumulative erosion and deposition after 5 years.

*Note: The initial adjustment produced in the model during Year 1 was not included in the calculations.*

Figure 30 presents a comparison between initial and final bed levels. The formation of a new channel network in the outfall area and deposition in the areas between the bifurcating channel network is apparent.

To quantify the deposition and erosion volumes, the model domain was divided into polygons. Annual deposition and erosion volumes were then calculated for each polygon (Figure 31). Polygon C shows the largest deposition volume while polygon J shows persistent erosion throughout the 5 years.



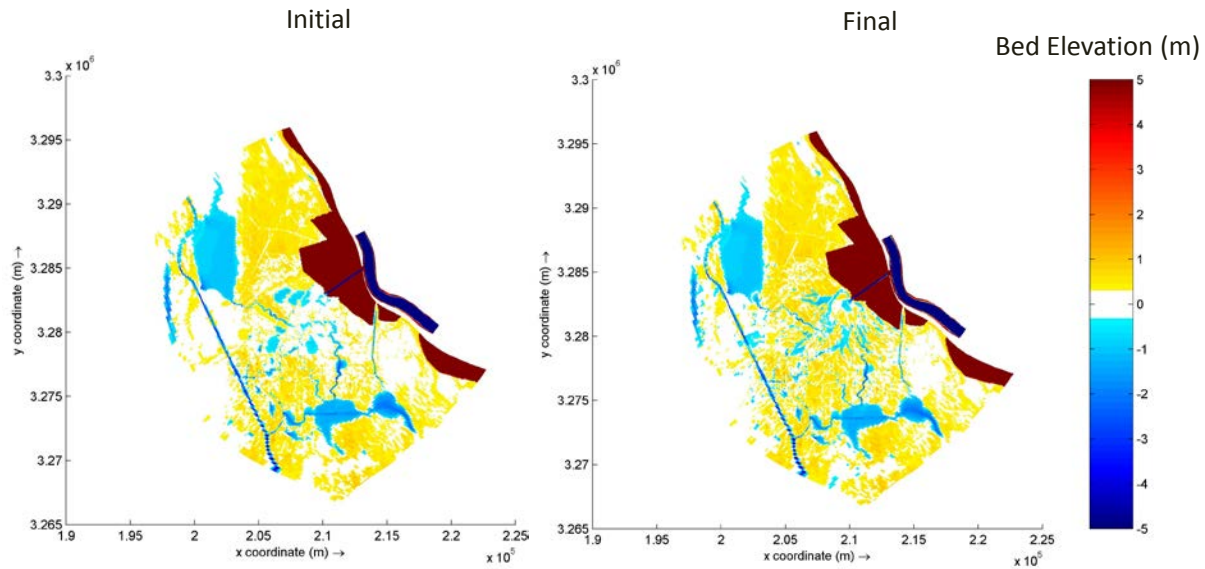


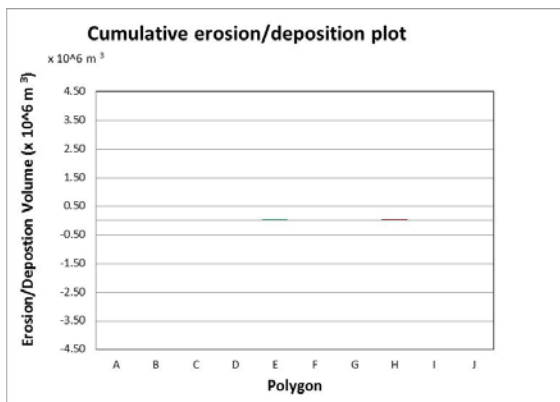
Figure 30. Simulation #1.1: Initial bed level (left panel) and Year-5 bed level (right panel).

*Note: The initial adjustment produced in the model during Year 1 was not included in the calculations.*

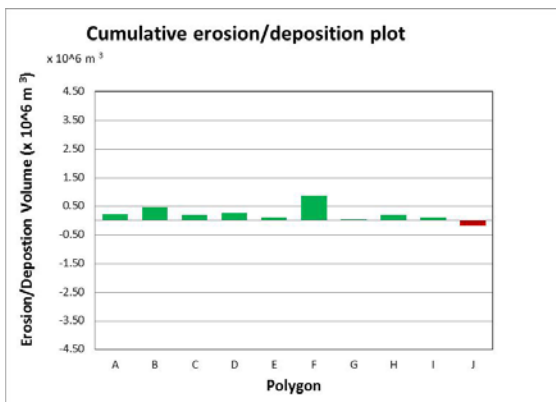
The cumulative volume change over the 5 years for each polygon is shown in Figure 32. It can be seen that the largest deposition volume occurred in polygon C, while the only erosional polygon is J. The erosion registered in polygon J is more likely due to a boundary effect than due to an actual physical process. Polygons G, H, I and J will likely produce results less reliable than the other polygons due to their proximity to the model boundaries. A net deposition volume of approximately 13.6 million  $\text{m}^3$  occurs over the 5-year modeling period.



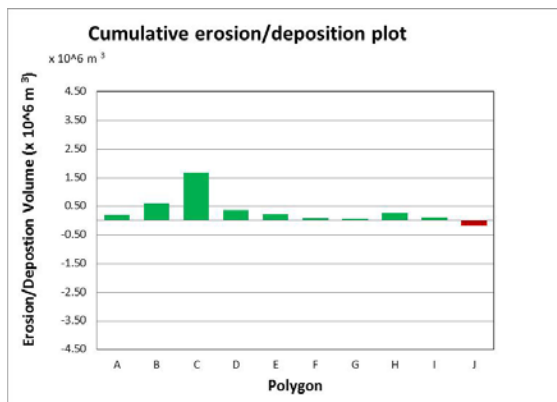
Year 1



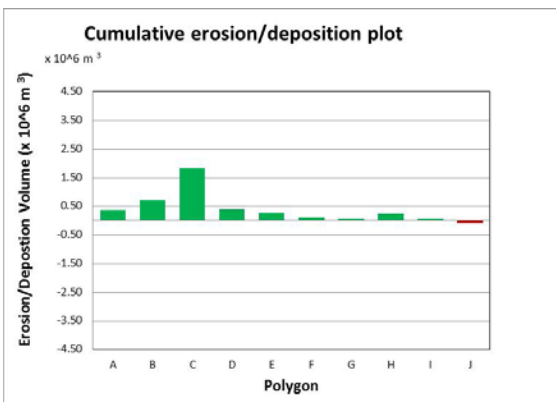
Year 2



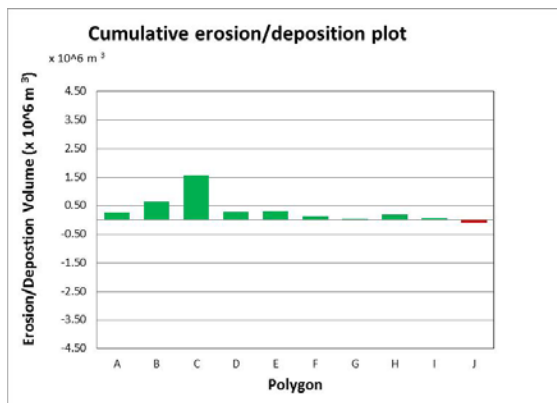
Year 3



Year 4



Year 5



Polygons

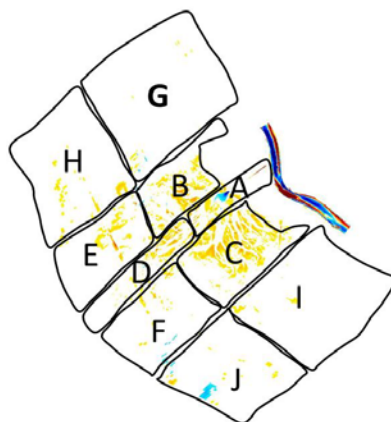


Figure 31. Simulation #1.1: Annual erosion and deposition volumes.

Note: The initial adjustment produced in the model during Year 1 was not included the calculations.



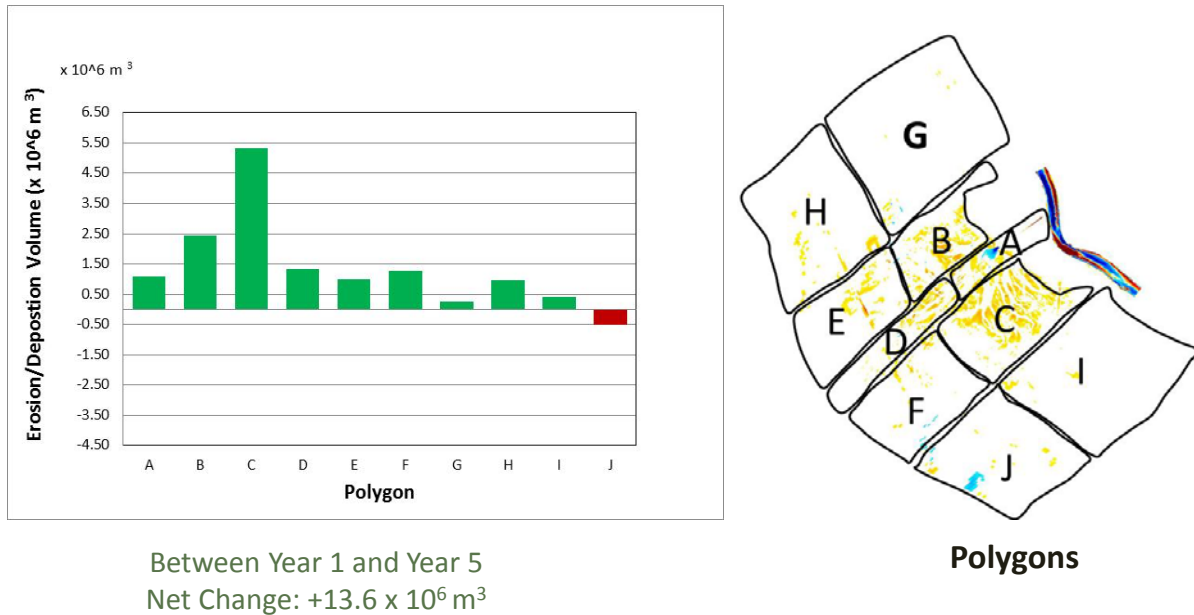


Figure 32. Simulation #1.1: Cumulative erosion and deposition volumes for the 5-year simulation.

*Note: The initial adjustment produced in the model during Year 1 was not included in the calculations.*

The calculation of how much sediment enters and leaves the receiving basin is key to developing a sediment budget and calculating sediment retention efficiency in the outfall area. Table 8 presents the retention rates by sediment size-class for Simulation #1.1. The majority of the silt remains in the basin and all of the sand is retained. As expected, clay is the size-class with the lowest retention rate (61%). Overall, approximately 87 % of the sediment diverted remains in the 8 X 8 mile proximal receiving area during the first five years. It should be noted that the period of simulation is too short to fully analyze the retention rates. As such, the rates presented below in Table 7 should not be viewed as the equilibrium (or average) retention rates.

Size-Class	Inflow (tonnes)	Outflow (tonnes)	Retained (tonnes)	Retained (%)
Clay	1,986,136	781,609	1,204,527	61%
Silt	6,009,005	568,995	5,440,009	91%
Very Fine Sand	937,383	0	937,383	100%
Fine Sand	1,342,551	0	1,342,551	100%
Medium Sand	190,241	0	190,241	100%
<b>Total</b>	<b>10,465,315</b>	<b>1,350,605</b>	<b>9,114,711</b>	<b>87%</b>

Table 8. Simulation #1.1: Retention rates by sediment size-class for the modeling period.

*Note: The initial adjustment produced in the model during Year 1 was not included in the calculations.*



### Simulation #1.2: Critical shear stress for erosion of clay equal to 0.1 Pa

The cumulative erosion and deposition change over the 5 years for Simulation #1.2 is presented in Figure 33. The highest erosion quantities occurred in the immediate vicinity of the mouth of the outfall. The formation of a network of channels is visible and overall, the channels are longer and deeper than those seen with Simulation #1.1. The lower value of critical shear stress for erosion of the substrate material used in this simulation explains the differences in the results obtained with the two simulations.

A comparison between the initial and Year 5 bed levels is shown in Figure 34. The figure illustrates the formation of new channels in the outfall area and the deposition in areas between the channels. The calculations of volume change by polygon (Figure 35 and Figure 36) confirm that more erosion occurs in the outfall area for Simulation #1.2 compared to Simulation #1.1. Also, the amount of deposition is smaller. Nonetheless, the largest amount of deposition is still recorded in polygon C, while polygon J continues to indicate erosional tendencies. The annual erosion volume decreases with time and the net volume change for the basin is again depositional and amounted to approximately 2.8 million  $m^3$  over the 5 years.

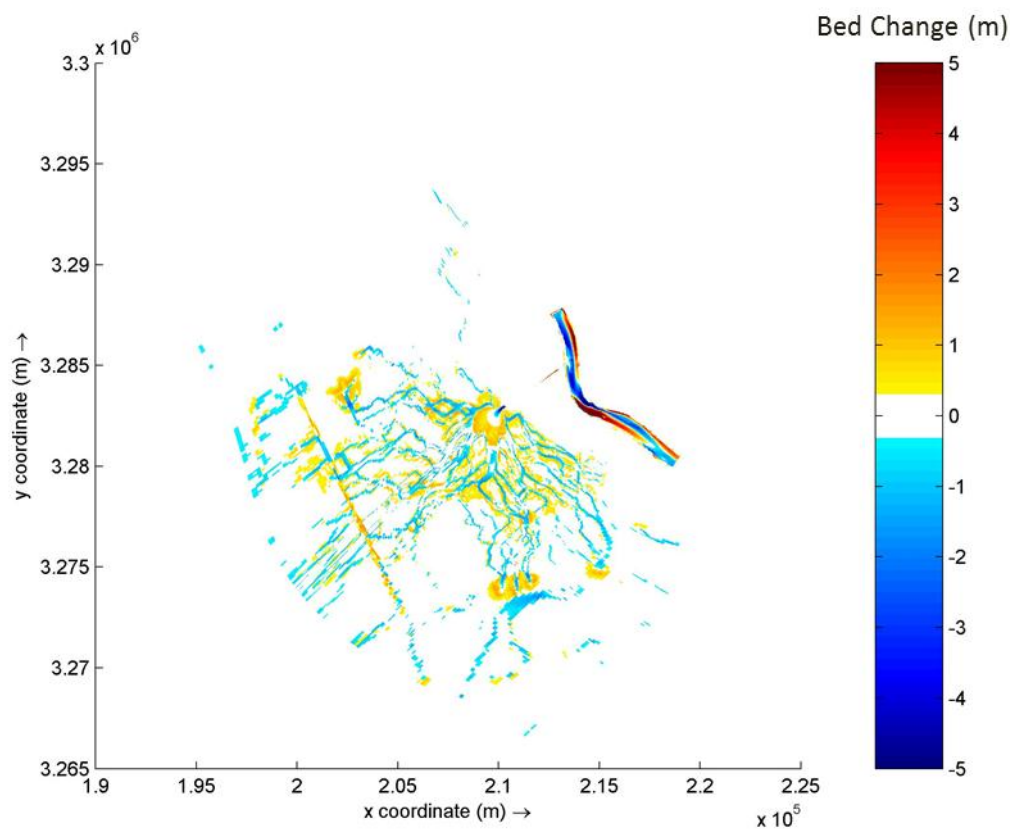


Figure 33. Simulation #1.2: Cumulative erosion and deposition after 5 years. A positive value indicates deposition and a negative value indicates erosion.



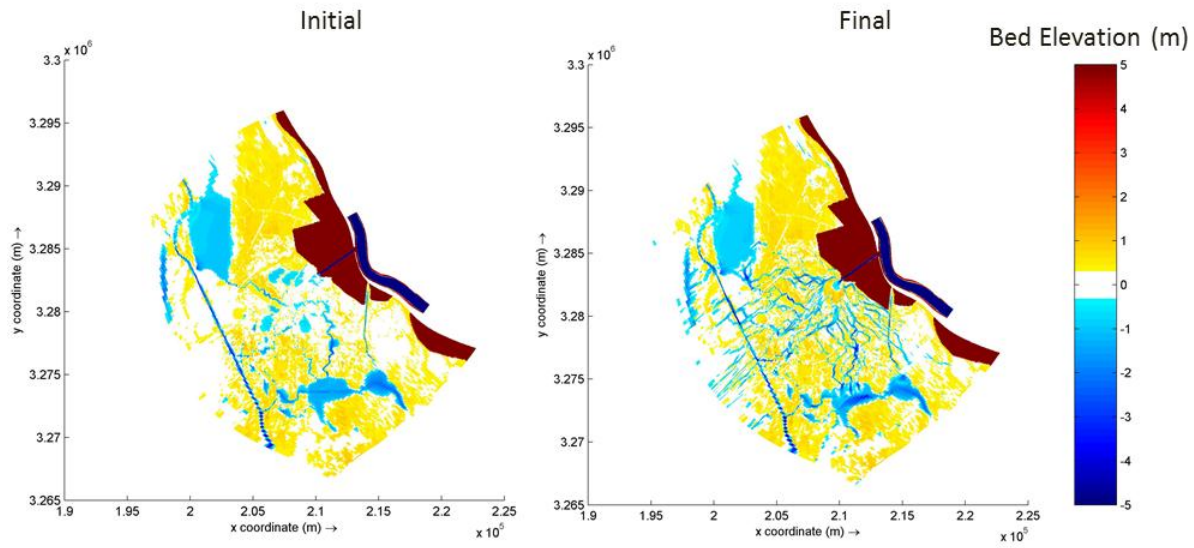
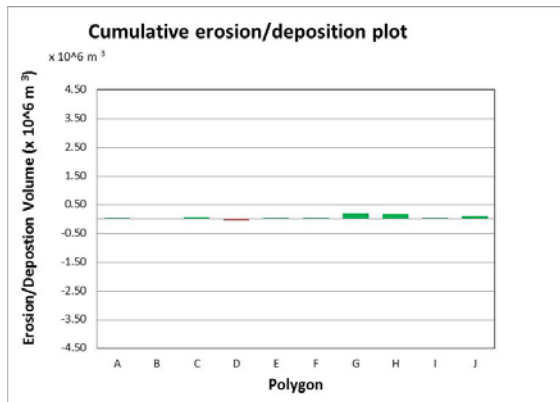


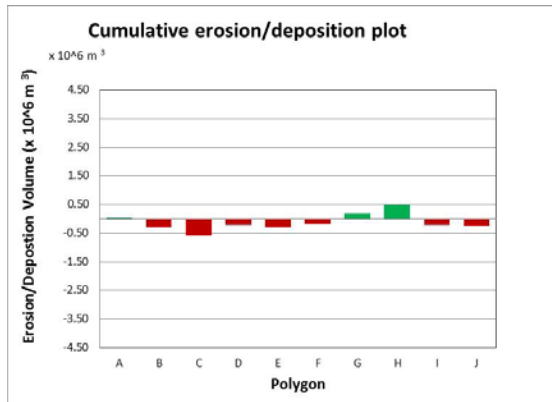
Figure 34. Simulation #1.2: Initial bed level (left panel) and Year 5 bed level (right panel).



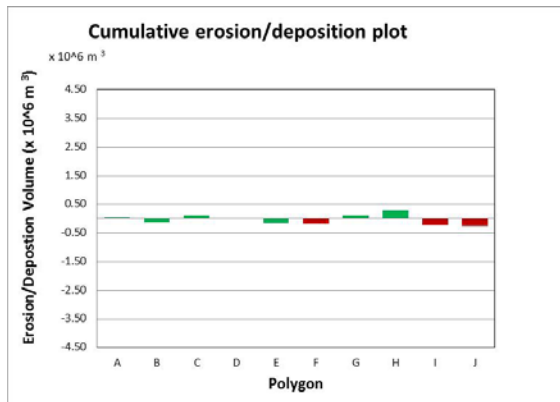
Year 1



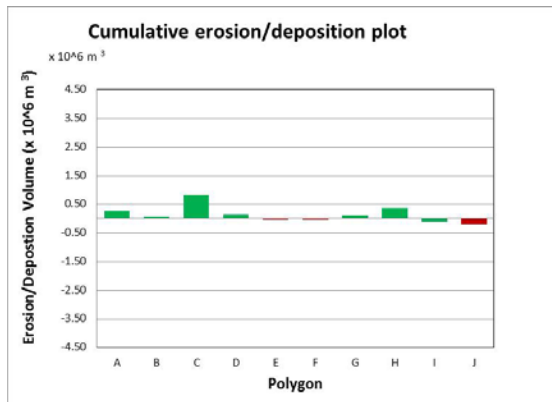
Year 2



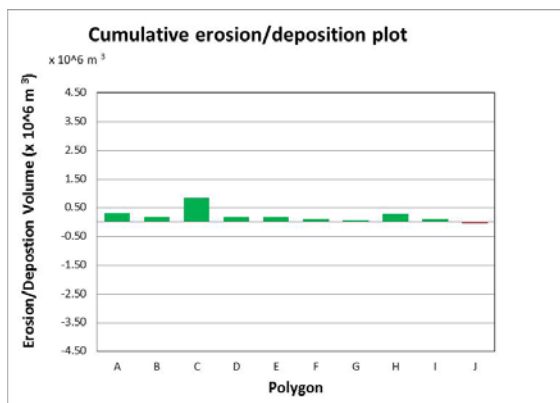
Year 3



Year 4



Year 5



Polygons

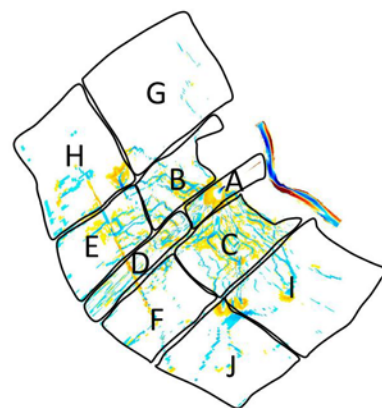
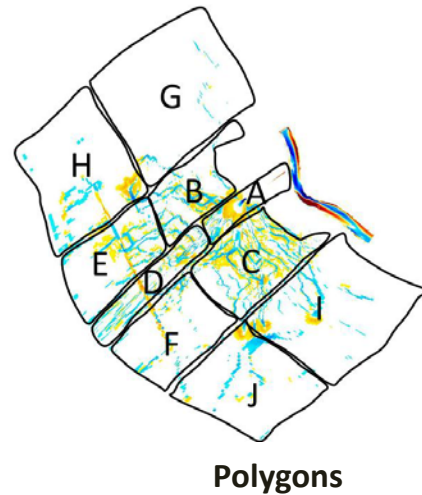
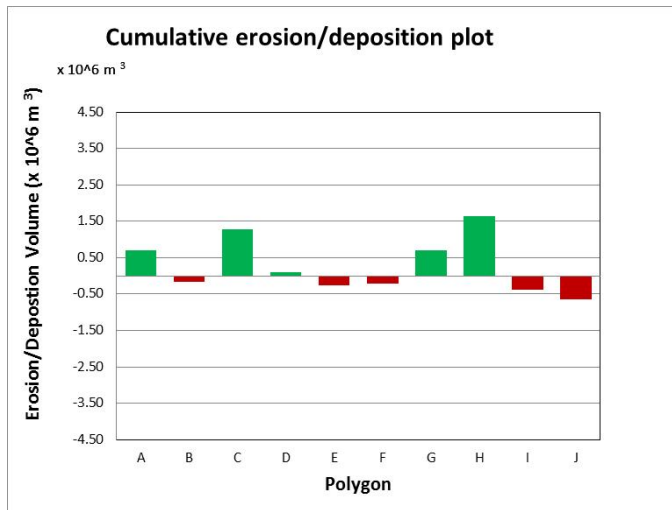


Figure 35. Simulation #1.2: Annual erosion and deposition volumes.

Note: The initial adjustment produced in the model during Year 1 was not included in the calculations.





Between Year 1 and Year 5  
 Net Change: +2.8 x 10<sup>6</sup> m<sup>3</sup>

Figure 36. Simulation #1.2: Cumulative erosion and deposition volumes.

Table 9 shows the retention rates by size-class for Simulation #1.2. The results for sand are identical to those for Simulation #1.1 with all of the sand being retained in the outfall area. The result obtained for silt is similar to the one obtained for Simulation #1.1. The major difference between the two simulations is observed for the clay. In this case, the amount of clay-sized fraction leaving the system is three times the amount of clay that enters the basin. The cause for this discrepancy in the results is the value for critical shear for erosion. Overall, about one third of the sediment diverted remains in the system during the five years modeled. As discussed before, the period of simulation is too short to fully analyze the retention rates. As such, these numbers should be considered to understand the behavior of the outfall area in the near term (5 years). Additional analysis should be performed over a longer period and using a large basin side domain to support broader scale conclusions.

Size-Class	Inflow (tonnes)	Outflow (tonnes)	Retained (tonnes)	Retained (%)
Clay	2,193,806	6,585,000	-4,391,194	-200%
Silt	6,635,990	964,446	5,671,544	85%
Very Fine Sand	1,047,097	0	1,047,097	100%
Fine Sand	1,481,491	0	1,481,491	100%
Medium Sand	203,111	0	203,111	100%
<b>Total</b>	<b>11,561,495</b>	<b>7,549,446</b>	<b>4,012,049</b>	<b>35%</b>

Table 9. Simulation #1.2: Retention rates by sediment size-class for the modeling period.

*Note: The initial adjustment produced in the model during Year 1 was not included in the calculations.*



### Comparison of Simulations #1.1 and #1.2

This section of the report focuses on additional comparisons between Simulations #1.1 and #1.2 to further understand the land building evolution in the near-field outfall area of the diversion.

Figure 37 shows the longitudinal profile of bed elevation and stage in the outfall channel and part of the receiving basin for peak flow conditions (i.e., river flow of 1,180,000 cfs). There is a head-drop in the stage from approximately 10 ft-NAVD88 on the riverside to approximately 2 ft-NAVD88 near the mouth of the outfall channel on the basin side. The water surface profiles of both simulations are similar as the bed change along the length of the outfall channel is similar. It can also be seen that the outfall channel has an adverse slope, i.e., it is deeper at the intake (river side) than at the mouth (basin side).

A longitudinal profile of velocity in the outfall channel and part of the receiving basin is presented in Figure 38. In the intake area, the velocities reach approximately 15 fps near the intake and within the rectangular portion of the outfall channel, then slow to approximately 5 fps resulting in in some accretion along the trapezoidal reach of the outfall channel.

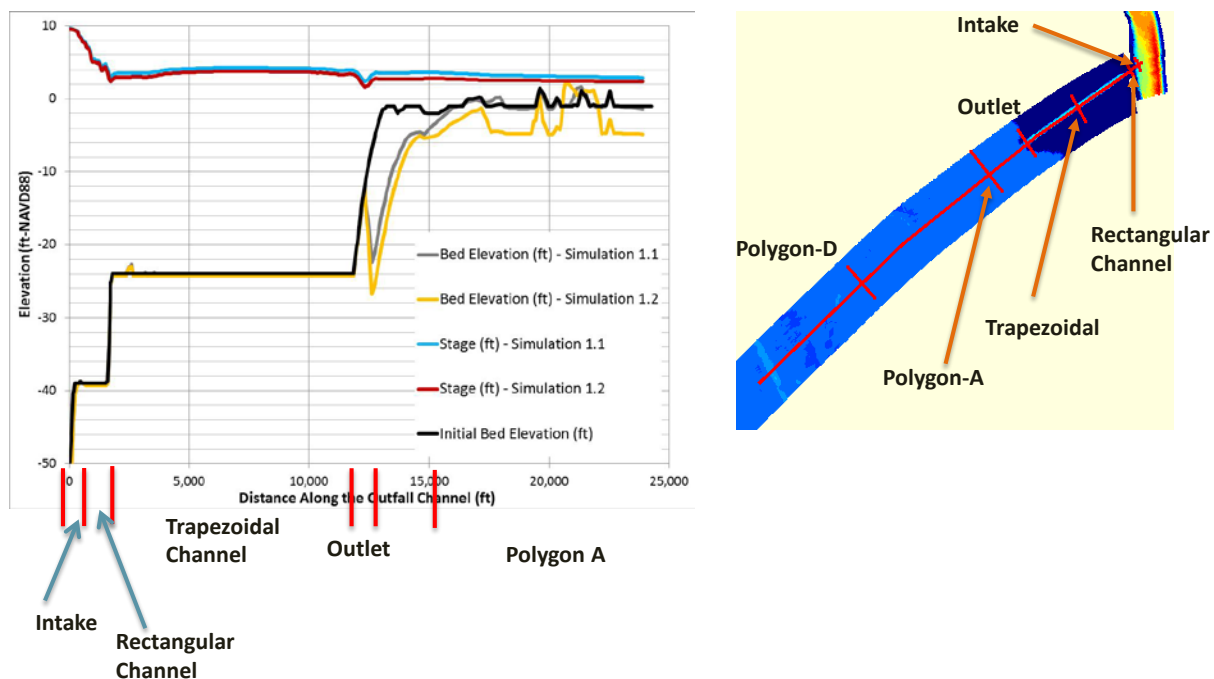


Figure 37. Simulations #1.1 and #1.2: Longitudinal profile of bed elevation and stage for peak flow (year 3;  $q=1,180,000$  cfs) - outfall channel and part of the outfall area.



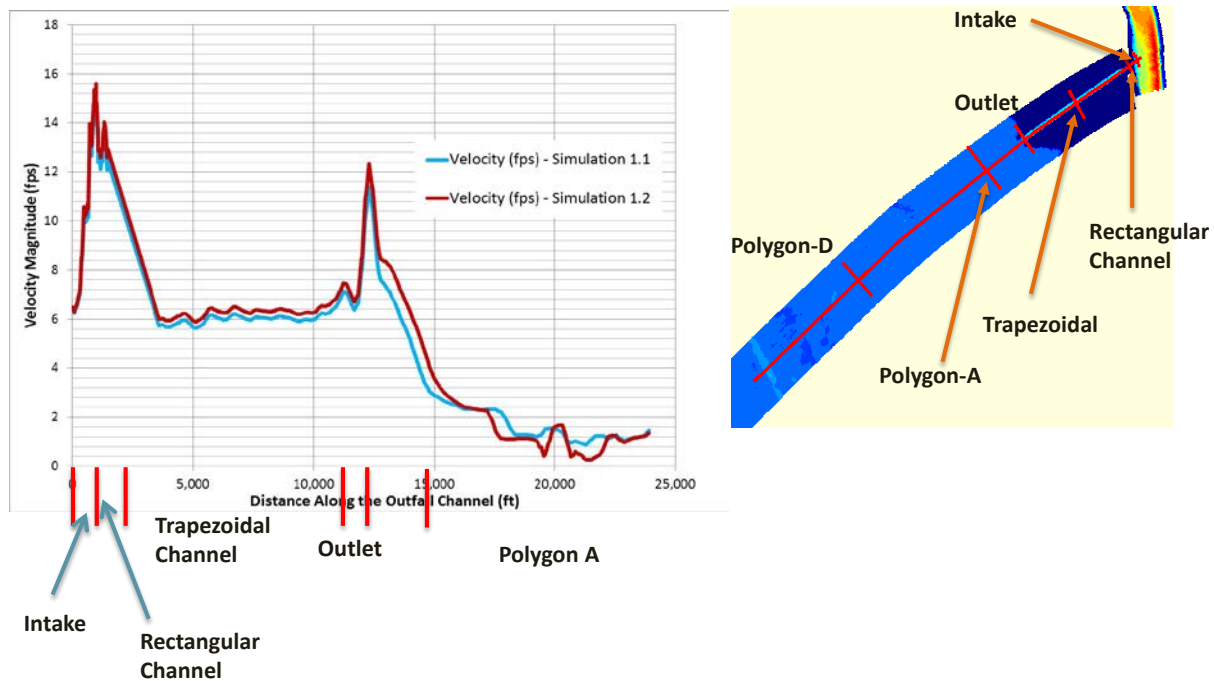


Figure 38. Simulations #1.1 and #1.2: Longitudinal profile of velocity for peak flow ( $q = 1,180,000$  cfs) - outfall channel and part of the outfall area.

The increase in the velocity magnitude near the outlet is due to the rapid decrease in flow depth (water depth in the outfall channel is much larger than the water depth in the receiving basin).

A comparison between the cumulative erosion and deposition patterns for the two simulations is presented in Figure 39. The patterns displayed are similar but as mentioned earlier, the channels formed in Simulation #1.2 are deeper and longer. The similarity between the patterns is also evident while comparing the final bed level results, shown in Figure 40.



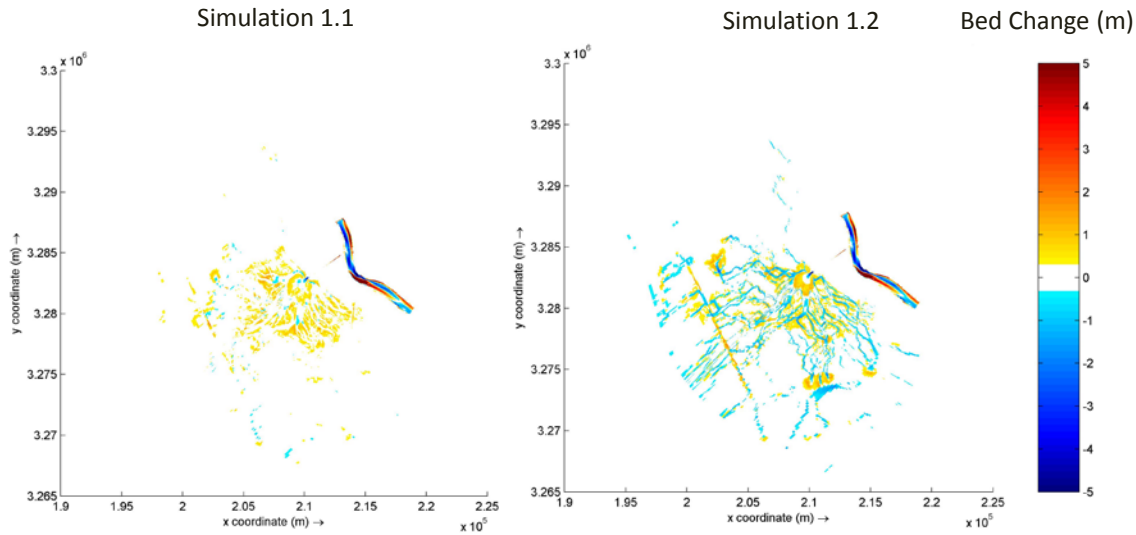


Figure 39. Simulations #1.1 and #1.2: Cumulative erosion and deposition after 5 years. A positive value indicates deposition and a negative value indicates erosion.

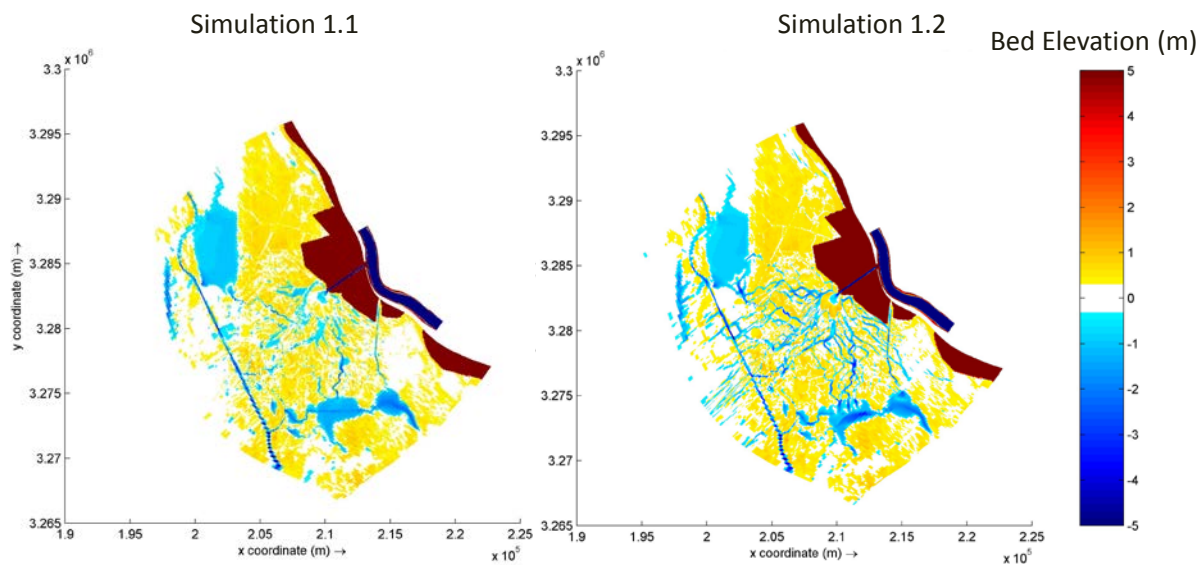
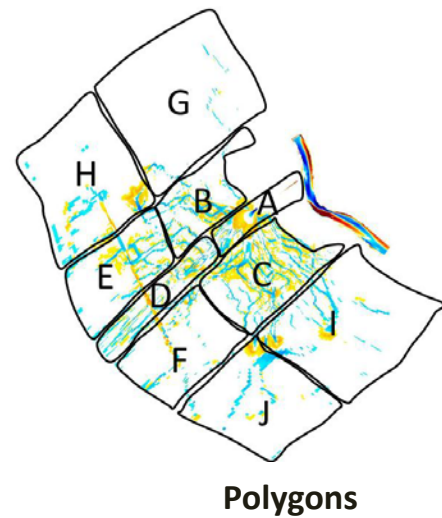
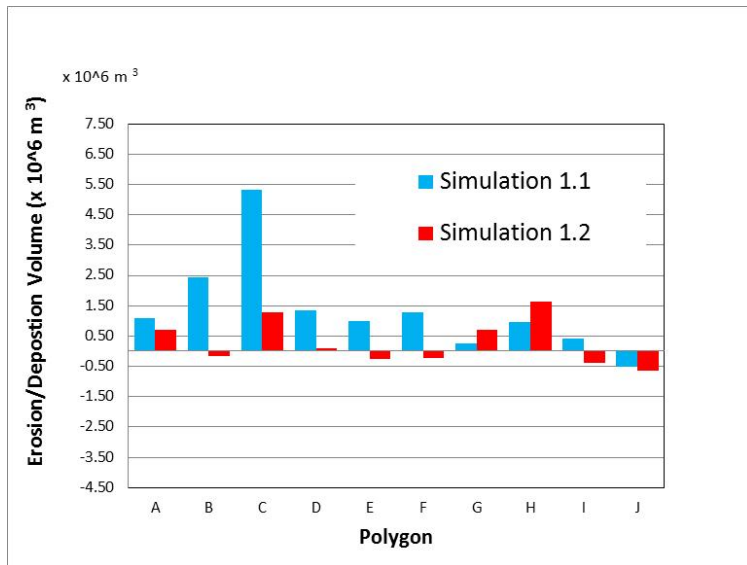


Figure 40. Simulations #1.1 and #1.2: Comparison of final bed level.

A summary of the 5-year cumulative changes by volume for each of the outfall area polygons is shown in Figure 41. Both simulations indicate that over the 5 years, deposition occurs in the outfall area and the highest amount of deposition occurs in polygon C, where also the formation of new channels is most noticeable. The results show that over the initial 5 years of operation, the net deposition volume in the outfall area ranges between 2.8- to 13.6 million  $m^3$ . Such a range could perhaps be narrowed with additional data collection of the substrate material. The annual progression of the net volume change over the first 5 years of the diversion operation is shown in Figure 42.





Between Year 1 and Year 5  
 Net Change:  
 Simulation 1.1: +13.6 x 10<sup>6</sup> m<sup>3</sup>  
 Simulation 1.2: +2.8 x 10<sup>6</sup> m<sup>3</sup>

Figure 41. Simulations #1.1 and #1.2: Comparison of cumulative erosion and deposition by polygon.

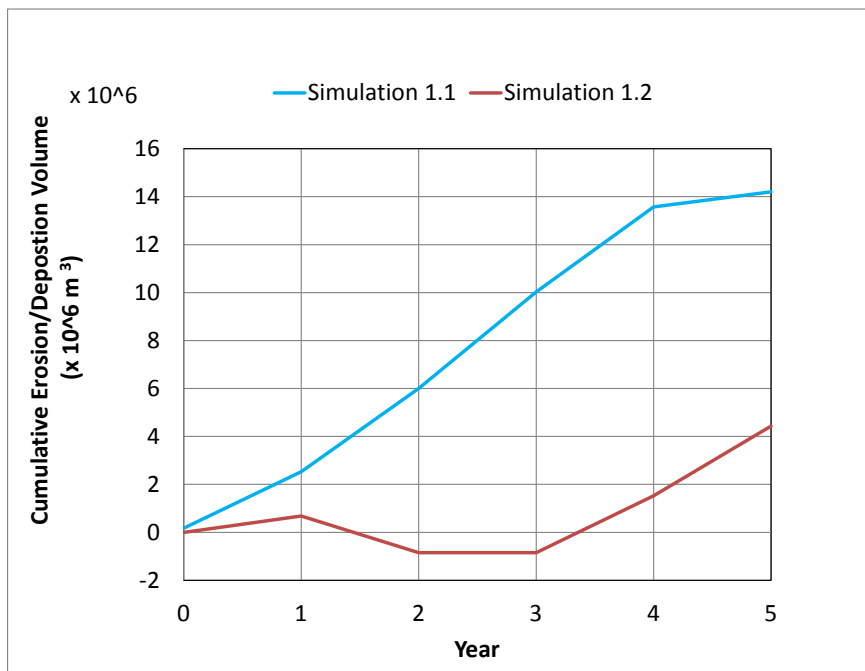


Figure 42. Annual evolution of the net volume change in the outfall area.

*Note: The initial adjustment produced in the model during Year 1 was not included in the calculations.*



Figure 43 presents the hypsometric curves of land evolution in time for the two simulations. The changes in area in the receiving basin occur for elevation values between 3 ft (1 m) and -10 ft (-3 m). For Simulation #1.1 only depositional behavior is observed resulting in a gain of land across the different elevations. For Simulation #1.2, deeper channels were carved in the receiving basin. However, land gain is seen at elevations near and above 0.0 NAVD-88. These curves emphasize the fact that both simulations show land building over the modeling period.

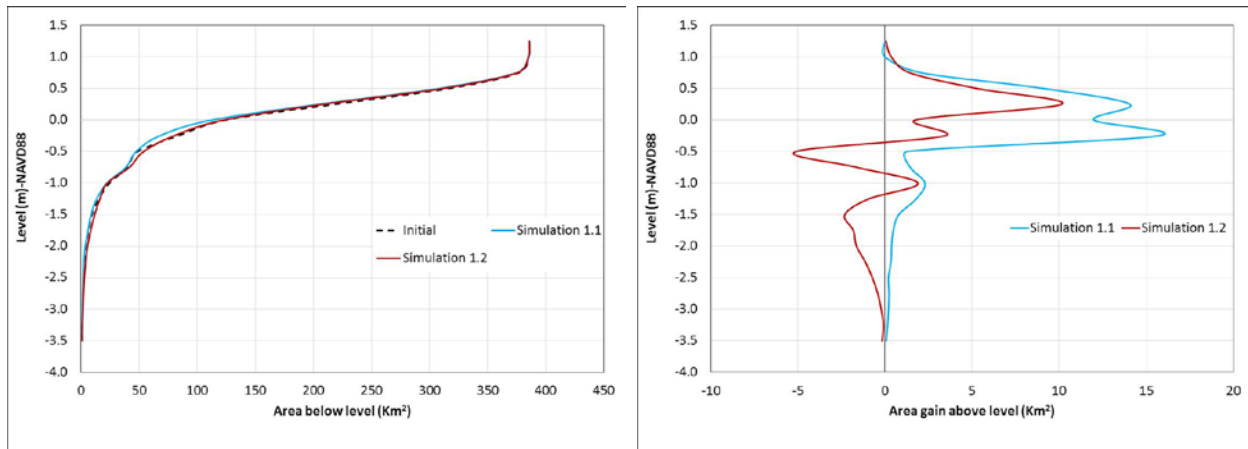


Figure 43. Hypsometric curves showing the land evolution in time.

This modeling effort could also be used to investigate the water surface elevation increase near the mouth of the outfall channel.

Figure 44 shows a comparison between the water stage time-series results obtained with the two simulations at selected locations within the outfall area. The differences between the two simulations were approximately 1.0 ft and the maximum stage (Simulation #1.1) is slightly higher than 3.5 ft-NAVD88. The typical stage during high tide in the outfall area is approximately 2.0 ft-NAVD88, meaning an increase in stage generated by the introduction of the diversion of approximately 1.5 ft is expected near the mouth of the outfall channel.



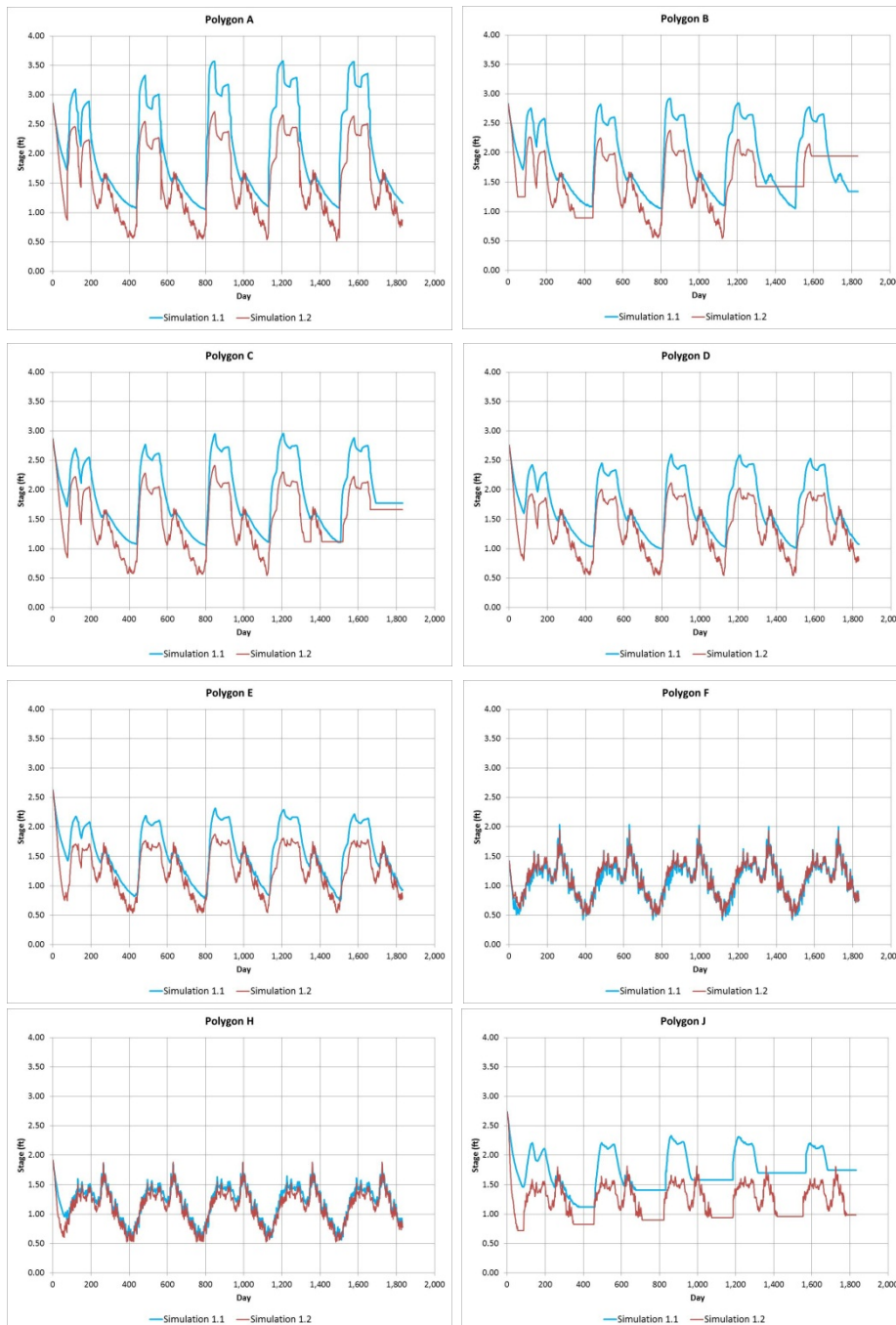


Figure 44. Simulations #1.1 and #1.2: Comparison of stage at selected polygons. The points were selected near the center of the polygons. The points were mostly in open water areas.

Finally, the sediment / water ratios (SWRs) are calculated to determine the diversion’s ability to capture sediment from the main Mississippi River channel:

$$SWR = \frac{\text{Sediment Load Diverted} / \text{Sediment Load in the River}}{\text{Water Discharged Diverted} / \text{Water Discharged in the River}}$$



Instantaneous SWR results are presented in Figure 45. There is consistency between the results obtained with the two simulations. As expected, the SWR for mud is 1.0 when the diversion is open. The SWRs for sand are around 0.6 and do not seem to vary significantly in time, meaning that the SWR for sand is the same during a 700,000 cfs flow or a 1,180,000 cfs flow. The results for sand are lower than previous estimates with the conceptual design of the diversion structure and outfall channel. The main factor that might have contributed to the difference is the variability in the tail water elevation. Further, the grid resolution used here might have contributed to some smoothing of the outfall channel geometry and, consequently, to a reduction in the diverted flows. For this 30% design work we relaxed the grid resolution to save computational time. In future phases of the project, a refined grid would be considered to determine the SWR more precisely. As such, it is recommended to evaluate the behavior generally without considering the land building projection of the SWR as final quantities. Overall, the sustained sediment capture efficiency over the five years is an important behavior that indicates that the land building taking place during the first five years has not diminished the diversion performance. It is also indicative that mechanical means to remove material may not be necessary since the performance is sustained. Longer time period should be tested to verify that the performance is sustained over longer durations.

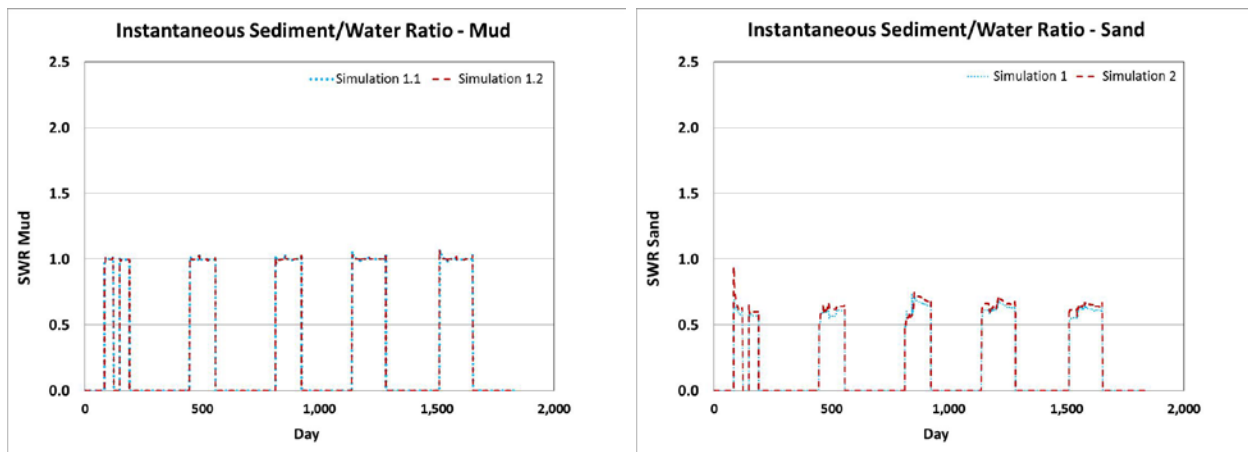


Figure 45. Simulations #1.1 and #1.2: Comparison of instantaneous SWRs.

*The calculation is performed by using a cross-section immediately above the diversion in the main stem and the rectangular cross-section area in the outfall channel.*



#### 1.4. PRODUCTION RUN WITH THE COMPLETE MODEL – ALTERNATIVE 2 – 50,000 CFS

Following the production runs for Alternative 1 (75,000 cfs diversion), production runs with an outfall channel designed to divert 50,000 cfs were also conducted. The methodology used in the model setup was identical to that followed for Alternative 1 production runs. The outfall channel geometry for the 50,000 cfs simulations was provided by HDR. All other model inputs (i.e., model coefficients, initial conditions and boundary conditions) were the same for both Alternatives 1 and 2.

The model results for Alternative 2 are presented in the same manner as they were for Alternative 1.

##### Simulation #2.1: Critical shear stress for erosion of clay equal to 1.0 Pa

The cumulative erosional and/or depositional change over the 5 year simulation for Simulation #2.1 is presented in Figure 46. The highest erosion values in the receiving basin are in the immediate vicinity of the outfall channel mouth, where high velocities are observed. Predominant change resulting from deposition is observed in the remainder of the model domain. Further, the carving of the channel bifurcation network is visible (Figure 47). These outcomes are similar to those from the Alternative 1 model runs.

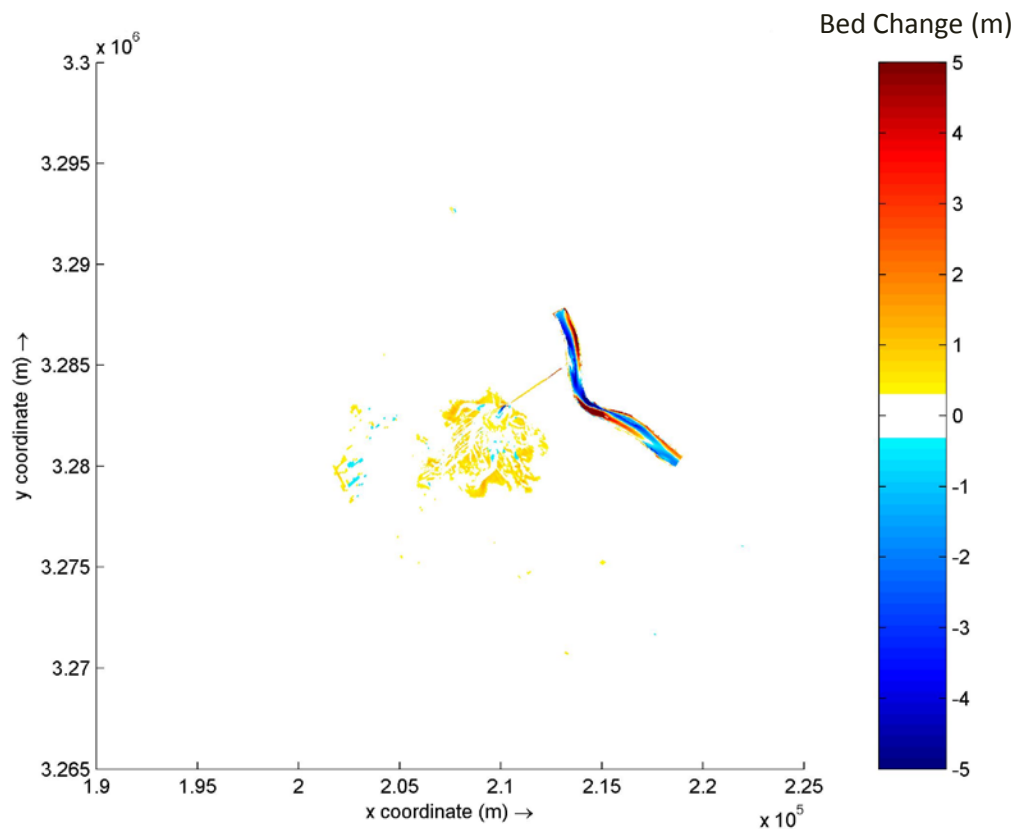


Figure 46. Simulation #2.1: Cumulative erosion and deposition after 5 years. A positive value indicates deposition and a negative value indicates erosion.



Figure 47 presents a comparison between the initial and the final bed levels. This comparison shows the formation of a new channel network in the outfall area and the deposition in the areas between the bifurcated channel network. As described previously, the model domain was divided into polygons, and annual deposition and erosion volumes were quantified within each polygon (Figure 48). Polygon C shows the largest deposition volume, and polygon J exhibits persistent erosion throughout the 5 years. Overall, the amount of erosion seems to decrease from year to year, but the rate of deposition persists. This is similar to outcomes of simulation #1.1.

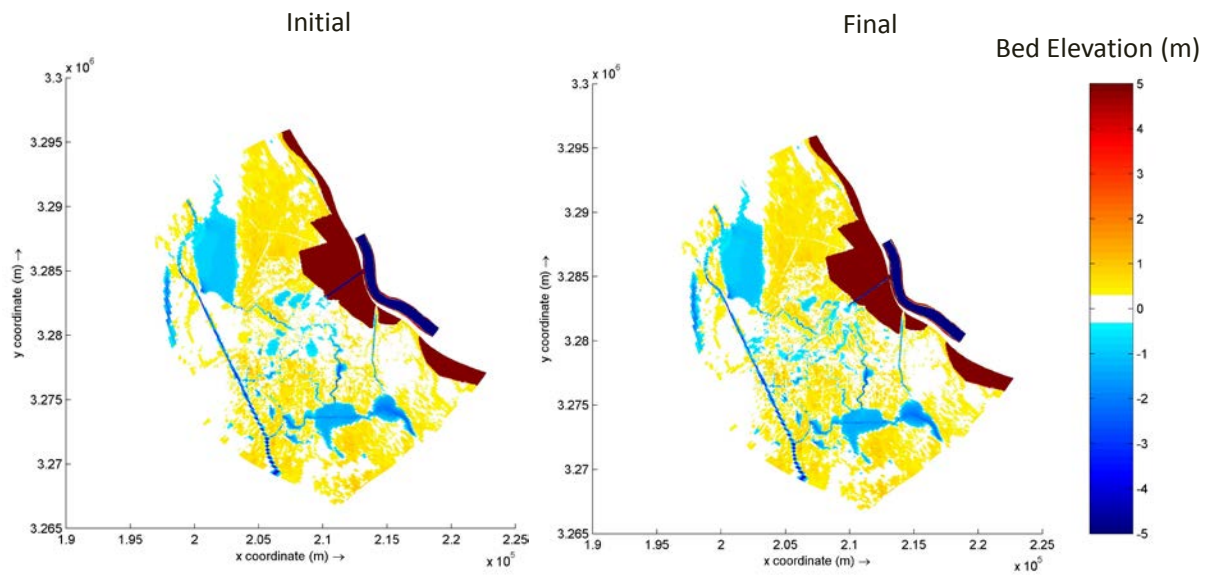
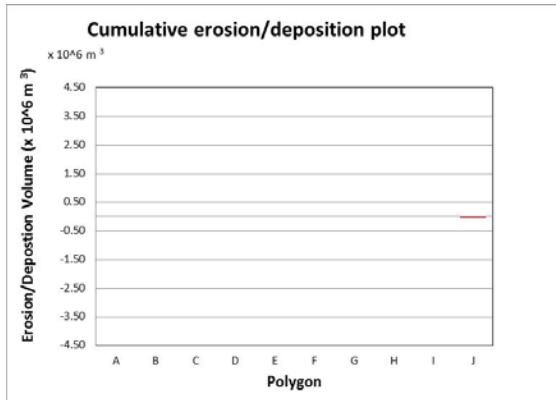


Figure 47. Simulation #2.1: Initial bed level (left panel) and Year-5 bed level (right panel).

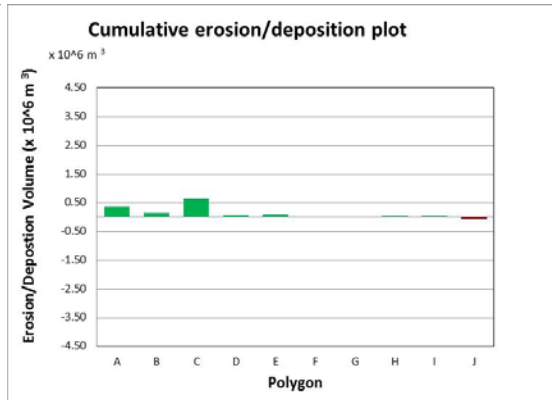
The cumulative volume change over the 5 years for each polygon is shown in Figure 49. The largest deposition volume occurred in polygon C, with a net deposition volume of approximately 7.4 million  $\text{m}^3$  over the 5-year modeling period. This value is about half of the deposition observed for simulation 1.1. (designed to divert 75,000 cfs). Polygon J was the only one with net erosion. Erosion was registered mostly in areas of open water (higher velocity values). Deposition occurred mostly in marsh areas, where velocity values are lower and sediment trapping is easier.



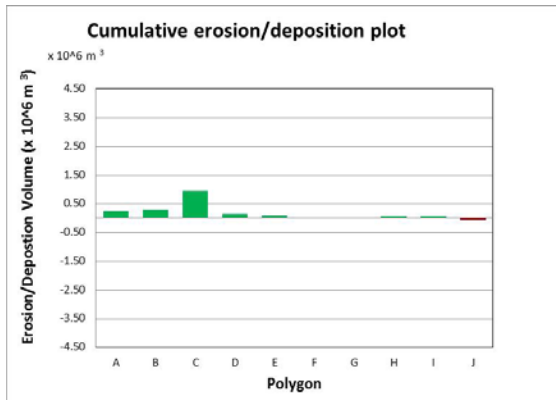
Year 1



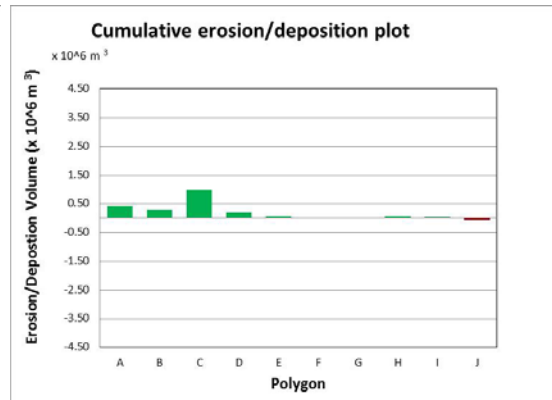
Year 2



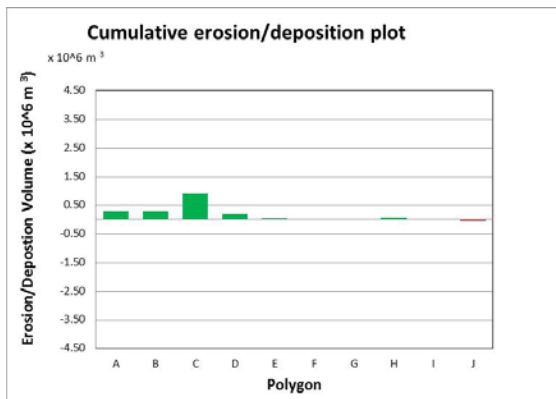
Year 3



Year 4



Year 5



Polygons

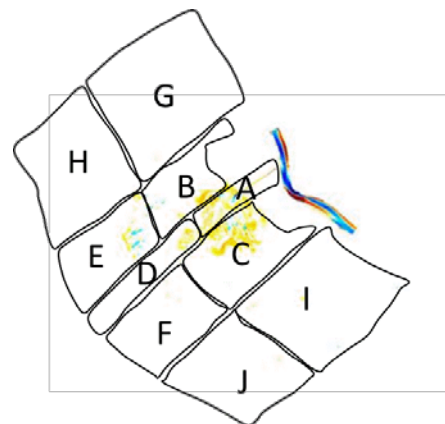


Figure 48. Simulation #2.1: Annual erosion and deposition volumes.

Note: The initial adjustment produced in the model during Year 1 was not included in the calculations.



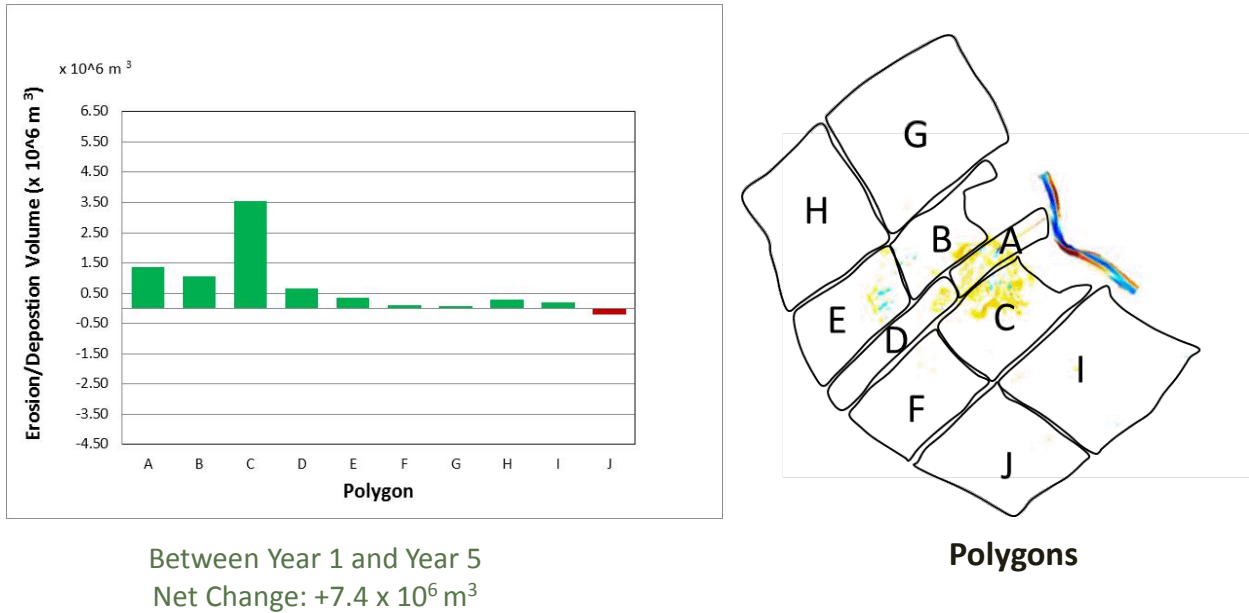


Figure 49. Simulation #2.1: cumulative erosion and deposition volumes for the 5-year simulation.

*Note: The initial adjustment produced in the model during Year 1 was not included in the calculations.*

Table 10 presents the retention rates by sediment size-class for Simulation #2.1. All of the sand is retained in the basin, as is the majority of silt (93%). As expected, clay is the size-class with the lowest retention rate (78%). Overall, approximately 91 % of the sediment diverted remains in the receiving area during the first five years. It should be noted that longer simulation periods are needed to fully analyze retention patterns and rates. As such, the retention rates presented below in Table 10 should not be considered the equilibrium (or average) rates. These results are consistent with outcomes from simulation #1.1.

Size-Class	Inflow (tonnes)	Outflow (tonnes)	Retained (tonnes)	Retained (%)
Clay	995,506	219,594	775,912	78%
Silt	3,029,887	206,483	2,823,404	93%
Very Fine Sand	417,849	0	417,849	100%
Fine Sand	479,743	0	479,743	100%
Medium Sand	47,619	0	47,619	100%
<b>Total</b>	<b>4,970,603</b>	<b>426,077</b>	<b>4,544,527</b>	<b>91%</b>

Table 10. Simulation #2.1: Retention rates by sediment size-class for the modeling period.

*Note: The initial adjustment produced in the model during Year 1 was not included in the calculations.*



### Simulation #2.2: Critical shear stress for erosion of clay equal to 0.1 Pa

The cumulative erosion and deposition change over 5 years for Simulation #2.2 is presented in Figure 50. The highest net erosion quantities occurred in the immediate vicinity of the mouth of the outfall, similar to what was observed for other simulations. The formation of a network of channels is visible, and overall the channels are longer and deeper than those seen in Simulation #2.1 output. The lower value of critical shear stress for erosion of the substrate material used in this simulation explains the differences in the results obtained with the two simulations. A comparison between the initial and Year 5 bed levels is shown in Figure 51. The figure illustrates the formation of new channels in the outfall area and the deposition in areas between the channels.

The calculations of volume change by polygon (Figure 52 and Figure 53) confirm that more erosion occurs in the outfall area for Simulation #2.2 compared to Simulation #2.1. Also, the amount of deposition is smaller. These results are logical because it is more difficult to erode sediment with a critical shear stress value of 1.0 Pa than with a value of 0.1 Pa. Nonetheless, the largest amount of deposition is still recorded in polygon C, which is consistent with what was seen for the other simulations. The annual erosion volume decreases with time, and the net volume change for the basin is again depositional, resulting in approximately 3.4 million  $m^3$  over the 5 year simulation.

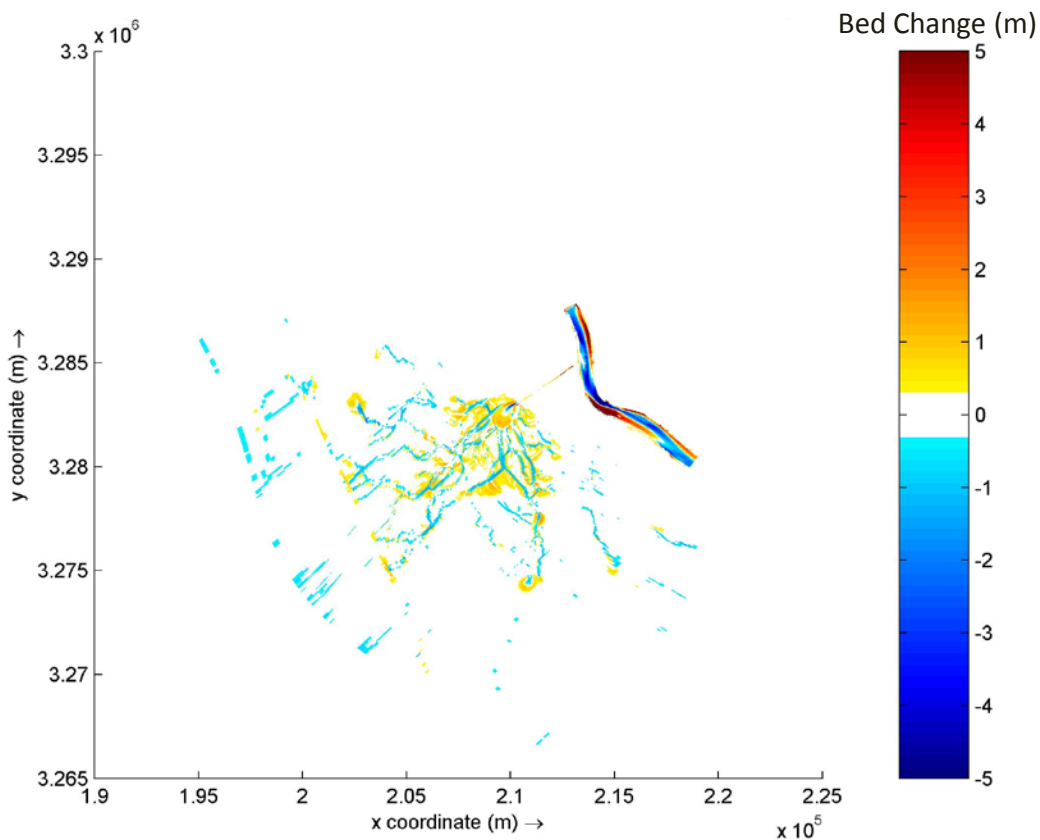


Figure 50. Simulation #2.2: Cumulative erosion and deposition after 5 years. A positive value indicates deposition and a negative value indicates erosion.



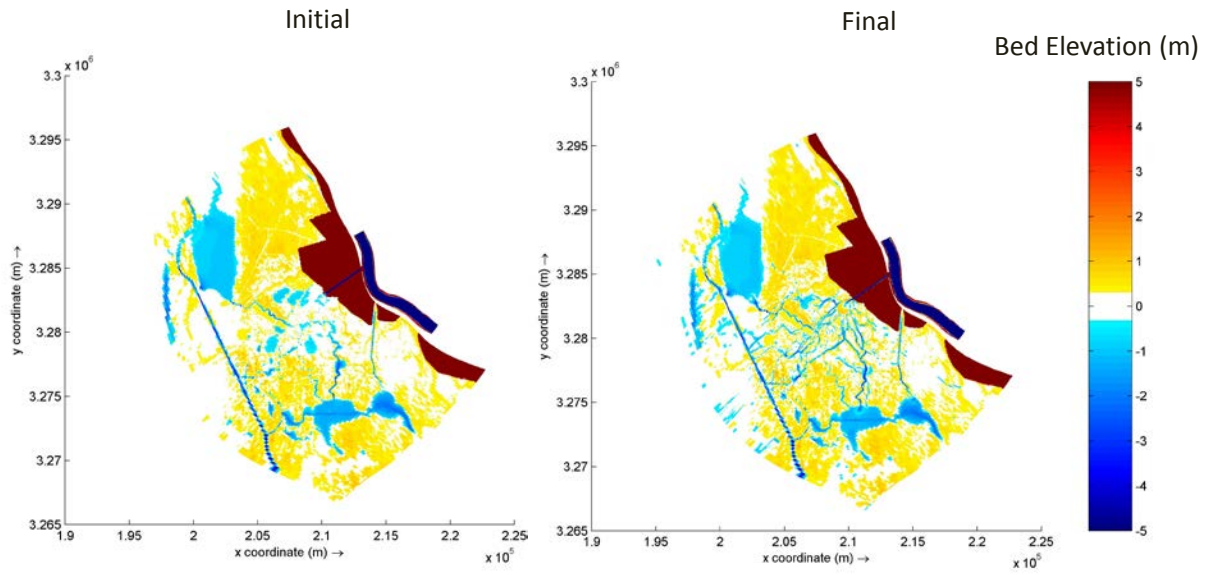
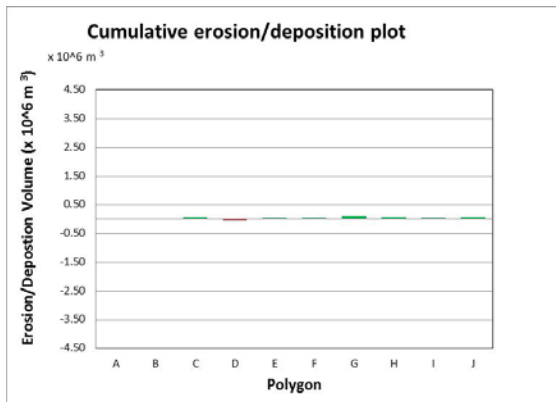


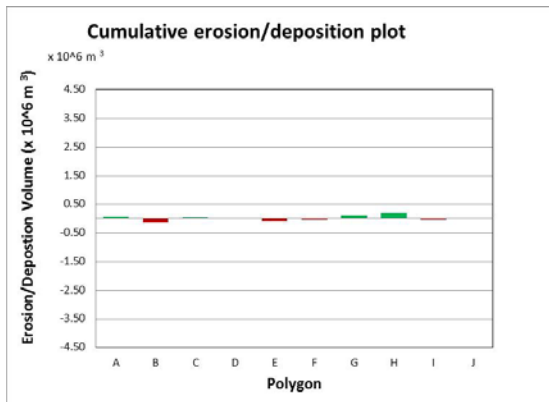
Figure 51. Simulation #2.2: Initial bed level (left panel) and Year 5 bed level (right panel).



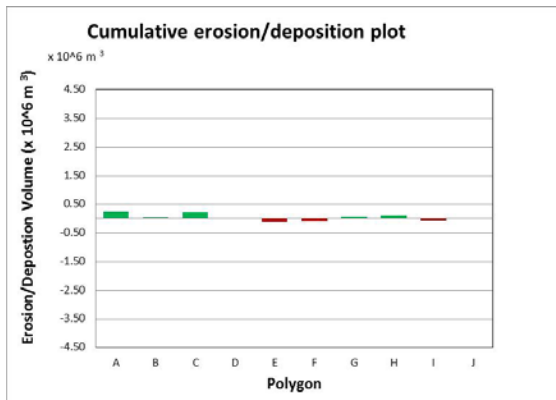
Year 1



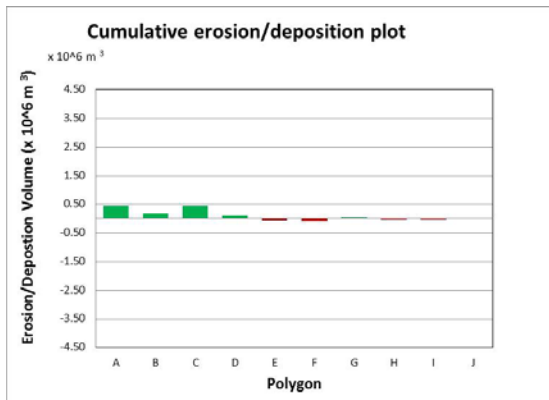
Year 2



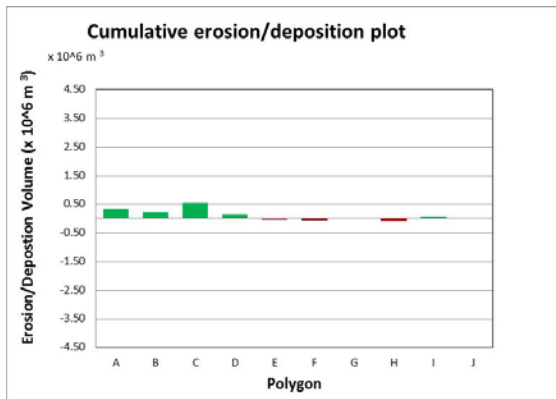
Year 3



Year 4



Year 5



Polygons

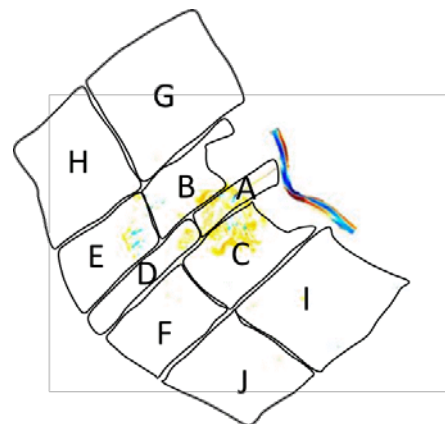


Figure 52. Simulation #2.2: Annual erosion and deposition volumes.

Note: The initial adjustment produced in the model during Year 1 was not included in the calculations.



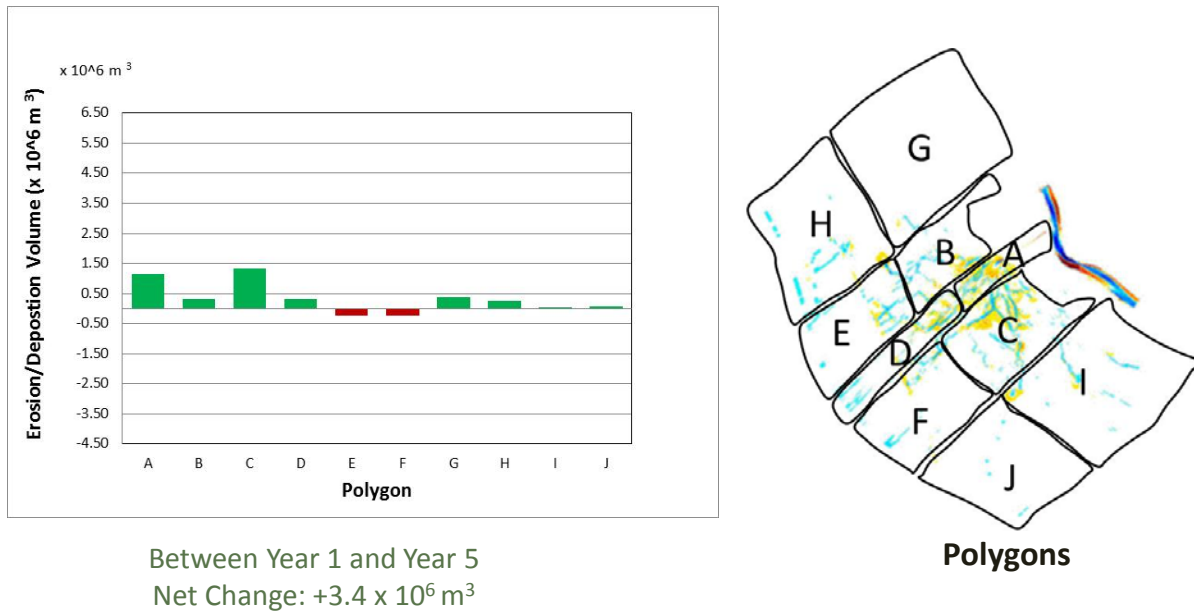


Figure 53. Simulation #2.2: Cumulative erosion and deposition volumes.

Table 11 shows the retention rates by size-class for Simulation #2.2. The results for sand are identical to those from the other simulations, with all of the sand being retained in the outfall area. The result obtained for silt is similar to the one obtained for Simulation #2.1. The primary difference between the two simulations is clay retention. In Simulation #2.2, the amount of clay leaving the system is more than 1.5 times the amount of clay that enters the basin. The cause for this discrepancy in the results (when compared to the outcomes of simulation #2.1) is the value for critical shear for erosion. Overall, about 40% of the sediment diverted remains in the system during the five years modeled. As previously discussed, the simulation period is too short to fully analyze the retention rates. As such, these outcomes should only be used to help understand the behavior of the outfall area in the near term (5 years). Additional analyses, including a longer time period and a large basin side domain would be necessary to draw any broader or longer term conclusions.

Size-Class	Inflow (tonnes)	Outflow (tonnes)	Retained (tonnes)	Retained (%)
Clay	1,054,701	2,816,332	-1,761,631	-167%
Silt	3,210,687	288,368	2,922,319	91%
Very Fine Sand	448,391	0	448,391	100%
Fine Sand	514,851	0	514,851	100%
Medium Sand	50,375	0	50,375	100%
<b>Total</b>	<b>5,279,006</b>	<b>3,104,700</b>	<b>2,174,306</b>	<b>41%</b>

Table 11. Simulation #2.2: Retention rates by sediment size-class for the modeling period.

*Note: The initial adjustment produced in the model during Year 1 was not included in the calculations.*



## Comparison of Simulations #2.1 and #2.2

This section of the report focuses on additional comparisons of Simulations #2.1 and #2.2 to further understand the short-term land building evolution in the near-field outfall area of the diversion. Figure 54 shows the longitudinal profile of bed elevation and stage in the outfall channel and part of the receiving basin for peak flow conditions (i.e., river flow of 1,180,000 cfs). There is a head-drop in the stage from approximately 10 ft-NAVD88 on the riverside to approximately 2 ft-NAVD88 near the mouth of the outfall channel on the basin side. The water surface profile and bed change along the length of the outfall channel are similar in both simulations, and the outfall channel has an adverse slope, i.e., it is deeper at the intake (river side) than at the mouth (basin side). These results are similar to those of Alternative 1.

A longitudinal velocity profile in the outfall channel and part of the receiving basin is presented in Figure 55. In the intake area, the velocities reach approximately 13 fps near the intake and within the rectangular portion of the outfall channel. They slow to approximately 3 fps and increase to about 4 fps, which results in mild deposition along the trapezoidal reach of the outfall channel. These velocity values are lower than those from Alternative 1.

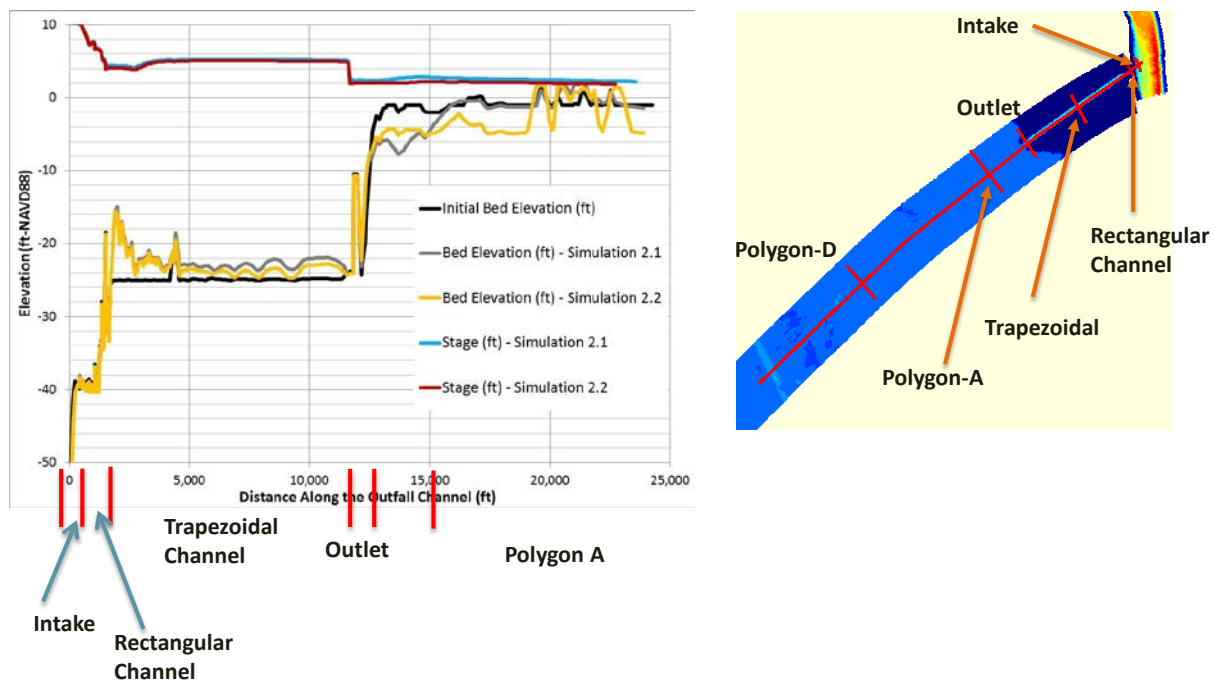


Figure 54. Simulations #2.1 and #2.2: Longitudinal profile of bed elevation and stage for peak flow (year 3;  $q=1,180,000$  cfs) - outfall channel and part of the outfall area.



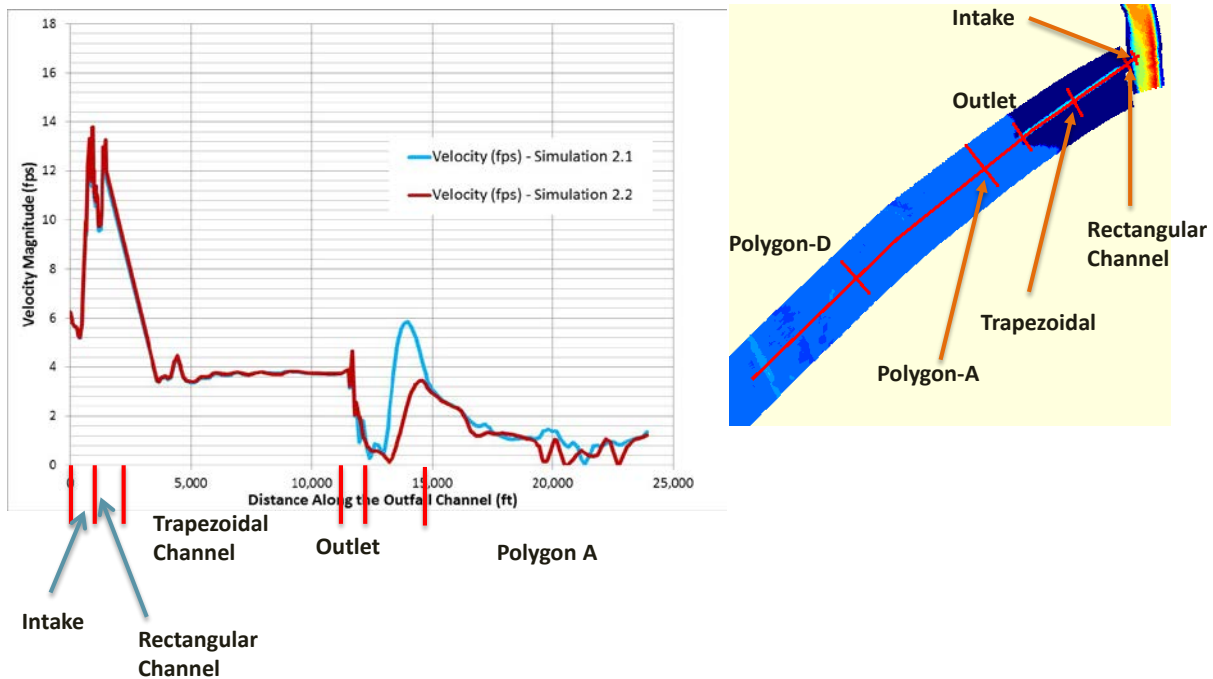


Figure 55. Simulations #2.1 and #2.2: Longitudinal profile of velocity for peak flow ( $q = 1,180,000$  cfs) - outfall channel and part of the outfall area.

A comparison between the cumulative erosion and deposition patterns for the two simulations is presented in Figure 56. The patterns displayed are similar but as previously described, the channels formed in Simulation #2.2 are deeper and longer. The similarity between the patterns is also evident when comparing the final bed level results, shown in Figure 57.

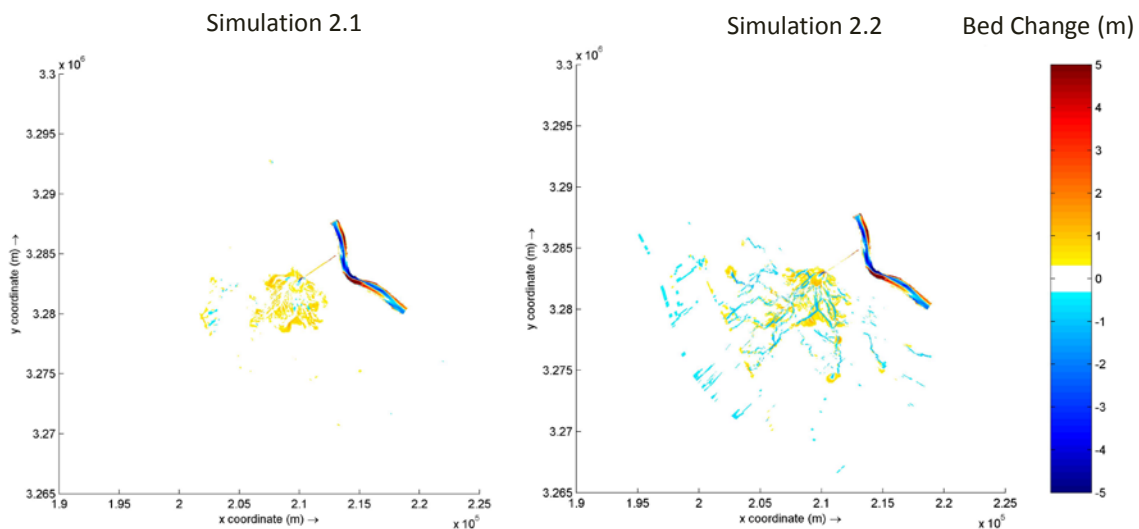


Figure 56. Simulations #2.1 and #2.2: Cumulative erosion and deposition after 5 years. A positive value indicates deposition and a negative value indicates erosion.



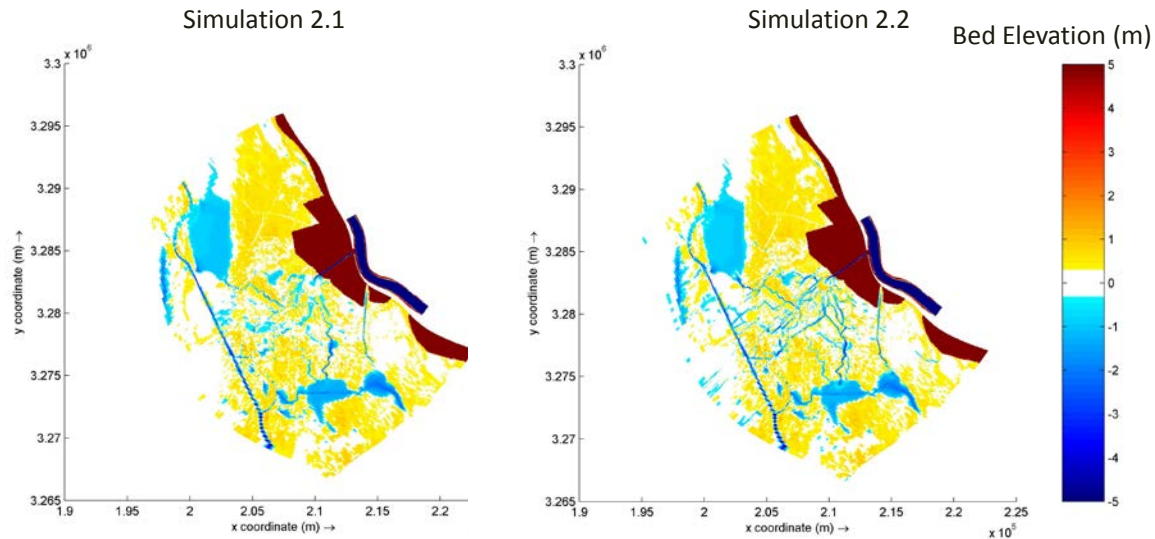
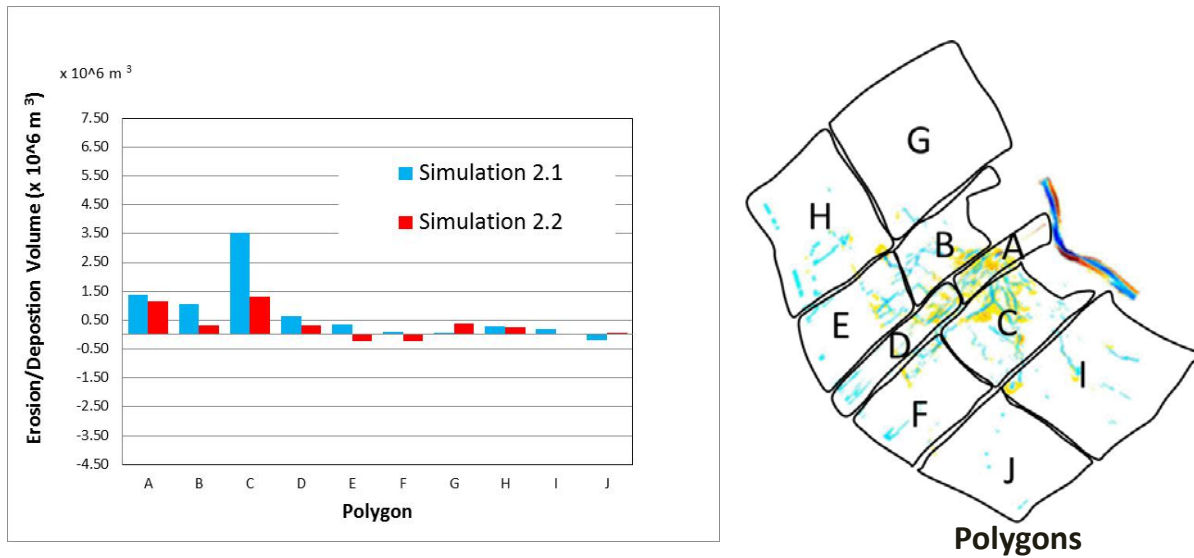


Figure 57. Simulations #2.1 and #2.2: Comparison of final bed level.

The summary of the 5-year cumulative changes by volume for each of the outfall area polygons is shown in Figure 58. Similar to what was observed for Alternative 1, both Alternative 2 simulations indicate that over the 5 years deposition occurs in the outfall area, the largest amount of deposition occurs in polygon C, and the formation of new channels is most noticeable in this area. The net deposition volume in the outfall area ranges from 3.4 - to 7.4 million  $m^3$ . It is noted that Simulation #2.2 resulted in larger net deposition volume despite being smaller diversion than Simulation #1.2. It is possible that the velocities exiting the outfall channel at the basin side for smaller diversion ( $\sim 50,000$  cfs) are lower than the velocities for the larger diversion ( $\sim 75,000$  cfs). Lower velocities would result in less erosion and higher sediment retention. The annual progression of the net volume change over the first 5 years of the diversion operation is shown in Figure 59.





Between Year 1 and Year 5  
 Net Change:  
 Simulation 2.1: +7.4 x 10<sup>6</sup> m<sup>3</sup>  
 Simulation 2.2: +3.4 x 10<sup>6</sup> m<sup>3</sup>

Figure 58. Simulations #2.1 and #2.2: Comparison of cumulative erosion and deposition by polygon.

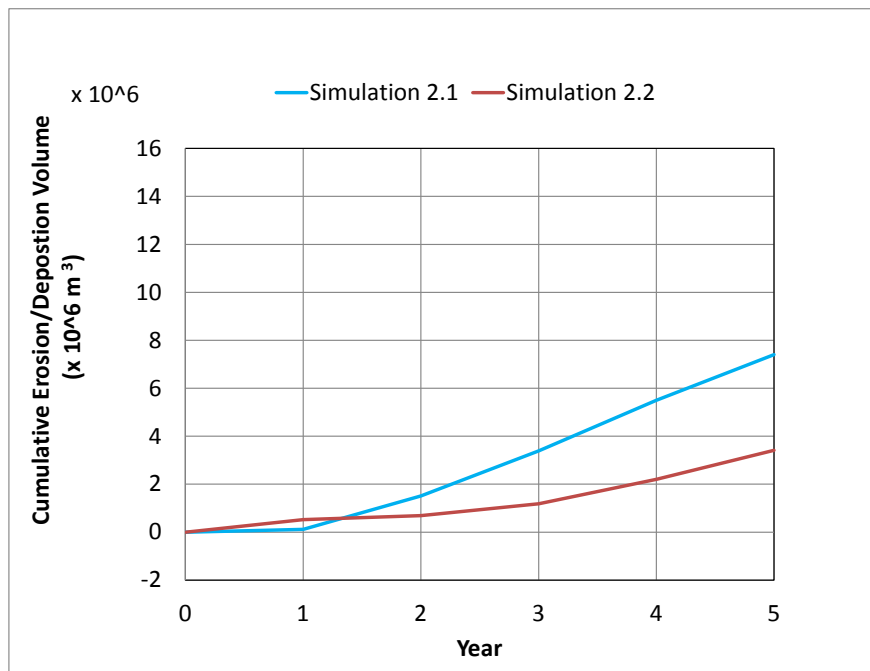


Figure 59. Annual evolution of the net volume change in the outfall area.

*Note: The initial adjustment produced in the model during Year 1 was not included in the calculations.*



Figure 60 presents the hypsometric curves of land evolution over time for the two simulations. In this case, changes in the existing area of land in the receiving basin occur at elevations between 3 ft (~1 m) and -7 ft (~-2 m). Similar to outcomes of Simulation #2.2, Simulation #2.1, only has depositional behavior which results in land gain across the different elevations. For Simulation #2.1, similar to the outcomes of Simulation #1.2, deeper channels are carved in the receiving basin. However, land gain is seen at elevations near and above 0.0 NAVD-88. These curves illustrate the fact that both simulations result in land building over the 5-year modeling period.

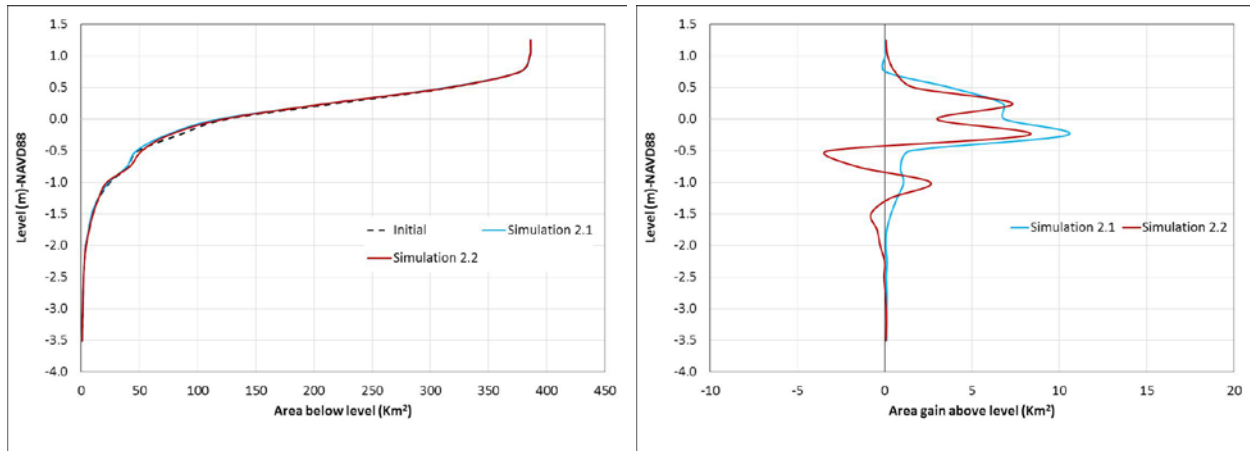


Figure 60. Hypsometric curves showing land evolution in time.

As previously stated, this work could also be used to investigate the water surface elevation increase near the mouth of the outfall channel. Figure 61 shows a comparison between water stage (time-series) from the two simulations at selected locations within the outfall area. The differences between the two simulations were within approximately 1.0 ft, and the maximum stage observed (Simulation #2.1) is just below 3.0 ft-NAVD88. High tide stage in the outfall area is typically 2.0 ft-NAVD88, and the outfall channel mouth could see an increase in stage (resulting from a diversion) of approximately 1.0 ft.



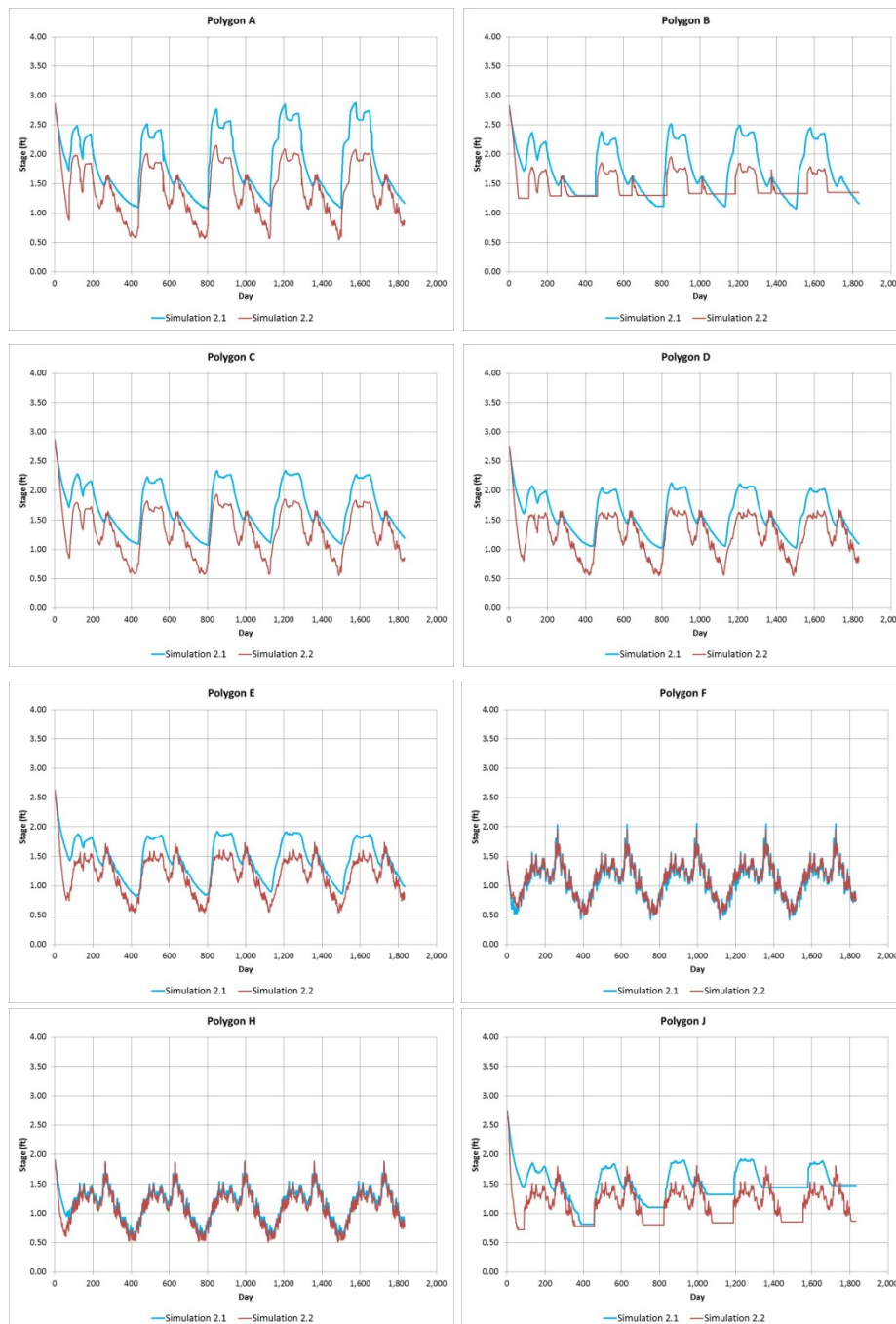


Figure 61. Simulations #2.1 and #2.2: Comparison of stage at selected polygons.

The instantaneous sediment/water ratio results for Alternative 2 are presented in Figure 61. Results from the two simulations are consistent. As expected, the SWR for mud is 1.0 when the diversion is open. The SWR for sand ranges from 0.4 to 0.5. It does not seem to vary substantially over time, meaning that the SWR for sand is just slightly lower during a 700,000 cfs flow than during a 1,180,000 cfs flow. Last, the results for sand are slightly lower for Alternative 2 (~0.5) than for Alternative 1 (~0.6).



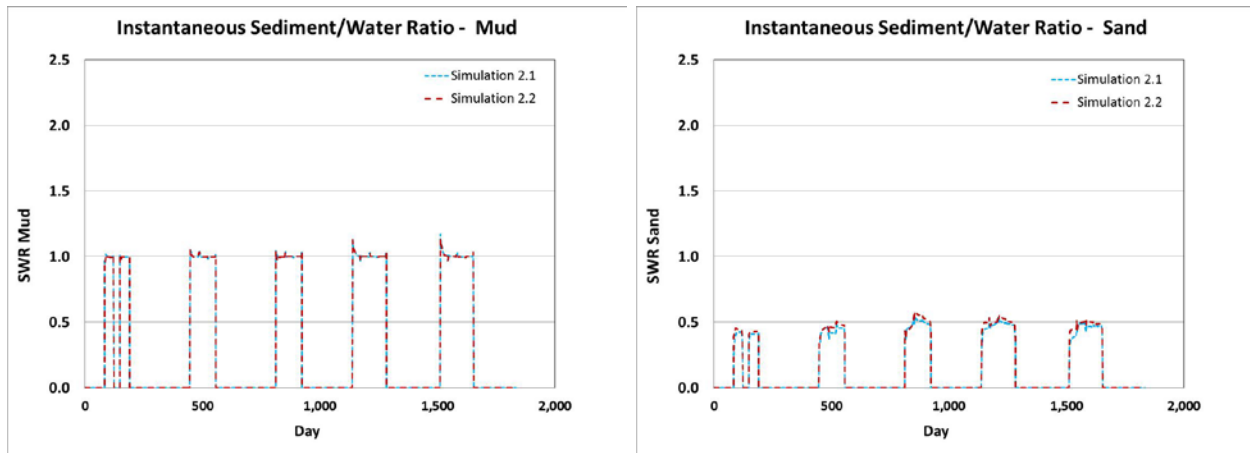


Figure 62. Simulations #2.1 and #2.2: Comparison of instantaneous SWRs.

*The calculation is performed by using a cross-section immediately above the diversion in the main stem and the rectangular cross-section area in the outfall channel.*



## 2. RIVER RESPONSE TO THE DIVERSION

At this intermediate phase of the modeling study, only small scale, short term analyses have been conducted for river response. For a broader analysis of river responses, it is recommended that a larger (spatial and temporal) analysis be conducted. It is recommended to perform such investigation in the future. Below is a brief description of the preliminary analysis of Mississippi River response to the Mid-Barataria diversion. It should be noted that the river model described in this section of the report is different from the model used in the outfall analysis described earlier. To investigate the morphological response of the river to the sediment diversion, a larger domain model is needed. Hence, a model domain between RM 76 and RM 56 (Figure 63) was used. The model has been calibrated and validated. Its performance has been assessed to ensure compliance with the metrics presented in Meselhe and Rodrigue (2013).

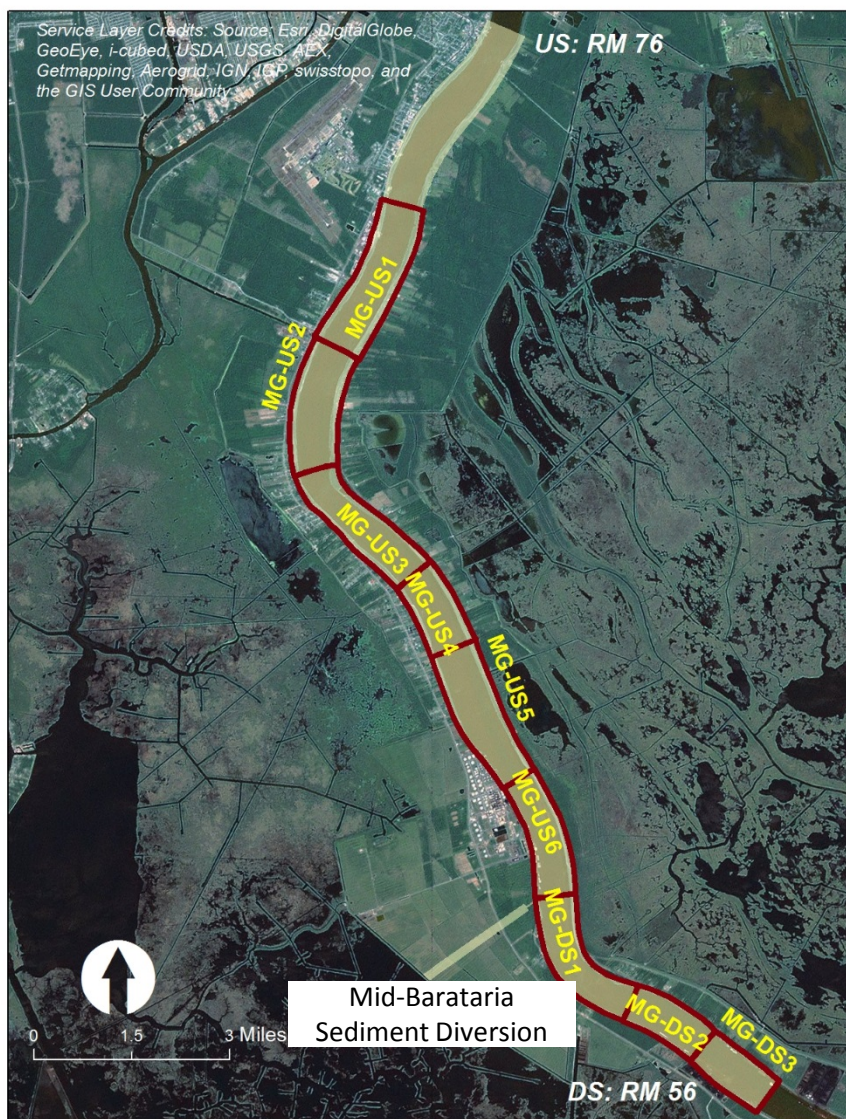


Figure 63. Extended model domain for the Mississippi River channel opposite the diversion site.



The model grid resolution for the extended model ranged from 10 m-by-10 m in the outfall channel and intake area, to 20 m-by-80 m closer to the upstream and downstream boundaries. A time-step of 0.10 min (6 sec) was used for the simulations. The model was used to simulate the operation of the Mid-Barataria diversion at a capacity of 75,000 cfs during the years 2008 to 2010.

The following boundary conditions were used:

- U/S Boundary: Flow at Belle Chasse (RM 76) (U.S. Geological Survey [USGS]); gap for October 2008 filled with Baton Rouge (RM 228) USGS data.
- D/S Boundary: Stage at RM 56 from a Mississippi River regional model (RM 138 to the Gulf); developed by the Water Institute.
- Outfall Boundary: Stage averaged between CRMS stations 0261 and 4103.

The following five size classes were used in the simulation:

- Sand: very fine sand ( $D_{50} = 83 \mu\text{m}$ ), fine sand ( $D_{50} = 167 \mu\text{m}$ ) and medium sand ( $D_{50} = 333 \mu\text{m}$ )
- Mud (fine material): clay ( $D < 2 \mu\text{m}$ ) and silt ( $2 \mu\text{m} < D < 63 \mu\text{m}$ )

Suspended sediment concentrations at the US boundary were prescribed daily based on rating curves developed using USGS measurements at Belle Chasse (RM 76) and presented in Section 1.1.

The simulated discharge at the intake is shown in Figure 64. Data show that the flow passed through the diversion matches well to the design capacity of the intake and outfall channel.

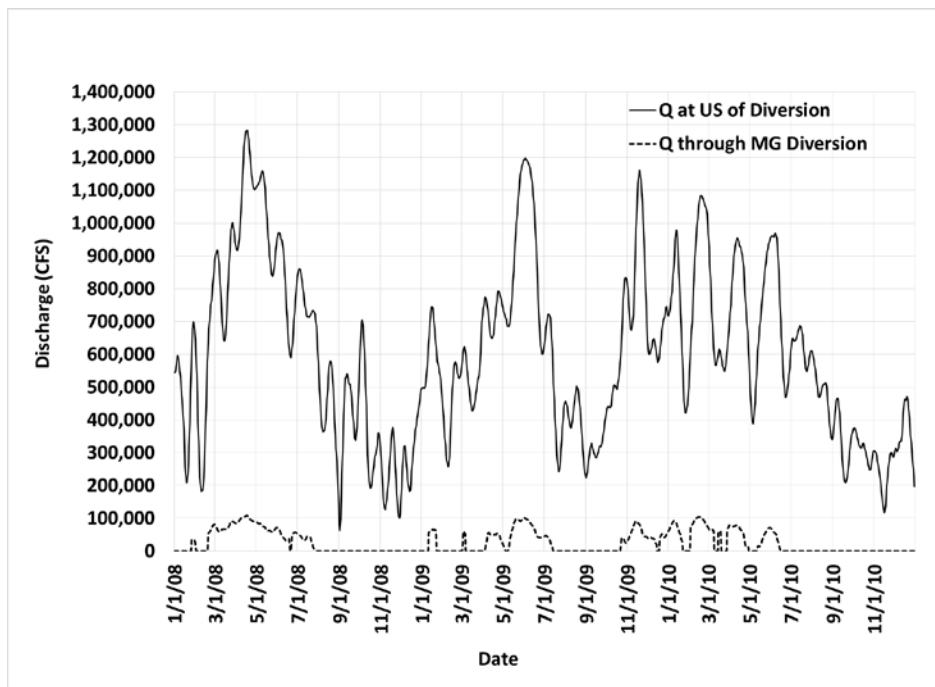


Figure 64. Simulated Mississippi River water discharge (Q) between 2008 – 2010.

To quantify the morphological changes in response to the diversion during a three-year period, the erosion and deposition volumes were calculated. These calculations were also performed for the same time period without the diversion in place. The quantities presented in the tables below represent the difference between the “with” and “without” project. The river channel was divided



into nine segments (polygons) to quantify the volume of the predicted deposition and erosion. The segments are labeled in Figure 63. Figure 65 shows that deposition occurring adjacent to and downstream of the diversion. There were little to no changes upstream of the diversion. This suggests that the diversion does not alter the morphology of the upstream sand bar, at least not during the short term (3 year) analysis provided by this modeling effort.

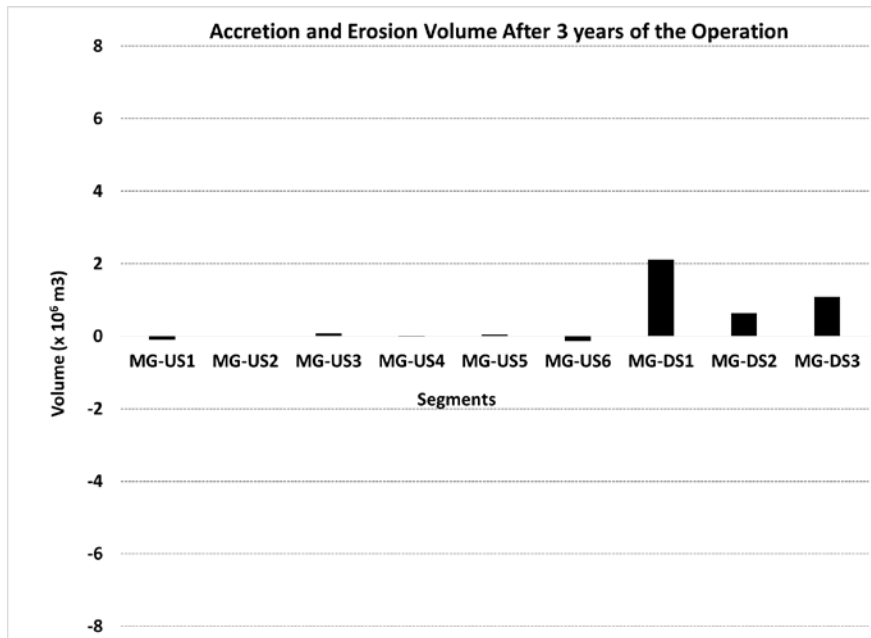


Figure 65. Erosion and deposition volume in response to the diversion during 2008 – 2010.

A sediment budget was developed to provide additional insights into the morphologic response of the river to the diversion. The budget shows the cumulative sediment mass and bulk volume: (a) entering/leaving the river segments mentioned above, (b) passing through the diversion structure, and (c) eroding or depositing within the river channel. The budget was computed during 2008 to 2010 both for Sand and Mud (fine material) sediment separately. The sediment budget (Table 12) shows that 14% of the inflowing sand load, which was about 6 million tonnes, was deposited on the riverbed and 79% exited through the downstream section. The model also shows that 6% of the inflowing sand load was diverted.

	Inflow at the U/S MR Section	Deposited US of the Diversion	Deposited DS of the Diversion	Deposited in the Outfall Channel	Diverted to the Receiving Basin	Outflow at the D/S MR Section
<b>Total Mass (10<sup>6</sup> tonnes)</b>	41.0	0.2	5.9	0.1	2.3	32.6
<b>Total Volume (10<sup>6</sup> m<sup>3</sup>)</b>	35.4	0.1	5.1	0.0	2.0	28.1
<b>% of U/S Inflow</b>		~ 0%	~ 14%	~ 0%	~ 6%	~ 80%

Table 12. Sediment budget for sand load for 2008 – 2010.



The sediment budget for fine sediment (clay and silt) indicates (Table 10) that 5% of the entering fine sediment load was diverted and 95% exited the system. There was no deposition of fine sediment occurring on the river bed.

Table 14 shows the budget for total load, i.e. the summation of the sand and fine sediment.

	Inflow at the U/S MR Section	Deposited U/S of the Diversion	Deposited D/S of the Diversion	Deposited in the Outfall Channel	Diverted To the Receiving Basin	Outflow at the D/S MR Section
<b>Total Mass (10<sup>6</sup> tons)</b>	184	0	0	0	10	175
<b>Total Volume (10<sup>6</sup> m<sup>3</sup>)</b>	159	0	0	0	9	151
<b>% with U/S</b>		~ 0%	~ 0%	~ 0%	~ 5%	~ 95%

Table 13. Sediment budget for fine sediment load for 2008 – 2010.

	Inflow at the U/S MR Section	Deposited U/S of the Diversion	Deposited DS of the Diversion	Deposited in the Outfall Channel	Diverted To the Receiving Basin	Outflow at the D/S MR Section
<b>Total Mass (10<sup>6</sup> tons)</b>	225	0	6	0	12	207
<b>Total Volume (10<sup>6</sup> m<sup>3</sup>)</b>	194	0	5	0	11	179
<b>% with U/S</b>		~ 0%	~ 3%	~ 0%	~ 5%	~ 92%

Table 14. Sediment budget for total load for 2008 – 2010.

This investigation shows that the operation of the diversion has minor impacts, at least in short term (< 5 years) at the upstream reach (including the sand bar) of the diversion. But, the stream power loss of the main channel for operating the diversion causes some shoaling downstream of the diversion.



### 3. FLOW-3D MODELING

This section provides an overview of the FLOW-3D modeling. It presents the calculations of sediment/water ratios (SWRs) for the 30% channel design based on 700,000 and 970,000 cfs Mississippi River discharge. The following approach was used:

- The previously calibrated/validated model was updated to include the most recent bathymetry, provided by HDR.
- The model domain was provided by HDR. The domain was shorter than the model used in Meselhe et al (2012) by approximately 4 miles (1 mile shorter on the upstream side and 3 miles shorter on the downstream side).
- Steady-state simulations were performed for different alternatives, and a SWR was calculated for each alternative run to quantify the performance of the sediment diversion channel.

#### 3.1. MODEL SET UP FOR ALTERNATIVE RUNS

The model calibration and validation were completed using a wall roughness for ADCP velocity data set collected in April 2009 (Mississippi River discharge at RM 62 was 700,000 cfs) and April 2010 (Mississippi River discharge at RM 62 was 970,000 cfs), respectively. Detailed information about the model calibration and validation can be found in Meselhe et al. (2012). The HDR team updated the model bathymetry and shortened the domain presumably for computational efficiency. Using the adjusted model provided by HDR, four alternative models were set up and simulated. Table 15 shows the specifications of the four alternatives, each being an individual model run.



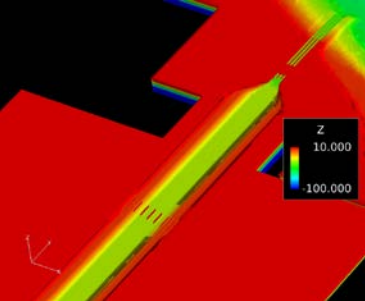
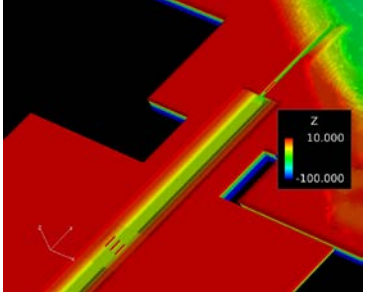
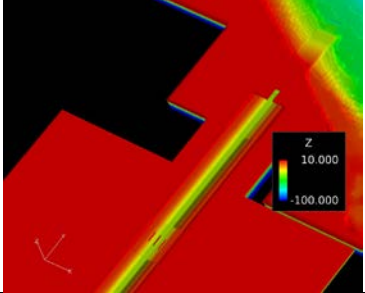
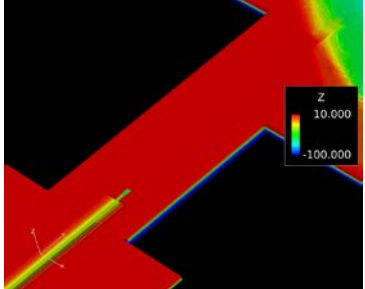
Alternative Runs	Flow Rate Diverted	Alternative Specification	Design configuration
Alternative 1 – Version 1	75,000 cfs	3 bay open channel inlet to 300 ft bottom width trapezoidal channel	
Alternative 2 – Version 1	50,000 cfs	2 bay open channel inlet to 200 ft bottom width trapezoidal channel	
Alternative 4 – Version 2	35,000 cfs	Rectangular submerged inlet invert -60 ft to rectangular box culvert to 100 ft bottom width trapezoidal channel	
Alternative 5 – Version 2	25,000 cfs	Rectangular submerged inlet invert -60 ft to triple 35 ft diameter tunnels west of LA 23 to 100 ft bottom width trapezoidal channel	

Table 15. Specifications of four alternative runs used in the FLOW-3D simulations (bathymetry colored by elevation (ft)).



Each alternative run consists of three different components in FLOW-3D to represent different surfaces: Mississippi River and diversion channel, intake structures, and Barataria Basin. Each component is defined by different wall roughness for wall shear stress calculation, which should correspond to the average height of surface imperfections like bumps and pits (Flow Science, 2010). Table 16 shows the wall roughness values used in the model runs.

Components	Surface Roughness	
	m	ft
Mississippi River and Diversion Channel	0.6	1.96
Structural Channel Components	5.2e-5	0.00172
Barataria Basin	0.5	1.65

Table 16. Wall roughness of model components.

The boundary conditions were estimated based on the calibrated and validated model results for 700,000 and 970,000 cfs flow conditions. This was done because as mentioned earlier, the model domain provided by HDR for the production runs is smaller than the model domain used for calibration and validation (See Table 17). The tailwater levels for the downstream boundary of the river were extracted from the previous simulations performed using the larger model domain. Table 17 shows the boundary conditions used in this study.

Model Runs	Q Upstream		Tailwater Downstream		Tailwater Outfall Channel		Model Domain
	cfs	cms	ft	m	ft	m	
Calibration/ Validation	700,000	19,822	7.50	2.29	4.20	1.28	RM 62.7 TO RM 56
	970,000	27,467	8.00	2.44	4.20	1.28	
Alternative 1 – Version 1	970,000	27,467	8.60	2.62	4.20	1.28	RM 61.8 TO RM 59.3
Alternative 2 – Version 1	970,000	27,467	8.60	2.62	4.20	1.28	RM 61.8 TO RM 59.3
Alternative 4 – Version 2	970,000	27,467	8.60	2.62	4.20	1.28	RM 61.8 TO RM 59.3
Alternative 5 – Version 2	970,000	27,467	8.60	2.62	4.20	1.28	RM 61.8 TO RM 59.3

Table 17. Boundary conditions used in the FLOW-3D simulations.



### 3.2. SEDIMENT / WATER RATIOS (SWRs)

The model simulations were conducted in two steps. First, hydrodynamic simulation using FLOW-3D was conducted to obtain steady state flow conditions for each alternative run. Second, using the steady state flow conditions, four size classes of sediment ranging from 64 to 250 µm were released at the upstream boundary of the model. The movement of the particles was then calculated.

Using the simulated results, the SWRs were calculated to determine the diversion's capability to capture sediment and its potential impacts on shoaling downstream of the diversion intake:

$$SWR = \frac{\text{Sediment Load Diverted} / \text{Sediment Load in the River}}{\text{Water Discharge Diverted} / \text{Water Discharge in the River}}$$

Table 18 shows the amount of river discharge diverted into the outfall channel and the SWRs for each alternative model run.

Alternative	Q (cfs) – Mississippi River	Q (cfs) – Diverted	SWRs by sediment size class				
			64 µm	96 µm	125 µm	250 µm	Total
<b>Alternative 1 – Version 1</b>	970,000	75,500	1.67	1.68	1.73	1.72	1.70
<b>Alternative 2 – Version 1</b>	970,000	46,356	1.62	1.61	1.77	1.72	1.69
<b>Alternative 4 – Version 2</b>	970,000	26,643	2.33	2.29	2.02	1.99	2.13
<b>Alternative 5 – Version 2</b>	970,000	26,102	2.54	2.51	2.27	2.20	2.35

Table 18. Sediment/Water Ratio (SWR) for different flow conditions.



## CONCLUSIONS AND CLOSING REMARKS

### Delft3D Modeling Effort

The Delft3D river channel model has been calibrated and validated for both hydrodynamics and sediment transport. The model results compare well against field measurements. The outfall area (receiving basin) model has also been calibrated and validated for hydrodynamics. There are no sediment field measurements available to date to validate the outfall area model directly. However, setup of the outfall area model for sediment transport and morphology was migrated from a validated Delft3D model for the West Bay Sediment Diversion which serves as a morphodynamic analogue.

To accommodate the uncertainty of the erodibility of the substrate material, two simulations were performed for each production run alternative (Alternative 1: 75,000 cfs and Alternative 2: 50,000 cfs), using a range of critical shear stress of the substrate soil. Only one operation plan for the diversion was tested herein; namely the diversion is open when the river discharge is higher than 600,000 cfs, and closed otherwise. It should be noted that this operation plan is significantly different from the 2012 Master Plan operation plan and as such it may not be possible to compare land building projections.

The results provide an envelope of potential land building quantities. It is worth noting that the critical shear stress was varied by a factor of 10. The resulting deposition volumes varied, in response, by a factor of approximately four for Alternative 1 (design diverted flow equal to 75,000 cfs) and two for Alternative 2 (design flow equal to 50,000 cfs). As mentioned earlier, it is also worth noting that due to boundary effects, the confidence in the results of the interior polygons (A, B, C, D, E, D, F) is higher than in the polygons at the edges (G, H, I, J). Expanding the model domain to more distal areas of the receiving basin would reduce the uncertainty of the results in these polygons. It is recommended that the outfall area model be linked to a basinwide model and longer temporal simulations are conducted to investigate the longer-term, far-field effects of the diversion.

Below is a summary of the overall observations from the results presented earlier in the report:

- The model showed that the efficiency of sediment capture and conveyance from the river side (as reflected in the persistent sediment/water ratio) to the outfall did not diminish over the course of the first 5 years of operation.
- The model showed an increase in the water surface elevation in the order of approximately 1.5 ft near the mouth of the outfall channel for a 75,000 cfs diversion and 1.0 ft for a 50,000 cfs diversion. . That increase is expected to dissipate/decrease farther away from the outfall channel mouth. That can be confirmed through a larger domain validated basin-wide model. The current model is too small to fully investigate the flooding of nearby coastal communities issue. This issue is more suitable to be addressed by larger model such as the RMA or larger scale Delft3D model.
- The model showed a trend of land building over the 5 years simulated for all the simulations.
- The exact amount of deposition volume should not be considered as final. Additional investigation of the substrate soil strength should be pursued prior to final design. Also, additional simulations with a longer temporal scale (20- to 50 years) should be performed to ensure that the performance of the diversion is within the acceptable range.



- The model showed that the sediment/water ratios (SWRs) for sand transport are only slightly higher for a 75,000 cfs than for a 50,000 cfs diversion. Nonetheless, absolute values of the SWR should be considered with care. A range of SWR should be provided rather than a single absolute value. The SWR varies with the size of the flood event, the duration of the flood event as well as with the natural variation in the tail water elevation.
- A three-year simulation showed that the diversion does not have significant impact on the morphology of the river reach upstream of the intake. As such, it does not appear that the sand bar will be impacted by the diversion operation. The model, however, showed that due to the loss of stream power, deposition may occur downstream of the diversion. Additional analyses using a larger domain model and longer simulation times are necessary to further investigate the morphology of the river in response to the operation of the diversion. This can be done in future phases of this project or through communications with ongoing studies such as the Mississippi River Hydrodynamic study.
- The model showed a high retention rate in the outfall area in the first 5 years of operating the diversion. It is possible that such high retention rates are reflective of the short duration of this modeling effort (5 years). Longer simulations would be required to fully assess the retention rates.

### **FLOW-3D Modeling Effort**

The FLOW-3D results for all the alternatives show high sediment water ratios compared to previous modeling effort presented in Meselhe et al (2012). Below are some insights and observations:

- For Alt 1 and Alt 2, the high sediment water ratio might be a direct result of shortening the model domain. The sediment distribution at the upstream end of the model is assumed to be uniform through the water column. It takes a certain distance for the sediment to be redistributed to a more natural profile of higher concentration near the bottom of the water column compared to near the surface. The smaller model domain provided by HDR (especially on the upstream side of the diversion) may skew the results into higher SWR.
- However, it does not appear that reducing the diversion size from 75,000 cfs to 50,000 resulted in a decrease in the sediment capture efficiency.
- For Alt 4 and 5, as expected, the sediment water ratios are quite high. Since the intake of these alternatives starts at an elevation of – 60 ft-NAVD88, it would capture sand from the bottom of the sand bar. It is unclear, however, how the intake would not be clogged since it is nearly 10 feet below the surface of the sand bar. There is a concern about the ability to convey and deliver sediment to the basin side over time. Such clogging would not be captured in this modeling effort, first because it reflects only steady-state conditions, and second because it is beyond the ability of most, if not all, numerical models to capture morphological behavior in a mixed system (free-surface flow coupled with pressurized closed conduit flows). In reality, unless there is a mechanical mechanism (e.g. pumps) to maintain the tunnel, it may not be possible to keep it open. This is especially true during the periods where the diversion is not in operation and material would settle to the bottom/floor of the tunnel. As such, it is in our opinion that this alternative be modeled in a physical scaled model to fully investigate its feasibility and verify whether it would clog over time and how to keep it open.



## REFERENCES

Deltares. (2009). Simulation of multi-dimensional hydrodynamic flows and transport phenomena, including sediments. Delft3D-FLOW User Manual, September.

Flow Science (2010). FLOW-3D – Excellence in Flow Modeling Software. User Manual 9.4 Volumes 1 and 2. Santa Fe, NM 87505, [www.flow3d.com](http://www.flow3d.com).

Léonard, J., & Richard, G. (2004). Estimation of runoff critical shear stress for soil erosion from soil shear strength. *Catena*, 57(3), 233-249.

Meselhe, E. A., Georgiou, I., Allison, M. A., & McCorquodale, J. A. (2012). Numerical modeling of hydrodynamics and sediment transport in lower Mississippi at a proposed delta building diversion. *Journal of Hydrology*, 472, 340-354.

Meselhe, E.A. and Rodrigue, M.D. (2013). Models Performance Assessment Metrics and Uncertainty Analysis. Louisiana Coastal Area Program Mississippi River Hydrodynamics and Delta Management Study. <http://www.lca.gov/Projects/22/Default.aspx>.

Pant, H. R. (2013). Erosional Resistance of Cohesive Sediments in Coastal Saltmarshes (Doctoral dissertation). Louisiana State University, Baton Rouge, Louisiana.

Ramirez, M. T., & Allison, M. A. (2013). Suspension of bed material over sand bars in the Lower Mississippi River and its implications for Mississippi delta environmental restoration. *Journal of Geophysical Research: Earth Surface*, 118(2), 1085-1104.

Rijn, L. C. van (1993). Principles of Sediment Transport in Rivers, Estuaries and Coastal Seas. Aqua Publications, The Netherlands.

Rijn, L. C. van (1984a). Sediment transport, Part I: bed load transport. *Journal of Hydraulic Engineering* 110 (10): 1431-1456.

Rijn, L. C. van (1984b). Sediment transport, Part II: suspended load transport. *Journal of Hydraulic Engineering* 110 (11): 1613 - 1640.

Sanford, L. P. (2008). Modeling a dynamically varying mixed sediment bed with erosion, deposition, bioturbation, consolidation, and armoring. *Computers & Geosciences*, 34(10), 1263-1283.

